HOKKAIDO UNIVERSITY

Pentosan Polysulfate: an Effective Treatment for Model of Rheumatoid Arthritis and a Novel Candidate for Inhibition of Cytokines-Induced Osteoclastogenesis

多硫酸ペントサン：関節リウマチの効果的な治療法およびサイトカイン誘発破骨細胞分化制御の新規薬剤としての検討

A Dissertation for the Degree of Doctor of Philosophy

H.M. Suranji Wijekoon

Graduate School of Veterinary Medicine

Department of Veterinary Clinical Sciences

Laboratory of Veterinary Surgery

2018

Dissertation Examination Committee:

Prof. Masahiro Okumura, Supervisor and Chair

Prof. Yasuhiro Kon

Associate Prof. Kenji Hosoya

Associate Prof. Kentaro Sakamoto

Pentosan polysulfate: an effective treatment for model of rheumatoid arthritis and a novel candidate for inhibition of cytokines-induced osteoclastogenesis

by

H.M. Suranji Wijekoon

A dissertation presented to the

Graduate School of Veterinary Medicine of Hokkaido University

in partial fulfillment of the requirements for the degree of Doctor of Philosophy

Hokkaido University

Japan

2018

Dedication

This thesis work is dedicated to my husband, W.M. Nuwan Wijeoon, who has been a constant source of support and encouragement during the challenges of graduate school and life. I am truly thankful for having you in my life.

This work is also dedicated to my parents, H.M. Somarathne and R.M. Ranjini Rajapaksha who have always loved me unconditionally and whose good examples have taught me to work hard for the things that I aspire to achieve.

Publications Related to the Dissertation

The contents of this dissertation are based on the following original publications and submitted manuscripts under review listed below by their Roman numeral I-VI of the research conducted during the period April 2014 - March 2018.

I. **Wijekoon, H.M.S.,** Toyota, K, Kim, S., Fang, J., Bwalya, E.C., Hosoya, K. and Okumura, M. **2017**. Differentiation potential of synoviocytes derived from joints with cranial cruciate ligament rupture and medial patella luxation in dogs. *Res Vet Sci* 114, 370-377.

II. **Wijekoon, S.,** Bwalya, E.C., Kim, S., Fang, J., Hosoya, K. and Okumura, M. **2017**. Chronological differential effects of pro-inflammatory cytokines on RANKL-induced osteoclast differentiation of canine bone marrow-derived macrophages. *J Vet Med Sci* 79 (12), 2030-2035.

III. **Wijekoon, S.,** Bwalya, E.C., Kim, S., Fang, J., Hosoya, K. and Okumura, M. **2017**. Inhibitory effect of pentosan polysulfate on formation and function of osteoclats derived from canine bone marrow. *BMC Vet Res* Under Review.

IV. **Wijekoon, S.,** Kim, S., Bwalya, E.C., Fang, J., Aoshima, K., Hosoya, K. and Okumura, M. **2018**. Anti-arthritic effect of pentosan polysulfate in rats with collagen-induced arthritis. *Res Vet Sci* Under Review.

List of abbreviations

ANOVA	One-way analysis of variance
AP1	Activator protein-1
BM	Bone marrow
BMMs	Monocyte-macrophages
CaP	Calcium phosphate
CCLr	Cranial cruciate ligament ruptured
cDNA	Complementary deoxyribonucleic acid
CIA	Collagen induced arthritis
COMP	Cartilage oligomeric matrix protein;
CII	Type II collagen
CO2	Carbon dioxide
CTK	Cathepsin K
DMARD	Disease-modifying anti-rheumatic drugs
DMEM	Dulbecco's modified eagle medium
DMOAD	Disease modifying osteoarthritis drug
EI	Edema index
ELISA	Enzyme-linked immunosorbent assay
FBS	Fetal bovine serum
FITC	Fluorescein isothiocyanate
GAPDH	Glyceraldehyde-3-phosphate dehydrogenase
H&E	Hematoxylin and eosin
HUVTH	Hokkaido University Veterinary Teaching Hospital
IL-1β	Interleukin-1β
IQR	Interquartile range
MAPK	Mitogen-activated protein kinase

M-CSF	Macrophage colony stimulating factor
MDP	N-acetylmuramyl-L-alanyl-D-isoglutamine;
MHC	Major histocompatibility complex
M-MLV	Murine Leukemia Virus Reverse Transcriptase
MMP9	Matrix metallopeptidase 9
MPL	Medial patella luxation
MSCs	Mesenchymal stem cells
MW	Molecilar weight
NFATc1	Nuclear factor of activated T-cells, cytoplasmic 1
NF-κB	nuclear factor kappa-light-chain-enhancer of activated B cells
NSAID	Non steroid anti-inflammatory drug;
OA	Osteoarthritis
OB	Osteoblast
OC	Osteoclast
OCP	Osteoclast precursor
PBS	Phosphate-buffered saline
PPS	Pentosan polysulfate
RA	Rheumatoid arthritis
RANK	Receptor activator of NF-kB
RANKL	Recombinant receptor activator of NF-kB ligand
RNA	Ribonucleic acid
RT-PCR	Real time polymerase chain reaction
SD	Sprague–Dawley
SEM	Standard error of mean
SM	Synovial membrane
TGF-β	Transforming growth factor
TNF-α	Tumor necrosis factor

TRACP-5b	Tartrate-resistant acid phosphatase 5b
TRAP	Tartrate-resistant acid phosphatase positive
TRITC	Tetramethylrhodamine

Contents

CHAPTER 3

3. Inhibitory effects of pentosan polysulfate on formation and function of osteoclasts derived from canine bone marrow

CHAPTER 4

4. Anti-arthritic effect of pentosan polysulfate in rats with collagen-induced arthritis

Preface

Pentosan polysulfate (PPS) is a Beechwood-derived hemicellulose semisynthetic compound which manufactured from sulfate esterification of the sugar ring hydroxyl groups (Burkhardt and Ghosh, 1987). PPS is a mean molecular weight (MW) of 5700 Da carbohydrate polymer (Fig. 1) and classified as a disease modifying osteoarthritis drug (DMOAD) because of its ability to preserve the integrity of articular cartilage and bone while improving the quality of joint synovial fluid (Burkhardt and Ghosh, 1987; Ghosh et al., 1992; Ghosh, 1999). Pentosan is able to improve anabolic activity of chondrocytes and fibroblasts while mitigating catabolic events associated with obliteration of the cartilage extracellular matrix (Ghosh, 1999). The chondroprotective activity of PPS has been demonstrated by stimulating proteoglycan synthesis in rat, rabbit and canine models of osteoarthritis (OA) (Ghosh et al., 1992; Ghosh, 1999). Further, hyluronan synthesis is restored when cells were incubated with PPS *in vitro* or with intra-articular injection into joints of OA patients (Ghosh, 1999). PPS has been available for over 40 years as an anti-thrombotic agent (Vinazzer, 1989; Joffe, 1976) and later identified it as anti-inflammatory agent, leading to use as a treatment for interstitial cystitis (Anger et al., 2011; Hanno et al., 2011).

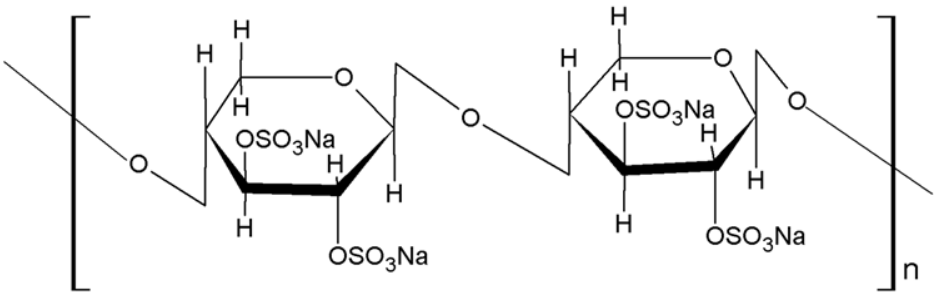

Fig. 1 Molecular structure of pentosan polysulfate

Currently Injectable PPS forms also are used to treat osteoarthritis in veterinary medicine (Cartrophen Vet® injection, PPS - 100 mg/mL; Biopharm Australia, Bondi Junction, NSW, Australia) (Kwan et al., 2012; McIlwraith et al., 2012).

One important difference between OA and rheumatoid arthritis (RA) is the massive inflammation seen in RA (Qvist et al., 2008). But chronic form of OA are progressively viewed as an inflammatory disease and "wear and tear disease" which starts through the growth of blood vessels and nerves from the subchondral bone into articular cartilage (Mobasheri, 2013). Rheumatoid arthritis is a chronic inflammatory disease that affects approximately 0.5 to 1 percent of the general population worldwide. It reasons joint destruction and significant debilitating morbidity and impairment in the quality of life of the patients by causing economic cost due to both health care expenditure and lost productivity (Firestein et al., 2005). The key characters of the inflammation related arthritis are progressive joint inflammation and destruction of marginal and sub chondral bone in the joint, deformity, loss of mobility, systemic manifestations and severe pain which ultimately impede basic motility functions (Walsh et al., 2014; Taylor et al., 2016).

Similar as many other forms of arthritis, RA is initially characterized by an inflammatory response of the synovial membrane, including hyperplasia, increased vascularity and infiltration of inflammatory cells, primarily antigen-driven CD4+ T cells (Quan et al., 2008). Cell to cell interaction and production of cytokines activate monocytes, macrophages and synovial fibroblast to produce the several pro-inflammatory cytokines, tumor necrosis factor-alpha (TNF-α), interleukin (IL) 6, 17 which appear to play a crucial role in the pathogenesis of RA (McInnes and Schett, 2007; Firestein, 2003) (Fig. 2). Other than above mentioned cytokines, many other cytokines, chemokines and angiogenic factors are also present in the inflamed synovium. They

trigger signal transductions pathways of cells and initiate the activation of transcription factors and variety of genes those are responsible for trigger the inflammation, tissue degradation and bone erosion (Quan et al., 2008). Bone erosion is a key outcome measure in RA and mainly happens via osteoclast (OC) secreted acids and cathepsin K (CTK) (Quan et al., 2008; Schett and Gravallese, 2012). Osteoclast generates from monocytes/macrophage lineage and differentiates within synovial membrane and plays critical role at inflammatory conditions (Redlich et al., 2002).

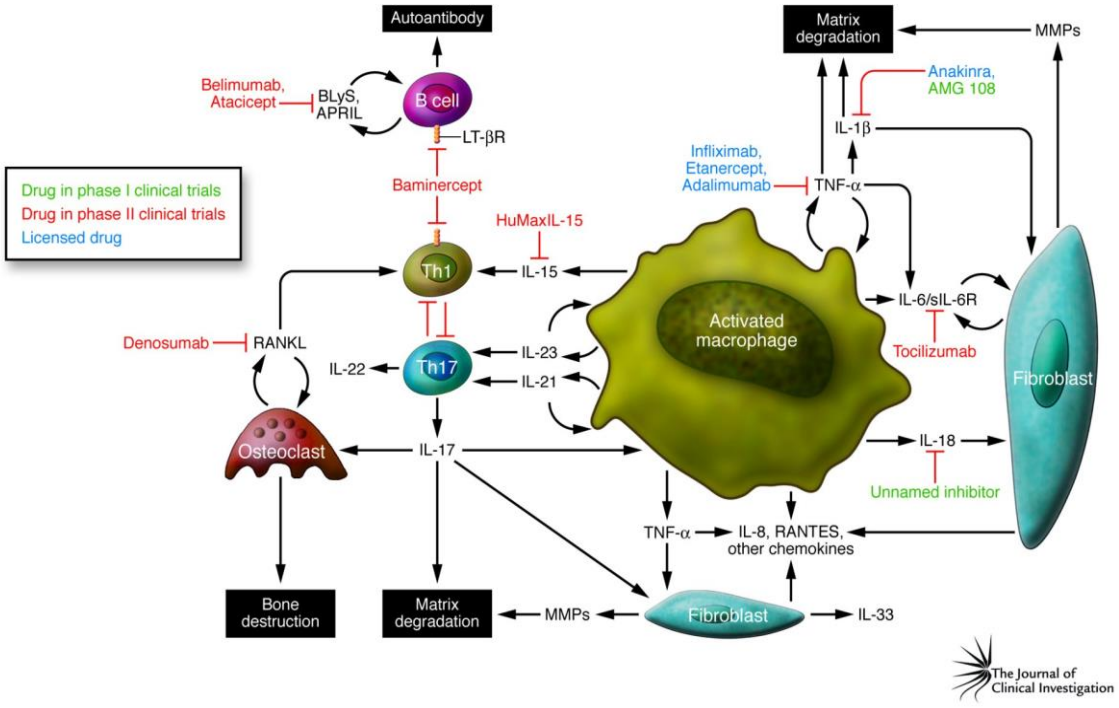

Fig. 2 Cellular interactions and cytokines playing significant role in the pathogenesis of rheumatoid arthritis. Cytokines and some immune cells are depicted as potential targets for novel therapies of inflammatory and immune-mediated diseases (Brennan and McInnes, 2008).

Synovium is a soft tissue lining the spaces of diarthrodial joints, tendon sheaths and bursae. It includes the continues surface layer of cells called intima which composed of macrophages and fibroblasts while the underlying tissue, sub intima includes blood and lymphatic vessels, a cellular content of both resident fibroblasts and infiltrating cells in a

collagenous extracellular matrix (Smith, 2011). The major functions of synovial membrane (SM) are maintenance of an intact non-adherent tissue surface, lubrication of cartilage, control of synovial fluid volume and composition and nutrition of chondrocytes within joints. Synovial joints are involved in a number of immunological and inflammatory disorders, including RA as well as synovium plays major role of pathology in such condition (Smith, 2011). The principle structure and cause of bone erosion is the pannus, which is found at the interface of bone, cartilage (Paleolog, 2002). After activation of synoviocytes through TNF-α, IL-1 and IL-6, secrete matrix metalloproteinase (MMP) in to synovial fluid and cause cartilage degradation (Smolen and Steiner, 2003; Smolen et al., 2007). Chondrocytes are also activated by cytokines, leading to direct release of additional MMP into the cartilage (Smolen and Steiner, 2003; Smolen et al., 2007).

Skeletal homeostasis is maintained by a highly regulated balance of continuous bone remodeling that couples new bone formation by osteoblasts (OB) and bone resorption by OC (Schwarz et al., 2006). In many pathologic conditions, such as postmenopausal osteoporosis, RA and periodontitis, the amount of bone removed by OC exceeds that laid down by osteoblasts and bone becomes deteriorated (Boyce et al., 2009). Osteoclasts are multinuclear cells derived from hematopoietic stem cells (Suda et al., 1992). During the process of osteoclastogenesis, monocytes differentiate into OC precursors (OCP) and subsequently assume a mature multinucleated OC phenotype with bone resorption activity (Ritchlin et al., 2003) (Fig. 3). Macrophage-driven osteoclastogenesis requires the presence of macrophage colony-stimulating factor (M-CSF) and results from the interaction of the receptor activator of nuclear factor kappa-B (RANK) and the RANK ligand (RANKL) (Karsenty and Wagner, 2002; Teitelbaum, 2000). Expression of

RANKL on the OCP is regulated by pro-inflammatory cytokines such as TNF-α, IL-1, IL-6 and IL-17 (Schett, 2007).

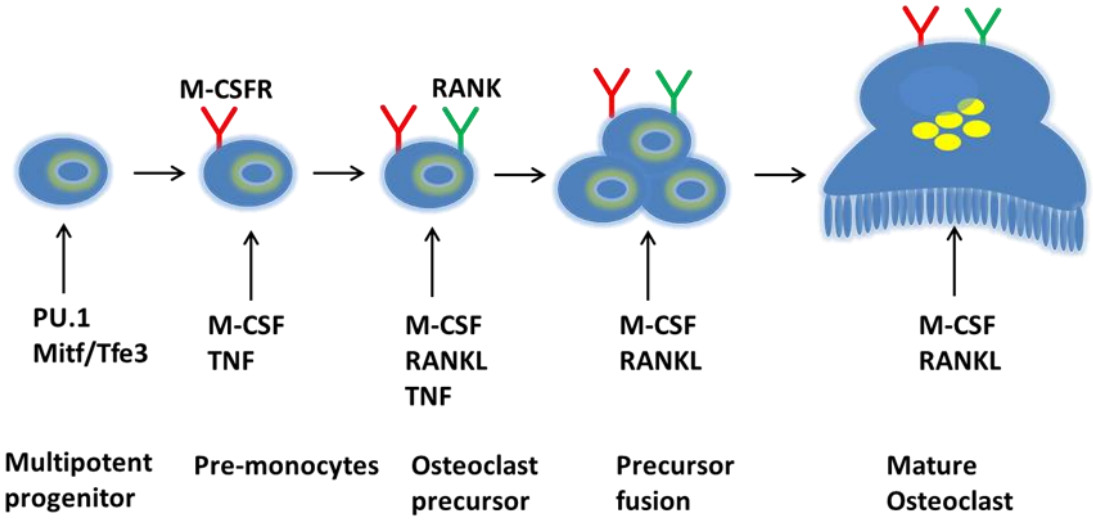

Fig. 3 Stages of osteoclast differentiation from hematopoietic lineage cells. M-CSF and RANKL are essential external stimuli for osteoclastogenesis.

RANKL binds to its receptor, RANK, on the surface of OCP activating signaling through nuclear factor kappa-light-chain-enhancer of activated B cells (NF-κB), c-Fos and nuclear factor of activated T cells c1 (NFATc1) to induce differentiation of OCP into OC (Takayanagi, 2007). Further, with RANKL binding, activates signal transduction pathways involving the adaptor protein TNF receptor-associated factor 6. Subsequently, several kinases such as p38 mitogen-activated protein kinase (MAPK) and JUN N-terminal kinase 1 are activated, which lead to induction of transcription via the various hetero- and (occasionally) homodimers of the activator protein-1 (AP1) family of proteins. This family includes the molecules FOS-related antigen 1 (FRA1), FRA2, JUN, JUNB and JUND, as well as activating transcription factor (Wagner, 2010; Schonthaler et al., 2011). Many of the drugs used to treat common bone diseases inhibit OC formation or activity with several limitations (Boyce et al., 2009). The identification and thoroughly understanding of cytokines and signaling pathways (Fig. 4) which activate in

osteoclast, might be greatly increased our understanding of how OC formation and bone resorption are regulated by its microenvironment.

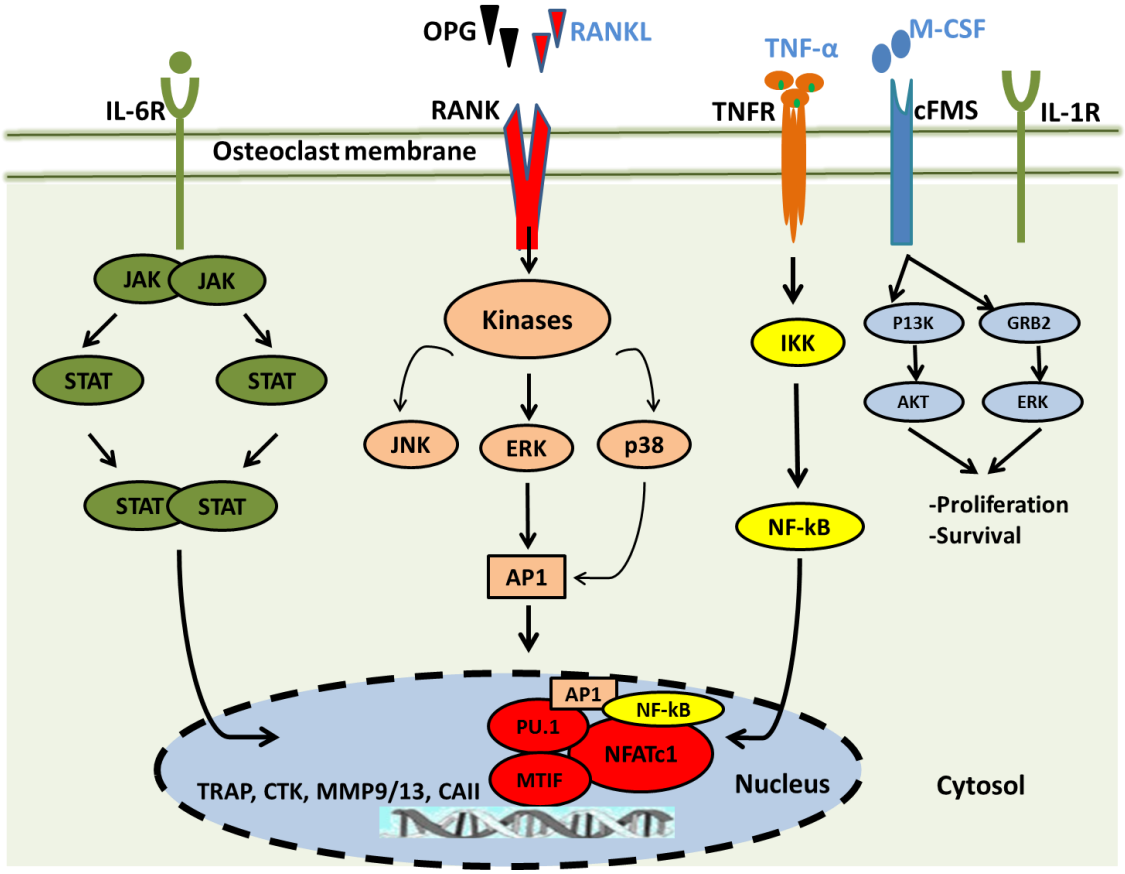

Fig. 4 Role of cytokines (RANKL, TNF-α, IL-1) in osteoclast differentiation. Osteoclast phenotype under the influence of RANKL, which signals trough the transcription factors AP1 and NFkB.

The management of patient with RA has dramatically changed last few decades. However, the ultimate goal in managing RA is to prevent structural joint damage and loss of function. Recent evidence suggests that early interference is essential in achieving this goal (Breedveld, 2002). In this new management setting, more attention is given to the differentiation between RA and other types of arthritis, particularly OA. Rapid and appropriate management of RA or OA disease activity is needed to prevent joint damage,

loss of function, and to maintain quality of life. Combination disease modifying anti-rheumatoid drug (DMARD) therapy may, in this respect, provide additive effects or allow dose reductions to avoid toxicity (Breedveld, 2002).

Many new therapeutic strategies are being investigated for RA in combination with methotrexate, a widely used DMARD. However, because methotrexate is cytotoxic and has serious and potentially life-threatening side effects its use cannot be justified for OA (Mobasheri, 2013). Novel treatment options for arthritis patient are focused on relief of pain and improvement of joint structure including analgesics, nonsteroidal anti-inflammatory drugs (NSAID), intraarticular injections of steroids and hyaluronans (Qvist et al., 2008). Further, NSAID reduce inflammation and pain, the most characteristic clinical outcomes of both RA and chronic form of OA. However long-term consumption of NSAID can cause stomach upset, cardiovascular problems, gastric bleeding and liver and kidney damage (Mobasheri, 2013).

This realization of various adverse effects of RA and OA therapeutic strategies has focused research effort on the development and evaluation of biological therapy that targets proinflammatory mediators, angiogenic factors and cytokines in articular cartilage, subchondral bone and synovium (Mobasheri, 2013). The good efficacy and general safety of these agents is well established and generally acceptable with a slight increase risk for infections (Chatzidionysiou, 2012). The central hallmark in the development of OA or RA is the progressive destruction of the joint tissue, a reasonable approach to the development of an effective medical treatment seems to be the search for drugs with the ability to slow down this process, or maybe even arrest it completely. These drugs, termed as DMOAD (Qvist et al., 2008). Till the date, the pharmacology industry has failed to bring effective and safe DMOAD to the human and animal suffering from debilitating RA or OA (Qvist et al., 2008).

Rationale for the thesis

The current study reasoned that cellular changes associated with different degree of synovitis would allow us to identify multiple differentiation capability of synovitis derived from common knee injuries associated with dogs. We hypothesized that the dogs with cranial cruciate ligament rupture and medial patella luxation, which carry different inflammatory severities, would be more likely to have a varying ability of multipotency. Comprehensive analysis of synoviocytes was carried out to speculate that the liability of synovial membrane-derived stem cells to re-establish the imbalance between OA catabolism and joint anabolism. Hence this study might serve as a platform for understanding the similarities and dissimilarities of the cellularity in synovitis associated with common knee injuries.

Inclusive clarification of osteoclast and its microenvironment were needed to classify the role in joint destruction and enabled the development of therapies aimed at reducing its resorptive capacity at inflammation-related arthritis. Part of this study was constructed to investigate osteoclastogenic properties of inflammatory cytokines at different time-points of osteoclastogenesis, in order to understand the precise mechanisms of osteoclasts at immune-mediated bone destruction. Additionally, this study reasoned that, *in vitro* and *in vivo* identification of action of PPS over the osteoclast and its microenvironment at the inflammatory nature by providing a novel mechanism as an inhibition of osteoclastogenesis and anti-arthritic. An additional aim of this work was to identify the effect of PPS over the cell signaling molecules of osteoclasts in dogs.

CHAPTER 1

Differentiation potential of synoviocytes derived from joints with cranial cruciate ligament rupture and medial patella luxation in dogs

1.1 Summary

The objective of this study was to assess the differentiation capability of synoviocytes derived from dogs with inflammatory joint conditions. Cranial cruciate ligament ruptured (CCLr) (n=12) and medial patella luxated (MPL) (n=10) knee joints of the dogs were used to collect the SM. Synoviocytes were enzymatically released from the SM and analyzed by flow cytometry for specific cellular markers (CD44 and CD90) of mesenchymal stem cells (MSCs), while doing histopathology from another part of SM sections. Under specific culture conditions, synoviocytes were forced to differentiate into chondrogenesis, adipogenesis, osteogenesis and osteoclastogenesis to investigate the multipotency. Upon treatments phenotypes of cell cultures were analyzed by histopathology and by semi-quantitative reverse transcriptase polymerase chain reaction for the expression of each differentiation marker genes. Although flow cytometry showing similar MSCs populations in CCLr and MPL synovium, synovial cells derived from CCLr showed higher multipotency compared to MPL-derived samples. Further, synovial changes such as vascularity, mononuclear cell infiltration and cellular hypertrophy were more pronounced in CCLr-derived synovial tissue than in MPL. Taken together, these findings suggested that the differentiation capability of SM-derived multipotent stem cells varies with inflammatory severity occurring in different joint conditions.

1.2 Introduction

Inflammatory joint diseases leading to severe functional disability are characterized by abnormal synovial proliferation as well as destruction of articular cartilage and bone (Danks et al., 2002). The synovium is the central area of pathology of OA, RA (Sakkas & Platsoucas, 2007) and other inflammatory joint diseases including canine common knee injuries such as CCLr and MPL (Doom et al., 2008; Witsberger et al., 2008). The study of degenerative changes of SM during pathological conditions in the joint contributes to the understanding and establishing of therapeutic options in regenerative medicine. During the inflammatory process, the cell population of SM is predominantly composed of mononuclear cells and includes T and B lymphocytes, activated tartrate-resistant acid phosphatase positive (TRAP) macrophages, major histocompatibility complex (MHC) class II+ dendritic cells and plasma cells (Lemburg et al., 2004; Muir et al., 2005). Proper understanding of cellularity in synovitis could be attained through elucidation of significant variations of microarchitecture in synovial tissue including the thickening of the intimal layer, increased vascularity, inflammatory cell infiltration of the sub synovial layer and the formation of multiple finger-like projections (villi) into the joint (Smith, 2011; Smith et al., 2011).

Stem cells, which are available in different organs and tissues, are capable candidates for the regeneration of tissue and organ systems. Mesenchymal stem cells are able to differentiate into lineages of mesenchymal tissues such as cartilage, bone, fat, and muscle (Branco De Sousa et al., 2014; De Bari et al., 2001). Isolation and characterization of MSCs from canine bone marrow (BM) have been previously described (Kisiel et al., 2012). Most of the studies have been focused on finding MSCs in different parts of the body for medical treatment. The synovial membrane is the most

specialized mesenchymal tissue among joint structures which, carrying resident MSCs (Branco De Sousa et al., 2014), have the potential of multiple differentiation (De Bari et al., 2001). Synovium is the closest tissue to articular cartilage having MSCs with higher chondrogenic capacity comparing with that in other structures of joint (Mochizuki et al., 2006; Sakaguchi et al., 2005) and is the only tissue that can produce hyaline cartilage in benign conditions, suggesting that SM act as a source of cells for articular cartilage repair (Nagase et al., 2008).

But the differentiation ability of synoviocytes in each individual case of CCLr or MPL with erratic inflammatory severity is yet to be elucidated. To our knowledge, there are no published studies confirming an association between synovitis and differentiation ability of synoviocytes in canine patients. The objective of the study reported in this chapter was to determine whether there was a relationship between the inflammation and multipotency of the cells from SM with CCLr or MPL. We hypothesized that the dogs with CCLr or MPL, which carry different inflammatory severities, would be more likely to have a varying ability of multipotency. The findings of this study support the hypothesis and suggest that pathological changes and differentiation capability of progenitors of SM in early synovitis could vary among CCLr and MPL.

1.3 Materials and Methods

1.3.1 Specimens

Synovial membrane samples were collected from dogs diagnosed with ruptured cranial cruciate ligaments (n=12) and medial patella luxation (n=10) while undergoing surgical exploration of the affected knee joint followed by surgical joint stabilization. Apart from ligament rupture, the animals were otherwise healthy. Twenty-two skeletally-mature, mixed small breed of genders, age 4 to 7 years (4.7 ± 1.3 years) and weighing 3 to 8 kg were used for this experiment after obtaining owner consent. All dogs were evaluated at Hokkaido University Veterinary Teaching Hospital. The use of clinical samples and all samples from experimental dogs was in accordance with Hokkaido University Institutional Animal Care and Use Committee guidelines (approval number: 12-0059). The medical history of each affected dog including information obtained from both the owner and the referring veterinarian was documented. Tentative diagnosis of CCLr was made on the basis of results of a drawer or tibial compression test in addition to diagnosing MPL by radiography and based on palpation of an unstable knee cap. For each dog, serum biochemical profile and urinalysis were performed.

1.3.2 Isolation and culture of synovial cells

The synoviocytes were isolated from the synovial tissue using a modification of published protocols (Burmester et al., 1987). The synovial tissue was dissected away, washed with Ca2+/ and Mg2+ free phosphate-buffered saline (PBS) twice and finely minced. The minced tissue was digested with 0.2% collagenase type I (Wako pure chemicals, Osaka, Japan) in Dulbecco's modified eagle medium (DMEM, Invitrogen, NY, USA) containing 10% heat-inactivated fetal bovine serum [(FBS) Nichirei

Bioscience INC., Tokyo, Japan] and antibiotic-antimycotic solution (100 units/ml penicillin, streptomycin and gentamycin; Wako) for 90 minutes at 37^{o}C. After filtering through the 70-mm cell strainer (Safar Co. Ltd., Osaka, Japan) the cell suspension (3 ml) was layered on 4 ml of ficoll/ paque (Pharmacia Biotech, Uppsala, Sweden) and centrifuged at 400 g for 30 minutes. The interface layer was re-suspended in 4 volumes of DMEM and washed three times by centrifugation at 250 g for 10 minutes. The cells were finally suspended in DMEM containing 10% FBS and seeded in (10^6 cells/ well) 48-well multi-well plates (Life Sciences, Oneonta, NY, USA).

1.3.3 Cytometry

Confluent monolayer primary cultured cells were washed 3 times with PBS and harvested by treatment with Ethylene diamine tetra acetic acid (0.05% EDTA, Dojindo institute, Tokyo, Japan) in 0.02% trypsin (Wako). After centrifugation (300 g), cell sediment was collected and washed with PBS in micro tube (BMbio, Tokyo, Japan). This was repeated 3 times. Aliquots of 1×10^5 cells suspension were incubated with rat anti-CD44 monoclonal antibody (clone YKIX337.8.7, AbD Serotec, Kidlington, UK), rat anti-Thy-1(CD90) monoclonal antibody (clone YKIX337.217, AbD Serotec) and negative control, rats IgG2b isotype (Institute of medical biological co. Ltd., Nagoya, Japan) for 30 minutes in dark at 4° C.

After 3 times of washing with PBS, cell suspension was incubated with fluorescein isothiocyanate (FITC) labeled anti-rat IgG antibody (Sigma, St. Louis, MO, USA) at 4° C in a dark place for 30 minutes. Sediment obtained in PBS suspension was filtrated through nylon mesh (Specimen advance science and technology, Tokyo, Japan) to get cell suspension. Flow cytometer (BD FACSVerse^{TM}, Becton Dickinson and Co.,

Piscatway, NJ, USA) was used for analyzing the expression of each of cell surface antigens.

1.3.4 *In vitro* chondrogenesis

The *in vitro* chondrogenesis assay was performed as described elsewhere (De Bari et al., 2001). Briefly, micromass cultures were obtained by pipetting 20-µl droplets of cell suspension from SM derived monolayer culture after trypsin treatment into individual wells of 48-well plates. The cells were allowed to attach without medium at 37° C and then chemically defined serum-free medium was added after 3 hours (Harrison et al., 1991). On the next day, 20 µg/ml dexamethasone, 10 ng/ml transforming growth factor (TGF)-β and 50 M ascorbic acid (all from Sigma) were added to the medium while adding identical amount of DMEM to parallel cultures as a control for treatment. After 21 days, media was removed from culture vessel, rinsed once with PBS and fixed cells with 4% formaldehyde solution (Kanto Chemical, Tokyo, Japan) for 30 minutes. After fixation, wells were rinsed with PBS and stained with 1% alcian blue 8 GS (Sigma) in 0.1 N HCl for 30 minutes. The wells were rinsed three times with 0.1 N HCl and added distilled water to neutralize the acidity.

1.3.5 *In vitro* adipogenesis

The *in vitro* adipogenesis assay was performed as described in another place (Kisiel et al., 2012). Briefly, SM-derived cells were cultured additional 5 days after 80% cell confluence. Then adipogenic differentiation medium which was consisting of growth medium supplemented with 1 mM dexamethasone, 0.5 mM methyl-isobutylxanthine, 10 mg/ml insulin, and 100 mM indomethacin (all from Sigma) was added to the wells. After 72 hours, the medium was changed to adipogenic maintenance medium (10 mg/ml

insulin in growth medium) for 24 hours. Cells were treated 4 times with adipogenic induction medium and propagated into adipogenic maintenance medium for 1 week before fixation. After 3 weeks, cells were rinsed twice with PBS, fixed with formaldehyde solution for 10 minutes, washed with distilled water, rinsed in 60% isopropanol, and covered with oil red O solution (0.1% oil red O [Sigma] in 60% isopropanol). After 10 minutes, cultures were briefly rinsed in 60% isopropanol and washed thoroughly in distilled water.

1.3.6 *In vitro* Osteogenesis

The *in vitro* osteogenesis assay was performed as described elsewhere (De Bari et al., 2001). Briefly, SM-derived cells were plated in growth medium at $3 \times 10^3/cm^2$ in 6-well tissue culture plates. From the following day onward cells were subsequently cultured for 21 days in the presence of 100 nM dexamethasone, 10 mM β-glycerophosphate, and 50 mM ascorbic acid (all from Sigma). Cells cultured in growth medium supplemented with DMEM and 10% FBS were used as control. Alizarin red S stain was prepared by adding (Sigma) 1 g into 100 ml of distilled water. Ammonium hydroxide 1000× dilution (Wako) was added to adjust pH 6.4. After 21 days, medium was removed and washed with PBS 3 times. After fixation with 10% formaldehyde solution for 10 minutes, plate was washed thoroughly by distilled water 3 times. Prepared alizarin red dye was added to the plate and kept 15 minutes and washed by distilled water. Images were visualized under light microscope for specific characteristics. Differentiation potential of chondrogenesis, adipogenesis and osteogenesis according to the strength of positivity of staining for mild, moderate and strong positivity was summerized. Cells cultured in normal growth medium supplemented with DMEM and 10% FBS were considered as controls for all the treatments.

1.3.7 *In vitro* Osteoclastogenesis

Isolated synovial cells (10^6 cells /well) were seeded to 48-well multi-well plates (Life Sciences) and cultured in the presence of 20 ng/ml recombinant human M-CSF (Invitrogen, Frederick, MD, USA), 50 ng/ml human recombinant RANKL (Sigma) and 10 ng/ml canine recombinant TNF-α (Kingfisher Biotech, INC., St. Paul, MN, USA) for 7 days. Cultured cells were fixed in 3% formaldehyde after treating PBS containing 0.002% pronase E (Sigma) and 0.02% EDTA (pronase E solution) for 5 minutes to remove synovial fibroblasts. Synovial cells were stained for TRAP according to the manufacturer's instructions of commercial kit (Cosmo Bio Co., LTD, Tokyo, Japan). Cells containing three or more nuclei were considered as OC.

1.3.8 Histopathology

After fixation in 4% formaldehyde, the biopsy specimens were embedded in paraffin, cut in 4-µm sections and stained with hematoxylin and eosin (H&E). Tissue sections were deparaffinised and TRAP staining was performed using a commercial acid phosphatase leucocyte kit (Sigma). Recently described comprehensive histological system (Brenner et al., 2005a) was used with some modification as a subjective histological grading. Briefly, SM was scored for synovial vascularity, synovial inflammation (mononuclear cell infiltration), elastic fibrosis and synovial fibrosis for (+) mild (1-10%), (++) moderate (11-50%) and (+++) strong (51-100%) positivity.

1.3.9 Tissue collection and RNA isolation

Total RNA was extracted from the cell culture and tissue homogenates according to the manufacturer’s instructions. Total RNA from cells was extracted using RNeasy Mini Kit® (QIAGEN, Germantown, MD, USA) according to the manufacture’s protocol.

Total RNA was quantified by spectrophotometry at 260 nm. RNA with a 260/280 nm ratio in the range 1.8–2.0 was considered high quality. Total RNA was reverse transcribed into cDNA with M-MLV RT kit (Takara Bio, Tokyo, Japan) according to manufacturer's recommended procedures. RNA concentrations were determined by spectrophotometry.

1.3.10 RT-PCR

One microgram of total RNA derived from the synovial tissue was reverse-transcribed into cDNA with random hexamers. Specific primers were used as shown in Table 1. PCR conditions were as follows: denaturation at 95 ^{o}C for 30 s, annealing temperature for 1 minute, extension aaut 72 ^{o}C for 1 min for 30 cycles, and final extension at 72 ^{o}C for 7 min. PCR products were separated on 1.5% agarose gel and stained with ethidium bromide.

1.3.11 Real-time PCR

Quantitative real-time PCR analysis was performed with KAPA SYBR® FAST qPCR kit (KAPA biosystems, Woburn, MA, USA). The amount of 2 μl of cDNA template was added to each 10 μl of premixture with specific primers. The mRNA level for the gene of interest was quantified as the percentage of that determined for glyceraldehyde-3-phosphate dehydrogenase (GAPDH).

1.3.12 Statistical analysis

Statistical analyses were performed using SPSS software (ver. 07 for Windows; SPSS Inc., Chicago, IL, USA). Relative gene expression of osteoclast specific genes was represented as the means ± S.E.M. (Standard Error Mean). An appropriate post-hoc test

was used to analyze the difference. Then comparison between groups was made by one-way analysis of variance (ANOVA). Statistical significances were achieved when $p < 0.05$ (* $p < 0.05$).

1.4 Results

1.4.1 Comparison of cell yield

Confluent primary monolayer culture cells were analyzed for expression of MSCs surface markers such as CD44 and CD90. In two dogs, one had CCLr and the other MPL strongly expressed CD44 (99.84% and 98.89%) and CD90 (86.85% and 99.46%), respectively (Fig. 5). According to the flow cytometric analysis, the greater yield of CD44 and CD90 positive cells were isolated from synovial cell fraction regardless the severity of inflammation in two different conditions.

1.4.2 Differential potential of SM-derived cells

Dexamethasone and TGF β1 treated micro masses displayed dark blue images under light microscope, indicating the synthesis of proteoglycans by chondrocytes (Fig. 6A). Alcian blue stain, marker of chondrogenesis was appeared in varying degree between the CCLr samples and MPL (Table 2). Different expression level of messenger RNA (mRNA) of collagen type II and aggrecan among CCLr and MPL, further confirmed that the chondrogenic potential of stem cells derived from SM (Fig. 6B). Differentiation potential of MSCs to adipocytes was confirmed by the accumulation of lipid vacuoles in cell cytoplasm as well as expression of adipocytes phenotype (PPARγ) of the tissue generated in vitro. Lipid vesicle stained with oil red O was distinguished in CCLr derived samples comparing with that in MPL (Fig. 7A). Spindle shaped SM-derived cells changed their morphology to cuboidal and formed large nodules that stained for alizarin red (Fig. 7B) with the presence of calcium deposits. Osteogenesis, evaluated by alizarin red was obtained in all samples tested without any major difference between phenotype

in CCLr and MPL samples. Varying degree of staining intensity for multipotency was shown between samples from CCLr and MPL, rendering them distinguishable (Table 2).

1.4.3 Osteoclast differentiation in synovial cell populations

After incubation of synovial cell culture with RANKL, M-CSF and TNF-α cytokine, TRAP (+) multinuclear osteoclast like cells appeared at day 7 by confirming the potential of synoviocytes to differentiate in to osteoclasts (Fig. 8A). Detecting of RANK expression in cultured SM cell fraction by semiquantitative RT-PCR confirmed the ability of osteoclastogenesis from SM (Fig. 8B). Messenger RNA expression level of osteoclast specific marker genes such as MMP9 and RANK significantly elevated ($p< 0.05$) in CCLr-derived samples (Fig. 8C). However, there was not significant difference in mRNA expression of carbonic anhydrase and CTK between CCLr and MPL.

1.4.4 Histochemistry and histopathology

Histopathology was done for 3 CCLr samples (dog 1-3) and 3 MPL samples (dog 1-3) (Table 3). Hematoxylin and eosin stained SM specimens of CCLr confirmed the presence of hypertrophy of laminar propria by fibroblast like cells, exuberant angiogenesis as well as cellular infiltration of lymphocytes and macrophages (Fig. 9). However, the specimens of MPL showed mild hypertrophy of fibroblasts cells in intimal layer, mononuclear cell infiltration and angiogenesis. According to grading of synovial changes in Table 3, mild to strong synovial changes were perceived in specimens from CCLr in addition to mild histological changes of MPL. Multinucleated OC-like cells were not detected with acid phosphatase leukocyte staining kit in both CCLr and MPL sections.

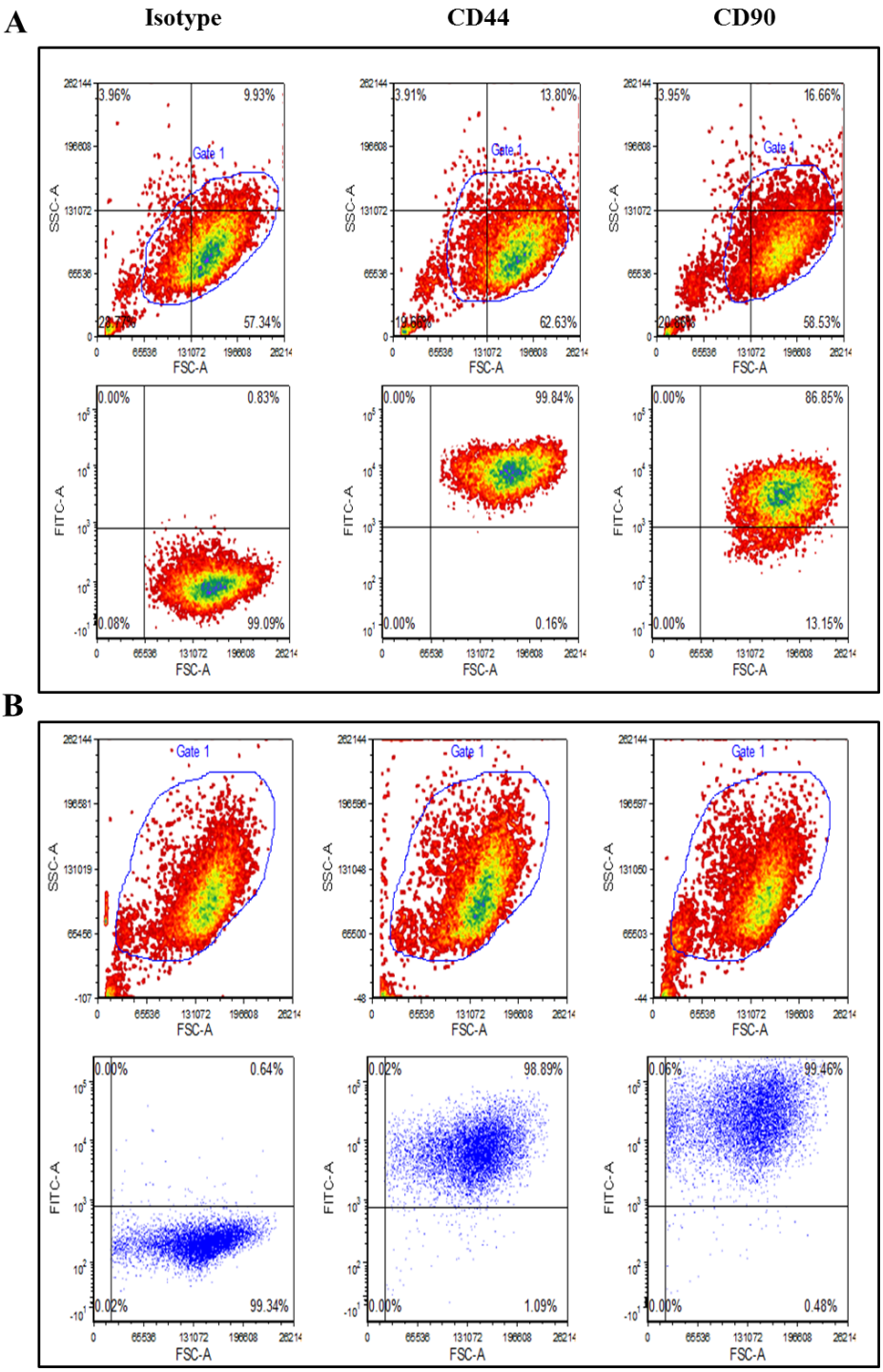

Fig. 5 Expressions of CD44 and CD90 surface marker of synovial membrane (SM) derived MSCs. Flow cytometry identified SM derived MSCs from (**A**) CCLr and (**B**) MPL samples for positive markers CD44, CD90 and negative control isotype. Representative dot plot shows that, the higher percentage of CD44 and CD90 markers positive cells in both CCLr and MPL samples.

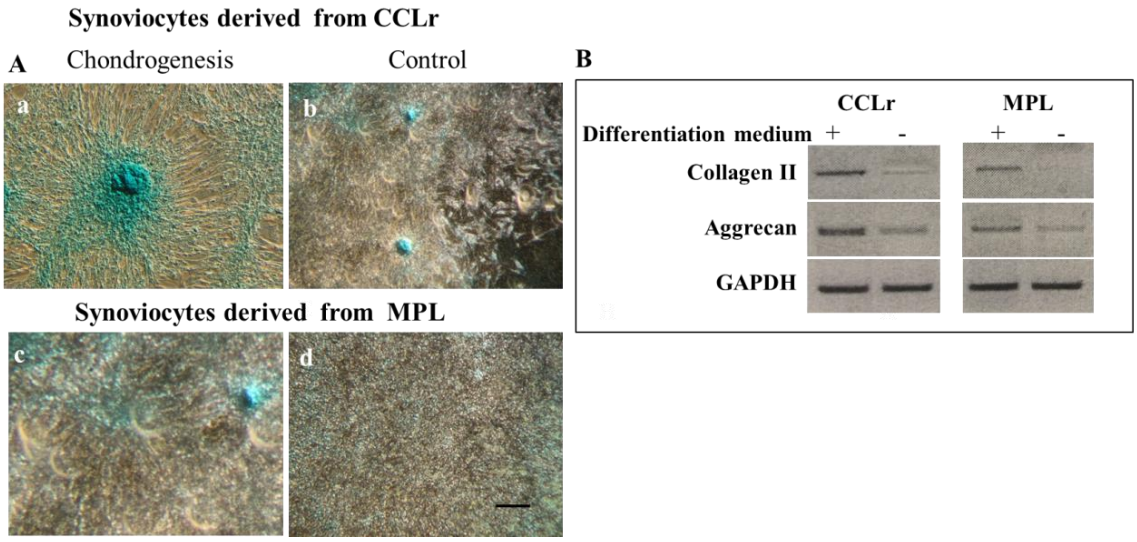

Fig. 6 Chondrocytes differentiation from SM-derived cells. A, Micromass were either treated (**a, c**) and not treated (**b, d**) with differentiation medium containing 20 µg/ml dexamethasone 10 ng/ml transforming growth factor β1 (TGF-β1) and 50 M ascorbic acid. After 3 weeks, cells were fixed and stained for alcian blue. Finding indicates that the presence of cartilage differentiation in cells derived from CCLr. Bar = 100 µm. **B**, Semi quantitative reverse transcription (RT)- PCR analysis for cartilage markers, collagen II and aggrecan from CCLr-derived samples were comparable with MPL sample. For each donor, the experiment was performed in duplicate. The samples cultured in growth medium containing DMEM and 10% FBS were considered as control group. GAPDH was used as a house keeping gene.

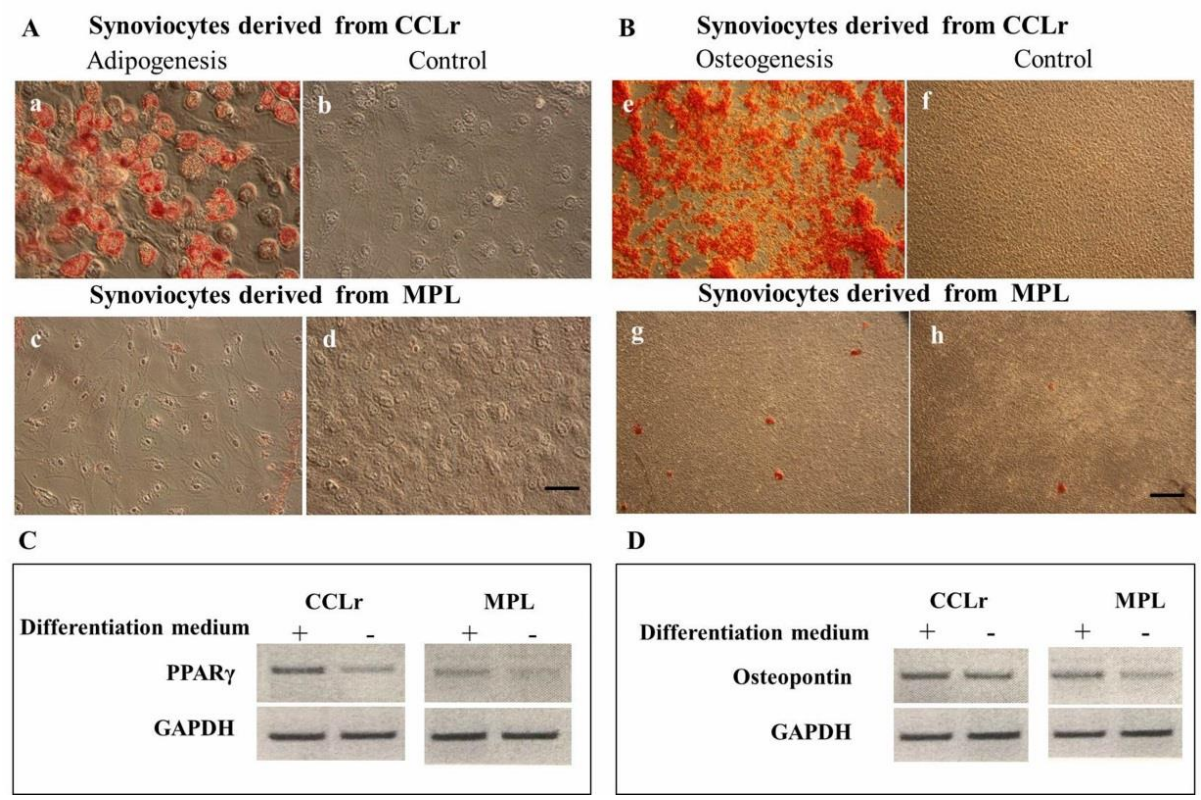

Fig. 7 Adipogenic and osteogenic differentiation of synovial membrane (SM)-derived cells. A, Monolayer SM derived cells were either treated (**a, c**) or not treated (**b, d**) with differentiation medium containing 1 mM dexamethasone, 0.5 mM methyl-isobutylxanthine, 10 mg/ml insulin, and 100 mM indomethacin. After 3 weeks, cells were fixed and stained for oil red O stain. **B**, Monolayer SM derived cells were either treated (**e, g**) or not treated (**f, h**) with differentiation medium containing 100 nM dexamethasone, 10 mM β-glycerophosphate, and 50 mM ascorbic acid. After 21 days, cells were fixed and stained for alizarin red. Finding indicates the presence of adipocytes differentiation in cells derived from CCLr. Bar = 50 µm. **C, D**, Gel electrophoresis results of specific marker genes of adipogenesis and osteogenesis. The mRNA expression level of PRARγ and osteopontin from CCLr were comparable with MPL sample. For each donor, the experiment was performed in duplicate. Controls for the all treatment groups were SM derived cells cultured in growth medium containing DMEM and 10% FBS.

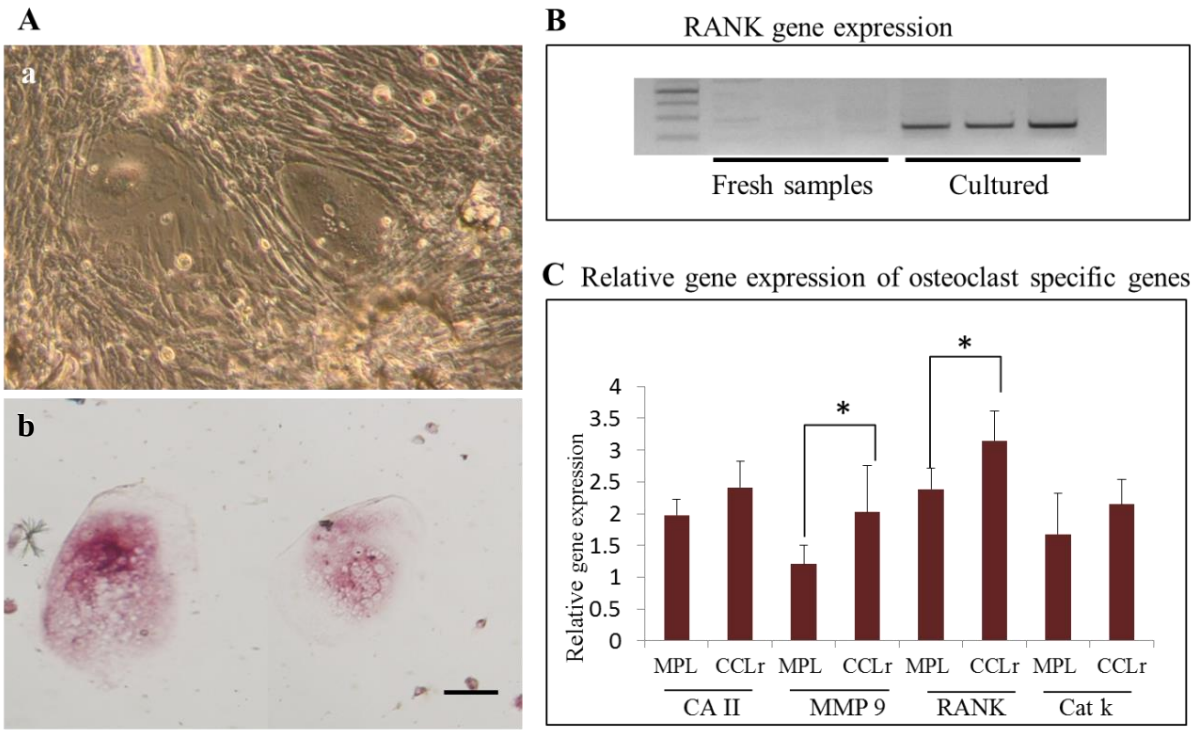

Fig. 8 Shows TRAP positive osteoclasts-like multinucleate giant cells formation from SM derived cells. A-a, Light photomicrograph of synovial cell culture after 7 days with the presence of MSC-F, RANKL, TNF-α shows that osteoclasts-like cells formation among fibroblasts. After treatment of pronase E (**b**) to remove the fibroblast, TRAP positive cells were appeared. Bar = 100µm. **B**, Osteoclast specific marker gene, RANK was expressed only in cultured samples which were treated with osteoclastogenic medium. **C**, Relative gene expression of osteoclasts marker genes, carbonic anhydrase II (CA II), MMP 9, RANK and CTK were statistically different (*: $p < 0.05$) amidst CCLr (n= 6) and MPL (n= 5) samples. Bars represent mean relative values normalized to GAPDH expression ± SEM.

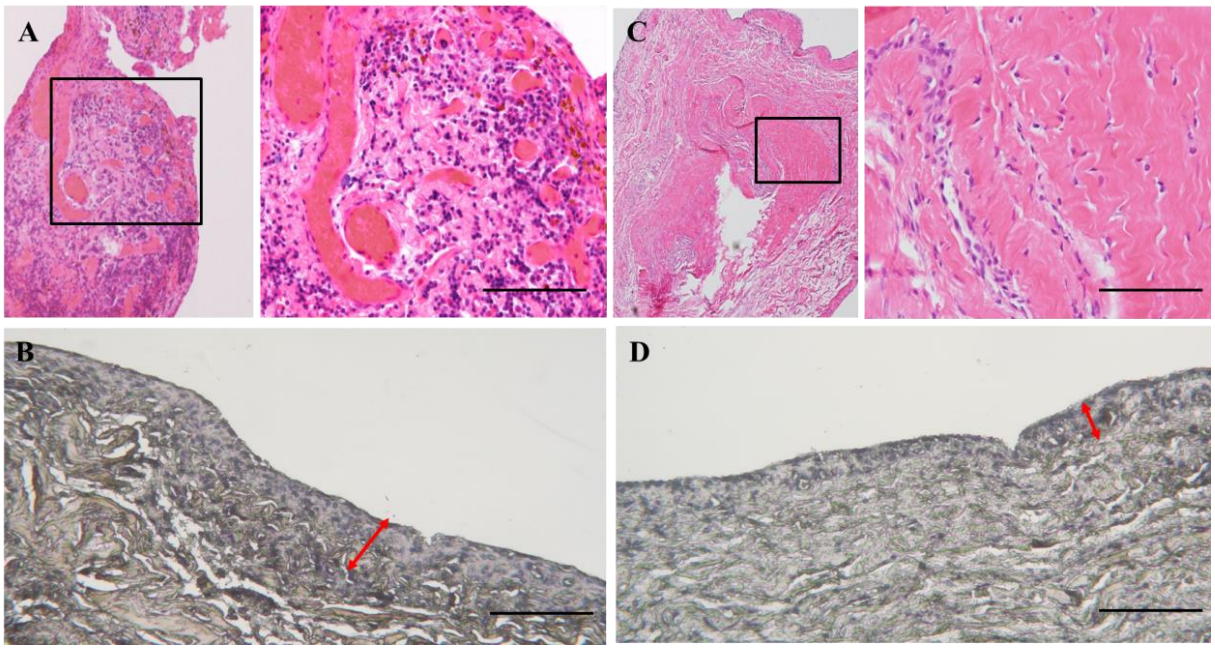

Fig. 9 Histopathological changes of synovial membrane specimens from CCLr and MPL patients. Histological examination was performed by H&E and acid phosphatase staining. Bar= 500 µm. **A, B,** Synovial membrane of CCLr, composed of elastic fibers, fibroblasts, blood vessels, infiltration of mononuclear cells and thickened synovial lining layer. **C, D,** Hyperplasia of fibroblasts with relatively thin synovial lining layer (red double arrow) was noticed in MPL derived samples.

Table 1 Primes used to polymerize the chondrocytes, adipocytes, OB and OC-specific function genes

Target gene	Sense and anti-sense (5-3)	Annealing temperature (^{o}C)	PCR fragment length (bp)
Collagen II	CACTGCCAACGTCCAGATGA	54.54	215
	GTTTCGTGCAGCCATCCTTC	54.16	
Aggrecan	ACTTCCGCTGGTCAGATGGA	54.98	111
	TCTCGTGCCAGATCATCACC	53.75	
PPARG	ATCAAGCCATTCACCACCGT	59.9	149
	GCAGGCTCCACTTTGATTGC	60.1	
Osteopontin	ACGATGTAGATGAAGATGATGG	59.8	548
	GCTTTGACTTAATTGGCTGAC	60.1	
Carbonic anhydrase II	AAGGAGCCCATCAGCGTTAG	59.82	104
	GGGCGCCAGTTATCCATCAT	60.25	
MMP9	GGCAAATTCCAGACCTTTGA	56.4	166
	TACACGCGAGTGAAGGTGAG	53.4	
RANK	CCCTGGACCAACTGTAGCAT	58.7	239
	ACCCAGTGCCACAAATTAGC	55.9	
Cathepsin K	ACCCATATGTGGGACAGGAT	57.79	169
	TGGAAAGAGGTCAGGCTTGC	60.25	
GAPDH	CTGAACGGGAAGCTCACTGG	54.92	129
	CGATGCCTGCTTCACTACCT	54.03	

Table 2 Differentiation potential of synovial membrane derived cells obtained from CCLr and MPL. Differentiation potential of SM derived cells was examined and graded as indicated in material and methods. (+ Mild positive, ++ Moderate positive, +++ strong positive, - Negative, NA Not available)

Origin	Animal	Chondrogenesis	Adipogenesis	Osteogenesis
CCLr	Dog 2	+ +	++	+ + +
	Dog 3	+ +	NA	+ +
	Dog 4	+ +	+	+ +
	Dog 5	+ +	-	+ +
	Dog 6	+ + +	+ + +	NA
	Dog 7	+ +	+ + +	+
	Dog 8	+	+ + +	NA
	Dog 9	-	-	+
	Dog 10	++	++	NA
MPL	Dog 4	+	-	NA
	Dog 5	-	+	+
	Dog 6	-	NA	+
	Dog 7	+	NA	+ +
	Dog 8	+	+	+ +
	Dog 9	-	-	+

Table 3 Histopathological findings of synovial tissue extracted from CCLr and MPL. Sections were stained with H&E and graded as indicated in material and methods. (+ Mild, ++ Moderate, +++ Strong and – Not recognized)

Origin	Animal	Vascularity	Mononuclear cells infiltration	Elastic fibrosis	Fibroblasts
CCL	Dog 1	+	+	+ +	+ +
	Dog 2	++	+	+	+
	Dog 3	+ + +	+ + +	+ + +	+ + +
MPL	Dog 1	-	-	-	_
	Dog 2	-	-	+	+
	Dog 3	+	-	+	+

1.5 Discussion

In the present study, canine synoviocytes derived from CCLr and MPL of male and female dogs with different inflammatory severities were isolated, characterized and successfully identified for their multipotency. Adherent cells obtained from SM specimens of CCLr and MPL displayed typical features of MSCs, which represent major cell type in synovial cell fraction with strong expression of CD44 and CD90 surface antigens. Our result corresponds with other papers which describe the CD44 and CD90 as markers of MSCs (Dominici et al., 2006; Pei et al., 2008). Synovial tissue can be used as a therapeutic option in regenerative medicine due it's a large amount of MSCs from a small section of SM tissue. Those MSCs isolated from SM is called as SM derives stem cells (De Bari et al., 2001) or synovial mesenchymal progenitor cells (Bertram & Krawetz, 2012). The original of MSCs within the SM are from blood that penetrates synovial tissue or from BM that connects to intra-articular space (Branco De Sousa et al., 2014).

The value of synovium was further confirmed as a potential source of MSCs which carry chondrogenic differentiation ability (De Bari et al., 2001; Nishimura et al., 1999; Sakaguchi et al., 2005), by the current study with the finding of availability of chondroprogenitor cells in adult canine SM. Chondral defects have been shown to repair spontaneously in different species (Jackson et al., 2001) by a population of chondroprogenitor cells resident in cartilage (Barbero et al., 2003; Candela et al., 2014) or an exogenous population of MSCs. One of the exogenous sources of chondroprogenitor cells might be SM, which is closely associated with articular cartilage for the repair of chondral defects. Although the aptitude of differentiation of canine MSCs into bone and fat tissue has been reported previously by using bone marrow

samples, (Tharasanit et al., 2011) scarce evidence is available on canine SM-derived MSCs. In this study, differentiation capability of MSCs into adipocytes and osteocytes was clearly identified.

Synovial biopsy obtained from CCLr patients carried higher multipotency (Table 2) when compared with cellular staining strength with MPL-derived samples. There might be some other specific factors affecting these differences among those two clinical presentations, however it showed the same MSC population. The study on chemokine profiles of synovial fluid from normal, OA and RA patients clearly showed that the number of MSCs recruited by SF from rheumatoid arthritis patients differs from OA and normal donors, suggesting that chemotactic factors contribute to the attraction of progenitors from subchondral bone (Endres et al., 2010), blood and bone marrow (Branco De Sousa et al., 2014). It is still unclear whether there is an effect of chemokines on improving the potency of MSCs. Inflammatory reactions of the affected area such as vascularity, mononuclear cell infiltration and cellular hypertrophy varied between CCLr and MPL, rendering them distinguishable. The findings in our study were consistent with those of previous reports (Brandt et al., 1991; Little et al., 2014) on the histopathologic changes of dogs with ruptured cranial cruciate ligaments. At the acute stage of arthritis, different immune cells secrete cytokines and other mediators which sustain and amplify the inflammatory environment (Krenn et al., 2006). Multipotency differing with diverse inflammatory conditions of joint space would be further consistent with previous studies on human synovial-derived MSCs, when disclosed higher proliferative and chondrogenic capacities than other MSCs especially when incubated with bone morphogenetic protein 2 (Sakaguchi et al., 2005; Shirasawa et al., 2006).

Additional investigation has been done for finding the differentiation capability of OC progenitors in SM with the presence of MCS-F, RANKL and TNF-α. Above

mentioned changes of cellularity and microenvironment in inflamed SM were used as an indicator for the level of bone destruction in some studies. The degree of destruction of articular cartilage and bone correlated with the number of synovial macrophages in the inflamed thickened synovial lining and the sub-intima, predominantly at the articular margins (Mulherin et al., 1996). Synovial tissue derived from CCLr showed significantly higher expression levels of OC-specific genes and emphasized that OC precursor's niche in SM might play an important role in the development of inflammatory arthritis at knee joints of dogs.

Some of the limitations of our study are the low number of animals and subjective histologic grading of the SM specimens. To the author's knowledge, no similar studies have previously been reported to determine a priori what the sample size of the present study should be. In the present study, the assessment of chronicity (duration of clinical signs) was based on the observation of lameness by the owner. Because CCLr and MPL in dogs may be deceptive at onset and not associated with trauma, the initial lameness may have not been noticed by the owner and not documented in the records of the referring veterinarians. Even though we do not believe that such an underestimation of chronicity affected the overall results of the study, proper assessment of chronicity of CCLr and MPL is needed for expanding this study using the fundamental phenomena we found. Further, we analyzed few specific genes for evaluation of gene expression of each differentiated cell types; quantification and additional genomic analysis would have been more desirable. The use of additional cell markers is needed for future study to identify the hematopoietic cell percentage in the SM with varying inflammatory changes. Finally, we elected for less time-consuming, subjective histologic grading of tissue specimens; more objective grading and quantification would have been preferable, particularly from a statistical viewpoint.

CHAPTER 2

Chronological differential effects of pro-inflammatory cytokines on RANKL-induced osteoclast differentiation of canine bone marrow-derived macrophages

2.1 Summary

Chronic inflammation is a key mediator for local and systemic bone loss in RA patients. Metabolic activation of osteoclasts for potentiating the bone-resorbing ability requires 'biochemical fueling' from complex cellular interactions between cells of the OC lineage and mesenchymal cells and lymphocytes at the pathological condition such as RA. Cytokines play an important role in inflammatory bone destruction by upregulating the RANKL. The role of cytokines at different stages of osteoclastogenesis in dogs has yet to be elucidated. The aim of this study was to investigate the osteoclastogenic properties of inflammatory cytokines at different time-points of osteoclastogenesis. Bone marrow macrophages derived from five healthy dogs were stimulated with the M-CSF and RANKL. Inflammatory cytokines, such as IL-1β, TNF-α and IL-17 were added to the culture system of osteoclastogenesis at two time-points. The 'early' effect of each cytokine was investigated at the time of first RANKL treatment, whereas the 'late' effect was investigated 48 h after the first RANKL challenge. Osteoclast differentiation and function were assessed by cell number, area/ cell ratio by TRAP staining and quantitative PCR of CTK and MMP9 genes. In the M-CSF/RANKL culture system, TNF-α enhanced osteoclasts formation and their function at particular concentrations, regardless of temporal differences while IL-1α and IL-17 suppressed the osteoclastogenesis at early phase of the process. Furthermore, IL-1β upregulated the expression of cathepsin k and MMP9 genes responsible for OCdifferentiation and

maturation at the late phase while enhancing the OC functional genes in a dose dependent manner. In conclusion, those outcomes have been revealed, even though the rate of IL-1β and IL17–driven bone destruction in RA can be restrained by its inhibitory action on early OCP to limit the extent of inflammation, targeting IL-1β, TNF-α and IL-17A may be a promising strategy to inhibit inflammatory associated bone destruction and osteoporosis.

2.2 Introduction

Rheumatoid arthritis is a chronic autoimmune disease, ultimately presents with extensive joint destruction as a consequence of severe inflammatory process. Chronic inflammation is the key mediator for local and systemic bone loss in arthritic joints where cytokines abundantly present in the synovium (Brennan and McInnes, 2008; Matei and Matei, 2002). Composed interaction of pro-inflammatory cytokines with T and B cells plays a key role in the pathophysiology of RA (Smolen et al., 2007; Smolen and Steiner, 2013). Immune and bone cells are functionally interconnected and derived from same progenitors in the bone marrow sharing common microenvironment (Zupan et al., 2013). Well-balanced activity of OC at the healthy joint is deregulated with excessive activation of the immune mediators under the inflammatory conditions (Gao et al., 2007). Based on the current evidence, pro-inflammatory cytokines are categorized into three groups, called osteoclastogenic (IL-1, 6, 8, 11 and 17, TNF-α), anti-osteoclastogenic (IL-4, 10, 13 and 18, IFN-γ, IFN-β) and both osteoclastogenic and anti-osteoclastogenic (IL-7, 12, 23, and 6, TGF-β) (Kotake et al., 2009; Takayanagi et al., 2002). However, the theories on activity of pro-inflammatory cytokines in different stages of osteoclastogenesis are still controversial. Recently, Moon et al., 2013 observed the enhancement of osteoclastogenesis with the treatment of IL-1β, regardless of the maturation status of mouse-derived precursor cells. However, previous human study shows that early treatment of IL-1β prior to or together with RANKL strongly inhibits osteoclastogenesis of human-derived precursor cells. The explanation for strong inhibition of human osteoclastogenesis induced by IL-1β is due to suppression of RANK expression by IL-1β-induced proteolytic shedding of the M-CSF receptor, c-Fms which is essential for RANK expression (Lee at al., 2010). Further, TNF-α could stimulate the

proliferation and differentiation of OC precursors (Pfeilschifter et al., 1989; van der Pluijm et al., 1991) in addition to maturation of OC (Kitazawa et al., 1994; Lerner and Ohlin, 1993; Thomson et al., 1987). The disputes regarding the cytokine-induced osteoclastogenesis which stems from the fact that previous experiments were performed under different conditions among different species were considered in this study. However, the direct effect of IL-1β, TNF-α and IL-17 on the differentiation stages and function of OC have not been fully understood in dogs. To our knowledge, this study was the first attempt to examine the role(s) of IL-1β, TNF-α and IL-17 on OC differentiation, function and expression of OC marker genes, CTK and MMP9 using canine bone marrow-derived OCP.

2.3 Materials and Methods

2.3.1 *In vitro* osteoclastogenesis

Proximal femurs of 1-year-old, healthy beagle dogs (n = 5) were used to collect the 5 ml of bone marrow samples into 10 ml syringe containing 1 ml DMEM (Life technologies) and 1000 U/ml of heparin (Nipro, Osaka, Japan). The use of clinical samples and all samples from experimental dogs were in accordance with Hokkaido University Institutional Animal Care and Use Committee guidelines (approval number: 12-0059). The bone marrow was preceded as described previously (Wagner and Eferl, 2005; Yagi et al., 2006). Briefly, the bone-marrow derived monocyte-macrophages (BMMs) fraction was obtained by density gradients centrifugation over lymphoprep (Axis-sheild PoC AS, Oslo, Norway) to remove red blood cells. Isolated BMMs fraction (5×10^6 cells/ml) was incubated with DMEM containing penicillin/streptomycin (100 units/ml, Wako) and 10% FBS (Nichirei) for 24 hr to separate the non-adherent and adherent cells. Non-adherent cells were collected as a source of immature OC precursors, suspended in DMEM and counted. The isolated cells were then cultured in DMEM with the presence of 20 ng/ml recombinant human M-CSF on 48-wells plates (Corning Incorporated, Corning, NY, USA) at $2x10^5$ cells/well for 3 days. After 3 days, adherent cells were used as OC precursors after washing out the non-adherent cells, including lymphocytes and further cultured in the presence of 25 ng/m*l* M-CSF, 50 ng/ml recombinant human RANKL (Sigma) to generate OC. Various concentrations of canine recombinant IL-1β, TNF-α and IL17 (1, 5, 10 ng/m*l*) (Kingfisher Biotech, INC., Minnesota, USA) and RANKL were added into the osteoclastogenesis culture system at two different time-points; early cytokine treatment was performed with the first RANKL administration and late cytokine treatment was performed on day 2, when the second

RANKL treatment was administered to the osteoclast culture media (Fig. 10). On day 2, the media was replaced with fresh medium containing M-CSF, RANKL and cytokines. Selected concentrations of cytokines were within the previous proved non-cytotoxic range for bone marrow derived cells (Moon et al., 2013). Precursor cells began to fuse between 36 and 48 hr and mature osteoclasts were observed at 60 hr after RANKL stimulation. TRAP staining, RNA extraction and RT-PCR were done as explained in chapter 1.

2.3.2 Bone resorption assay

Bone marrow cells were cultured on bone resorption assay plate 48 (PG Research, Tokyo, Japan) coated with calcium phosphate (CaP-coated, Sigma-Aldrich) and followed the same cytokines treatments. The resorption pit area was analyzed with image-J software (Image J software version 1.43, National Institute of Health).

2.3.3 Statistical analysis

Relative gene expression of level of MMP9 and CTK were analyzed with the t test using SPSS statistical software (ver. 16.0; SPSS, USA) and expressed as the mean ± standard error of mean (SEM). p values < 0.05 were considered statistically significant and determined using the Bonferroni modification of ANOVA. Each data point represents the mean ± SEM of 5 samples unless otherwise indicated.

2.4 Results and Discussion

This study demonstrated that cytokines have specific characteristic osteoclastogenic properties throughout the maturation stages. Consistent with the results of previous human study, our results confirmed that the rate of IL-1β driven dog osteoclastogenesis which restrained by its inhibitory action on early osteoclasts precursors, could limit the extent of inflammation in arthritis (Lee et al., 2001). Challenging many previous reports, this study found temporal differential effect of IL-1β, determined by varying degree of osteoclastogenesis, bone resorption and mRNA expression levels of OC-related specific genes (Jimi et al., 1999; Jimi et al., 1995; Kobayashi et al., 2000; Ritchlin, 2000). At all given concentration of IL-1β, number of TRAP-positive multinucleated cells and resorbed area were decreased compared with that in the control group at early phase (Fig. 11A-F).

However, previous work has also found that IL-1β could suppress bone resorption in selective *in vivo* models (Bajayo et al., 2005; Lee et al., 2010; Vargas et al., 1996). In this context, our findings suggest that suppressive functions of IL-1β on osteoclastogenesis may become apparent and biologically important in limiting the extent of bone resorption under conditions where exposure to IL-1β precedes initial steps of differentiation in response to RANKL. But the inhibitory action of IL-1β at early phase was not enough to overcome the stimulatory effects on bone erosion which is given by other factors. Lee et al., 2010 explained that the inhibitor action of IL-1β in human due to its down regulatory activity over receptor of M-CSF, ultimately ended up with concurrent inhibition of M-CSF-induced RANK expression. Additionally, the effect of IL-1β on osteoclastogenesis is strikingly time dependent and species dependent when

considering that in human (Lee et al., 2010), murine (Moon et al., 2013) and current canine-related study.

Osteoclast differentiation, bone resorption and CTK expression were amplified with TNF-α in dose dependent manner, while keeping 10 ng/m*l* as significant concentration (p<0.05) (Fig. 11E). Remarkably, IL-17 suppressed OC functional genes, CTK (Fig. 11E) and MMP9 (p<0.05) (Fig. 11F) with all the concentrations at early phase where those genes starting to express (Takeshita et al., 2000). Bone resorption-related genes CTK and MMP9 are highly expressed in OC and play an important role in skeletal remodeling (Reponen etal., 1994). Various patterns of osteoclastogenesis were observed with supplementation of TNF-α and IL-17. At the concentration of 5 ng/ml, TNF-α markedly upregulate all functional genes (p<0.05) while increasing OC differentiation and bone resorption (Fig. 11A-E). But challenging the previous study (Kitami et al., 2010), our findings of IL-17 indicated remarkable suppression of osteoclastogenesis (p<0.05) at highest concentration (10 ng/ml) in later phase by implementing the variation on differentiation capability of cytokines in temporal manner (Fig. 12A-F). Interestingly this study was able to postulate the differentiation patterns of inflammatory cytokines at different time-points of osteoclastogenesis.

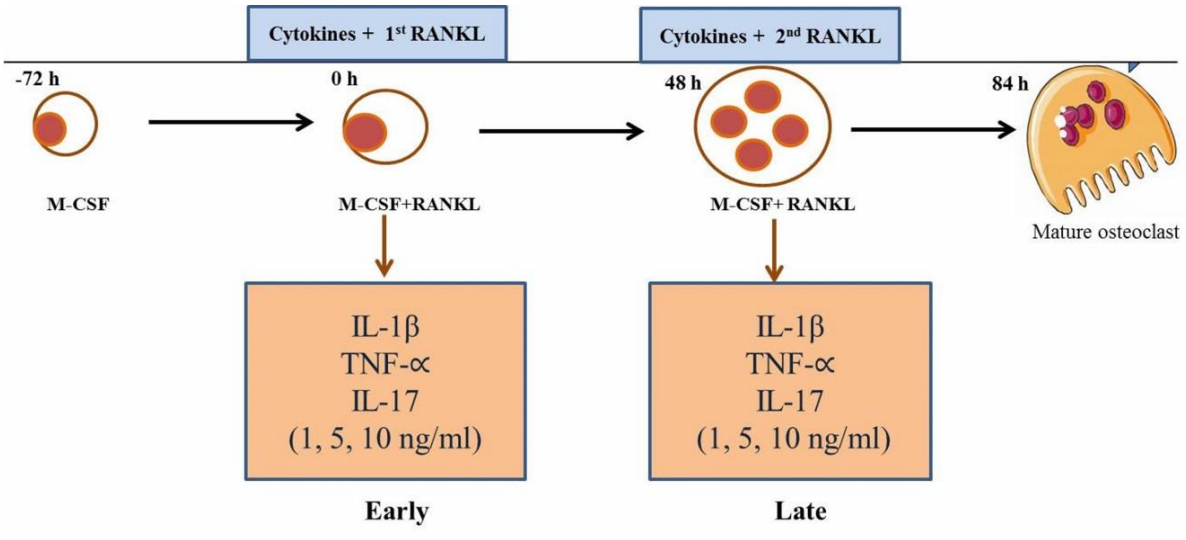

Fig. 10 Schematic description of the osteoclastogenesis process and cytokine treatments. Early and late challenges with cytokines were performed concurrently with the first RANKL stimulation (at 0 hr) and the second RANKL stimulation (after 48 hr).

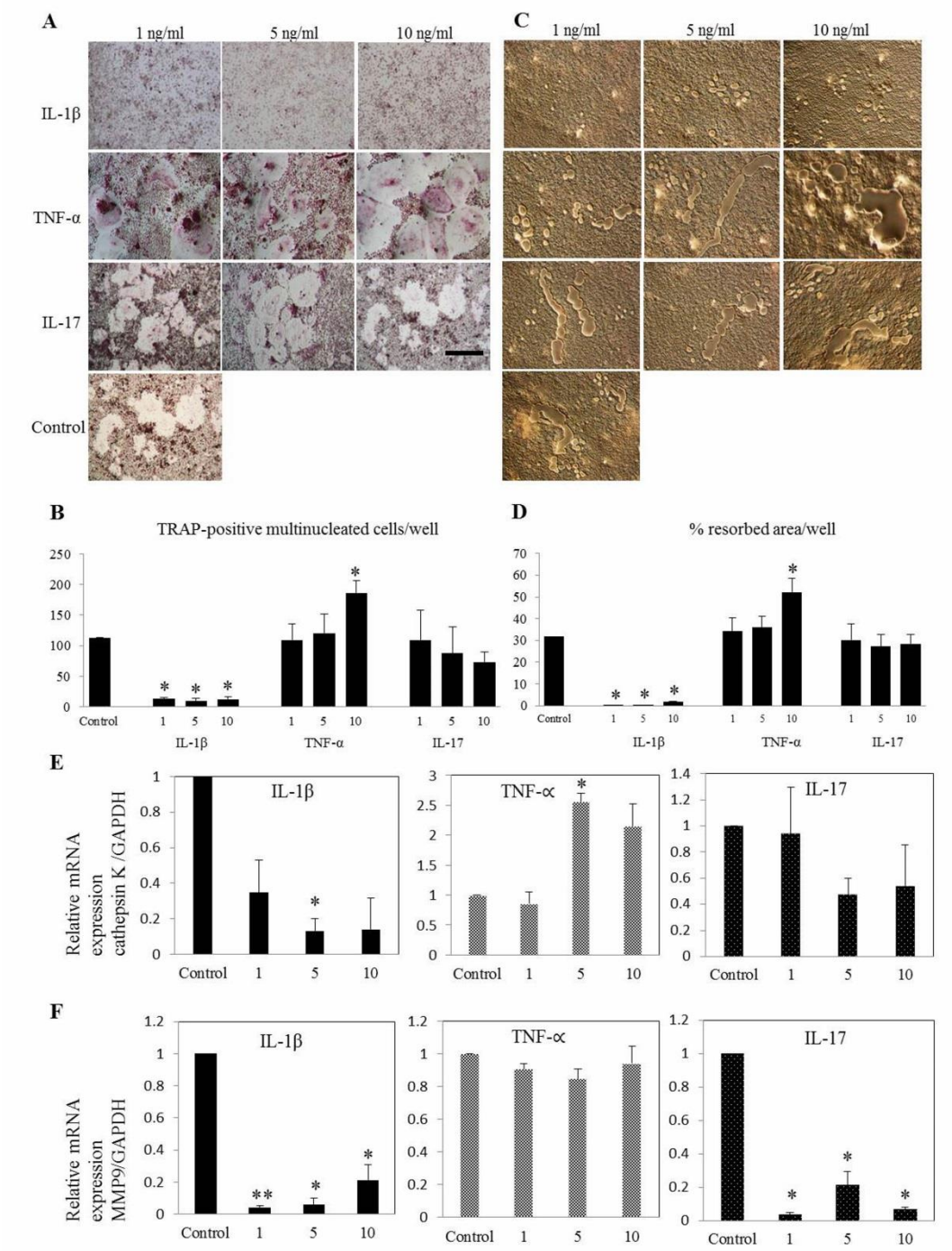

Fig. 11 Differential effect of IL-1β, TNF-α and IL-17 on osteoclast differentiation of canine bone marrow-derived macrophages (A) at early phase is shown. Early challenges with cytokines were performed concurrently with the first RANKL stimulation (at 0 hr). TNF-α increased the **B** number of OC and **C, D** area of resorption while IL-1β inhibits osteoclast formation in all concentrations. **E**, Relative mRNA expression of CTK was significantly upregulated with the presence of 5 ng/ml of TNF-α. **F**, Expression of MMP9 was significantly lower in all the treatments in early phase of maturation. Values are the means ± SEM of 5 independent experiments. *: $p<0.05$ and **: $p<0.001$ compared with control group. Scale bar = 200 μm.

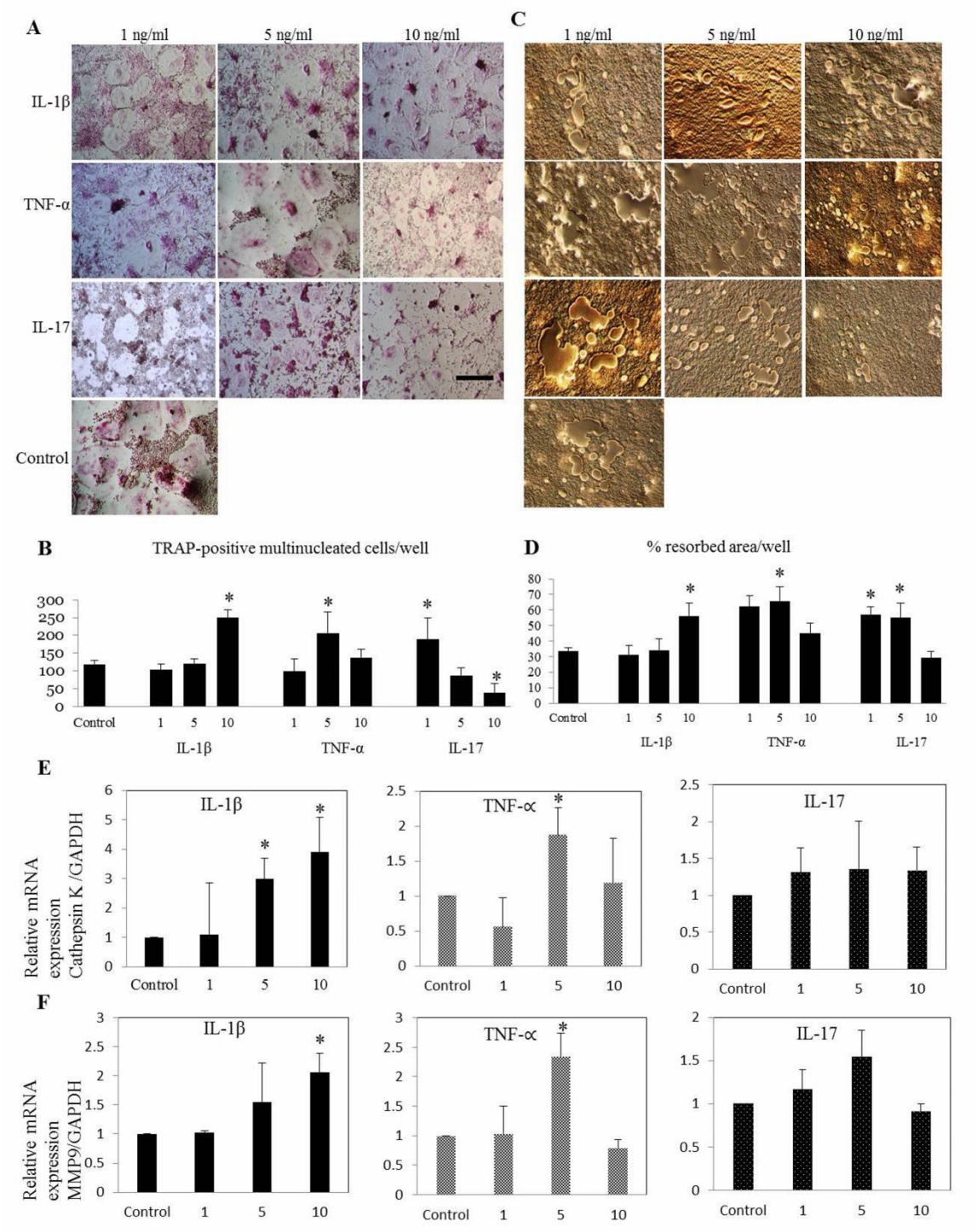

Fig. 12 Differential effect of IL-1β, TNF-α and IL-17 on osteoclast differentiation of canine bone marrow-derived macrophages (A) at late phase is shown. Late challenges with cytokines were performed concurrently with second RANKL stimulation (after 48 hr). IL-1β at 10 ng/ml and TNF-α at 5 ng/ml significantly increased the **B** number of OC and **C, D** area of bone resorption. At the late phase, 10 ng/ml of IL-17 attenuate the osteoclastogenesis. Relative mRNA expression of **E** CTK and **F** MMP9 was significantly upregulated with IL-1β and TNF-α. Values are the means ± SEM of 5 independent experiments. *: $p<0.05$ and **: $p<0.001$ compared with control group.
Scale bar = 200 μm.

CHAPTER 3

Inhibitory effects of pentosan polysulfate on formation and function of osteoclasts derived from canine bone marrow

3.1 Summary

Pentosan polysulfate was testified as a chondroprotective drug in with a detailed rationale of the disease-modifying activity. The purpose of this study was to determine the effect of this novel glycosaminoglycan over the differentiation and activation of OC derived from canine bone marrow. Isolated non adherent mononuclear cells were treated with receptor activator of RANKL and M-CSF to generate osteoclast-like multinucleated giant cells while treating PPS for 1-week by final well concentration of 0, 0.2, 1 and 5 μg/ml. Differentiation and activation of OC were monitored via tartrate-resistant acid phosphatase staining, filamentous-actin rings analysis, bone resorption assay and analyzing osteoclastogenesis-related markers such as NFATc1, c-Fos, CTK, MMP-9, AP-1 and CA II using quantitative reverse transcriptase polymerase chain reaction. The receptor activator of NF kappa B ligand-induced expression of NFATc1 and c-Fos, which are the key transcription factors for osteoclastogenesis, was reduced by treatment with PPS. Besides, disruption of the actin ring, decreased the expression mRNAs of CTK and MMP-9 both involved in bone resorption and tartrate-resistant acid phosphatase positive osteoclast number were attenuated with PPS in concentration gradient. Taken together, these results suggest inhibitory effect of PPS on OC differentiation and bone resorption by proving treatment option for osteoporosis or other bone diseases associated with excessive bone resorption and provides useful information for future pharmacokinetic studies and clinical trials *in vivo*.

3.2 Introduction

Bone homeostasis is crucial to maintain the integrity of bone functions that coordinated balance between bone resorption by OC and bone formation by chondrocytes/ OC (Corral et al., 1998; Karsenty and Wagner, 2002). Osteoclasts which originate from monocyte/macrophage family members derived from bone marrow hematopoietic precursors (Itonaga et al., 2004) are the principal multinucleate giant resorptive cells of bone which require two grave factors M-CSF and RANKL for their differentiation and maturation (Boyle et al., 2003; Kim et al., 2016; Nakamura et al., 2012). Receptor activator of NF kappa B ligand binds to its receptor, receptor activator of NF kappa B on OC precursors (Nakagawa et al., 1998), which involve the activation of NF-kB and Jun N-terminal kinase, eventually leading to the expression of AP1/ Fos, an essential regulator of osteoclast differentiation (Wagner and Matsuo, 20030. Previously reports have shown that OC precursors are found in both peripheral blood and synovial tissues of human with RA (Fujikawa et al., 1996; Itonaga et al., 2000). Osteoclast precursors which are unable to resorb bone (Yagi et al., 2005) stained positive for TRAP eventually fuse to form multinucleated mature TRAP-positive OC (Kong et al., 1999). Thus maturation and functional capability of OC while differentiation, are critical cellular process, understanding its regulation will have an important impact on the development of a new therapy to control bone loss among human and dogs.

In the past few years, the concept of DMOADs have been explored as an alternative treatment modality for OA (Altman, 2004) instead of using NSAIDs which has been frequently used for treat OA and associate with a high risk for gastrointestinal lesions with long-term uses (Wallace, 1997). Although PPS has been used for a number of years for the treatment of thrombotic and hyperlipidemic indications, it has only recently been

shown to be effective in improving the symptoms of human patients with OA (Ghosh, 1999; Ghosh et al., 2005; Kumagai et al., 2010). While the molecular mechanism of PPS action at the microenvironment of joint remains unclear, some previous reports shows that, PPS are capable in enhancing synthesis of proteoglycans such as aggrecan, which is intimately associated with resist compression throughout the extracellular matrix of articular cartilage (Takizawa et al., 2008). Hence, synovial changes in dogs with canine arthritis mimic human RA, dogs are potential useful model for studies of therapy (Schumacher et al., 1980). Recently, it has been reported that PPS can inhibit osteogenic differentiation in human bone marrow derived precursor cells while inducing chondrogenic differentiation (Ghosh et al., 2010). However, among the several previous human studies of PPS which were based on cartilage research, there was dearth of information on effect of PPS over the osteoclastogenesis, anti-resorptive capability and influence on cell signaling molecules of OC in dogs. To the best of our knowledge, present study is the first attempt to identify the interaction of PPS with *in vitro* cultured OC-derived from dog bone marrow. In this study, we examined the effect of PPS on dog OC differentiation and function stimulated by RANKL and M-CSF as an *in vitro* assay. This chapter provides useful preliminary information on the concentration of this drug and should help increase understanding and awareness of the opportunity and or limitation of its therapeutic use among dogs.

3.3 Materials and Methods

3.3.1 Differentiation of osteoclast derived from bone marrow of the dog

Proximal femur of one year old, healthy beagle dogs (n=6) were used to collect the 5 ml of bone marrow samples in to 10 ml syringe containing 1ml DMEM (Life technologies) and 1000U/ml of heparin (Nipro, Osaka, Japan). The use of clinical samples and all samples from experimental dogs was in accordance with Hokkaido University Institutional Animal Care and Use Committee guidelines (approval number: 12-0059). The bone marrow was preceded as described previously (Li et al., 2005; MacDonald et al., 1987). Briefly, the bone marrow mononuclear cell fraction was obtained by density gradients centrifugation over lymphoprep (Axis-sheild PoC AS) to remove red blood cells. Isolated BMMs cell fraction (5×10^6 cells/ml) was incubated with DMEM containing penicillin/streptomycin (100 units/ml, Wako) and 10% heat-inactivated FBS for 24 h to separate the non-adherent and adherent cells. Non-adherent was collected as a source of immature OC precursors, suspended in DMEM, counted, seeded on 48-well plates (Corning, New York, USA) at $2x10^5$ cells/well, and cultured in DMEM with the presence of 20 ng/ml recombinant human M-CSF (Invitrogen, Maryland, USA) for 3 days. After 3 days, adherent cells were used as OCP after washing out the non-adherent cells, including lymphocytes and further cultured in the presence of 25 ng/ml M-CSF, 50 ng/ml recombinant human RANKL (Sigma) to generate OC-like multinucleated giant cells and treated with PPS (Cartrophen Vet-Biopharm) for 1-week by final well concentration of 0, 0.2, 1 and 5 μg/ml, those are within the previous proved non-cytotoxic range for bone marrow derived cells (Ghosh et al., 2010). Triplicate cultures of each PPS (100mg/ml) concentration were used and cultures were maintained

with media changes containing the same PPS concentration in every 48 hours. TRAP staining was done as described in chapter 1.

3.3.2 Pit formation assay

Bone marrow cells were cultured on bone resorption assay plate 48 (PG Research, Tokyo, Japan) which was coated with calcium phosphate (CaP-coated) to generate mature OC as described above. Seven days after the culture with PPS at various concentrations in the presence of M-CSF (25 ng/ml) and RANKL (100 ng/ml), the CaP-coated plate was treated with 5% sodium hypochlorite (Sigma-Aldrich, St Louis, Missouri, USA) for 5 minutes according to the manufacturer's instructions. The resorption pit area was analyzed with Image-J software (Image J software version 1.43).

3.3.3 The actin ring formation assay

The actin ring formation assay was performed as described previously (Hurst et al., 2004). Briefly, BMMs cultured with M-CSF, RANKL and various concentrations of PPS for 7 days, washed with PBS and fixed with 4% paraformaldehyde (Wako) in PBS on ice for 20 minutes. Osteoclasts were detergent-permeabilized with 0.2% Triton X-100 (ICN Biomedicals, Germany) in PBS for 10 minutes, washed and blocked in 10% normal goat serum (Sigma) in PBS for 1 hour. The cells were incubated with primary rabbit anti-F actin polyclonal antibody (Bioss Inc., Woburn, MA, USA) (1:100 dilution) for 1 hour in PBS with 1% normal goat serum, washing three times with PBS, incubating for 1 hour with fluorescein isothiocyanate (FITC)-conjugated goat anti-rabbit antibody (Sigma) (1:100 dilution) in PBS with 1% normal goat serum, washing three times with PBS, and finally mounting with aqueous mounting medium. 4′,6-diamidino-2-phenylindole (DAPI) (Thermo Fisher Scientific, Eugene, OR, USA) was used to stain the nucleus and

mount the slides according to manufacturer's instructions. The images were observed under a laser scanning confocal microscope (Zeiss, Urbana, IL, USA).

3.3.4 Immunocytochemical detection of localization of PPS with actively transcribed gene

Osteoclasts resulting from canine bone marrow cells (2×10^5 cells) were cultured in 8-well culture slide (Iwaki, Tokyo, Japan) in 400 µl of DMEM, 10% FBS with osteoclasts differentiation factors. Cells were incubated with 10 µg/ml of TRITC-labeled PPS (Arthropharm, Bondi junction, New South Wales, Australia) for 24 hours. After fixation and blocking, cells were incubated with primary anti-human c-Jun (HT-9) rabbit polyclonal antibody (Santa Cruz Biotechnology, Dallas, TX, USA) (1:100 dilution) in 1% normal goat serum followed by incubation with FITC-conjugated goat anti-rabbit antibody (Sigma) (1:100 dilution) in 1% normal goat serum and observed under a laser scanning confocal microscope.

3.3.5 mRNA isolation and RT-PCR

Total RNA from cells was extracted using RNeasy Mini Kit (QIAGEN) according to the manufacture's protocol. Total RNA was quantified by spectrophotometry at 260 nm. RNA with a 260/280 nm ratio in the range 1.8–2.0 was considered high quality and then transcribed into cDNA with M-MLV RT kit (Takara Bio) according to manufacturer's recommended procedures. One microgram of total RNA derived was reverse-transcribed into cDNA with random hexamers. PCR conditions were as follows: denaturation at 95 ^{o}C for 30 seconds, annealing temperature for 1 minute, extension at 72 ^{o}C for 1 minute for 30 cycles, and final extension at 72 ^{o}C for 7 minutes. PCR products were separated

on 1.5% agarose gel (BM Equipment, Tokyo, Japan) and stained with ethidium bromide (Nippon Gene, Tokyo, Japan).

3.3.6 Real-time PCR

Quantitative real-time PCR analysis was performed with KAPA SYBR® FAST qPCR kit (KAPA). The amount of 2 μl of cDNA template was added to each 10 μl of premixture with specific primers (Table 4).

3.3.7 Statistical analysis

Statistical analyses were performed using SPSS software (SPSS software ver. 07 for Windows; SPSS Inc.). Relative gene expression of OC specific genes was represented as the means ± SEM. An appropriate post-hoc test was used to analyze the difference. Then comparison between groups was made by one-way analysis of variance, statistical significances were achieved when $p < 0.05$.

3.4 Results

The effect of different concentration of PPS on OC differentiation from BMMs stimulated with RANKL and M-CSF was evaluated. The number of TRAP-positive multinuclear cells (≥3 nuclei) generated in 48 well plate were reduced with the administration of PPS in dose dependent manner. Significant reduction of TRAP-positive multinuclear cell number at the concentration of 1 and 5 µg/ml PPS ($p< 0.05$) was noted (Fig. 13A, B). Osteoclast specific genes, CAII, CTK and MMP-9 expression was analysis after treatment of PPS in the concentration of 0.2, 1, 5 µg/ml. These specific genes were attenuated by the treatment with PPS dose-dependently (Fig. 13C, D, E). Furthermore, significant suppression of CTK and MMP-9 were observed ($p<0.05$) at 1, 5 µg/ml concentrations.

Effect of PPS on bone resorption was assessed with OC generated from 3 dogs. Cells were plated on CaP-coated plates and stimulated with M-CSF and RANKL in the presence or absence of PPS. Cells stimulated with M-CSF and RANKL formed a number of pits (Fig. 14A, B), suggesting that the bone resorption activity of RANKL-treated cells made them into functionally active state resembling OC. Treatment with 10 µg/ml PPS significantly reduced the formation of resorption pits in number and in overall area compared with treatment with M-CSF and RANKL alone. In the presence of RANKL exposure, BMMs can differentiate into mature OC and form distinct actin-ring structures (Figure 14C, D). However, PPS significantly reduced the size and the number of actin-ring structures in a dose-dependent manner, suggesting that PPS suppressed the formation of actin-rings in matured OC.

Canine OCLs were treated with fluorescently labelled (red) pentosan polysulfate (TRITC-PPS), then fixed in formalin and fluorescently stained for genetic DNA (blue)

and for c-Jun (green) which is one of the key components of AP-1 transcription factor (Yagi et al., 2005).

Invasion of PPS in to the cytoplasm and nucleus of mature osteoclast was visualized (Fig. 15A). The yellow to orange in the overlay image indicates that PPS and c-Jun proteins are in the same location (Fig. 15B). Pentosan inhibits NFATc1 and c-Fos expression and decreases AP-1 activation. The effect of PPS on the expression of NFATc1, c-Fos and AP-1 in the mature OC was examined and compared with the OC cells treated with the presence and absence of PPS. The cells with M-CSF, RANKL induced high level of expression of NFATc1, c-Fos and AP-1 mRNA (Fig. 15D, E, F). Treatment with PPS (5 μg/ml) significantly decreased ($p<0.05$) mRNA expression level of NFATc1, c-Fos and AP-1. As shown in Figure 15C, semi quantitative RT-PCR was correlated with quantitative PCR.

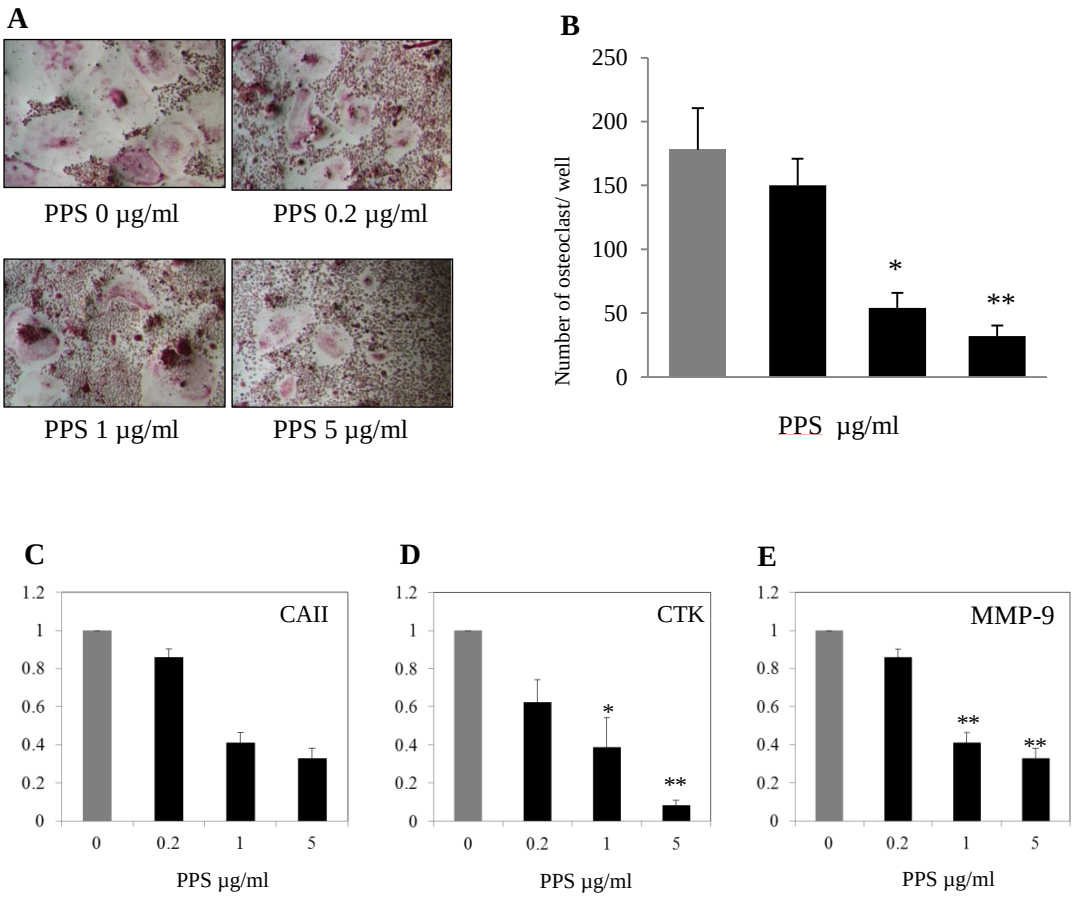

Fig. 13 Shows inhibitory effect of PPS on canine OC differentiation. A, The cells were treated with various concentration of PPS followed by M-CSF (20 ng/ml) and RANKL (50 ng/ml) for 7 days. The cells were stained for TRAP stain and **B** TRAP-positive cells (≥3 nuclei) were counted. Scale bar- 100µm. Bar graphs show the concentration effects of PPS on mRNA expression levels of **C** carbonic anhydrase II (CA II), **D** CTK and **E** MMP-9 determined by real-time PCR and results were normalized to the expression of GAPDH. Data are representative of five independent experiments and expressed as means ± SE. Means with * are significantly different from 0 µg/ml of PPS (*: $p < 0.05$, **: $p < 0.01$).

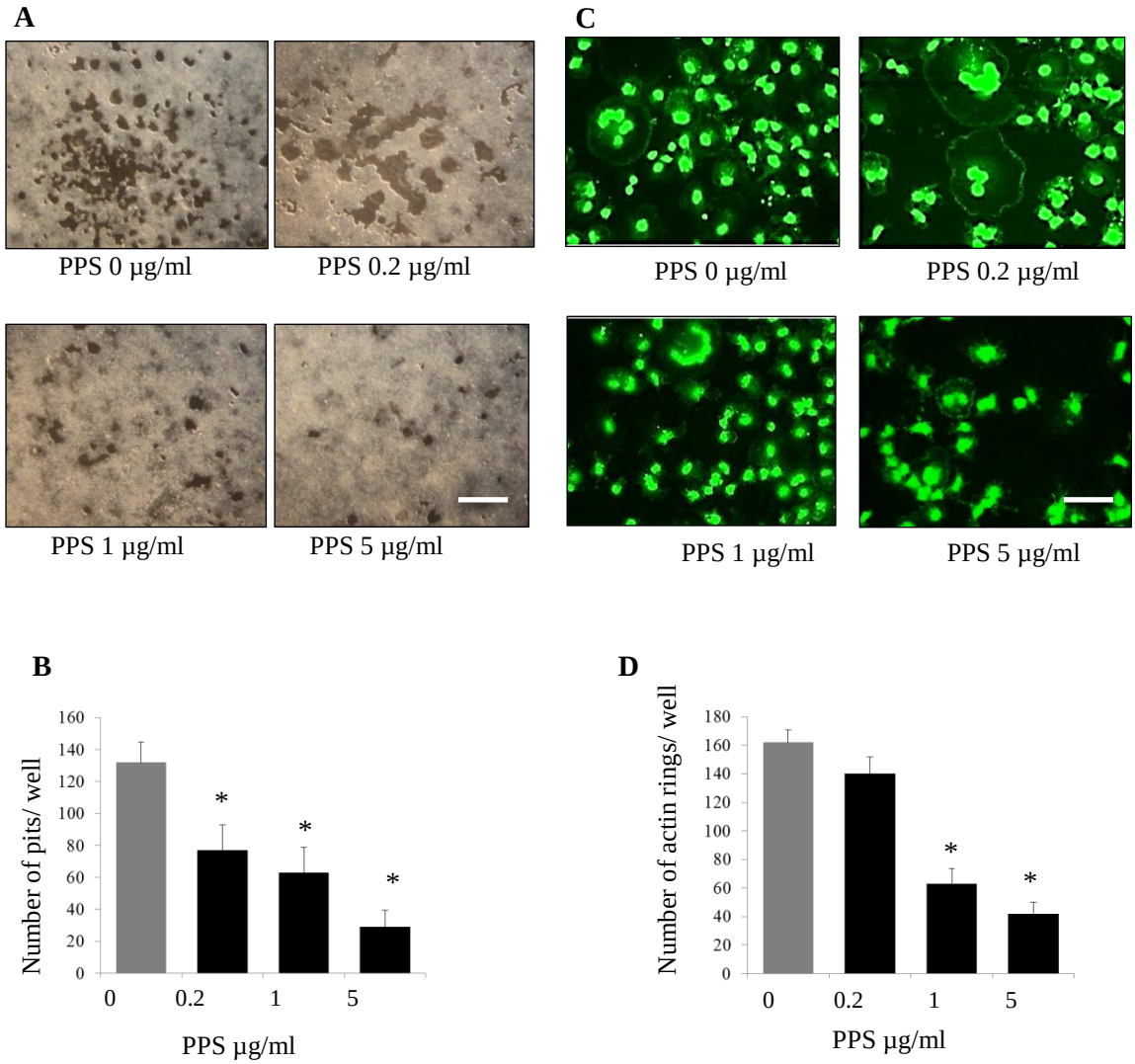

Fig. 14 Pentosan inhibits bone resorption and actin ring formation by concentration gradient. Canine BMMs, cultured with M-CSF (25 ng/ml) and RANKL (50 ng/ml) for 7 days with or without indicated doses of PPS. **A**, The cells were washed and the resorption pits were counted. **B**, The numbers of pits was analyzed with Image-J software. **C**, Cells were fixed, stained for F-actin formation (top) and **D** osteoclasts with actin ring were counted (bottom). Scale bar- 200µm. Column indicates means ± SE of three experiments performed in triplicate. Means with * are significantly different from 0 µg/ml of PPS (*$p < 0.05$).

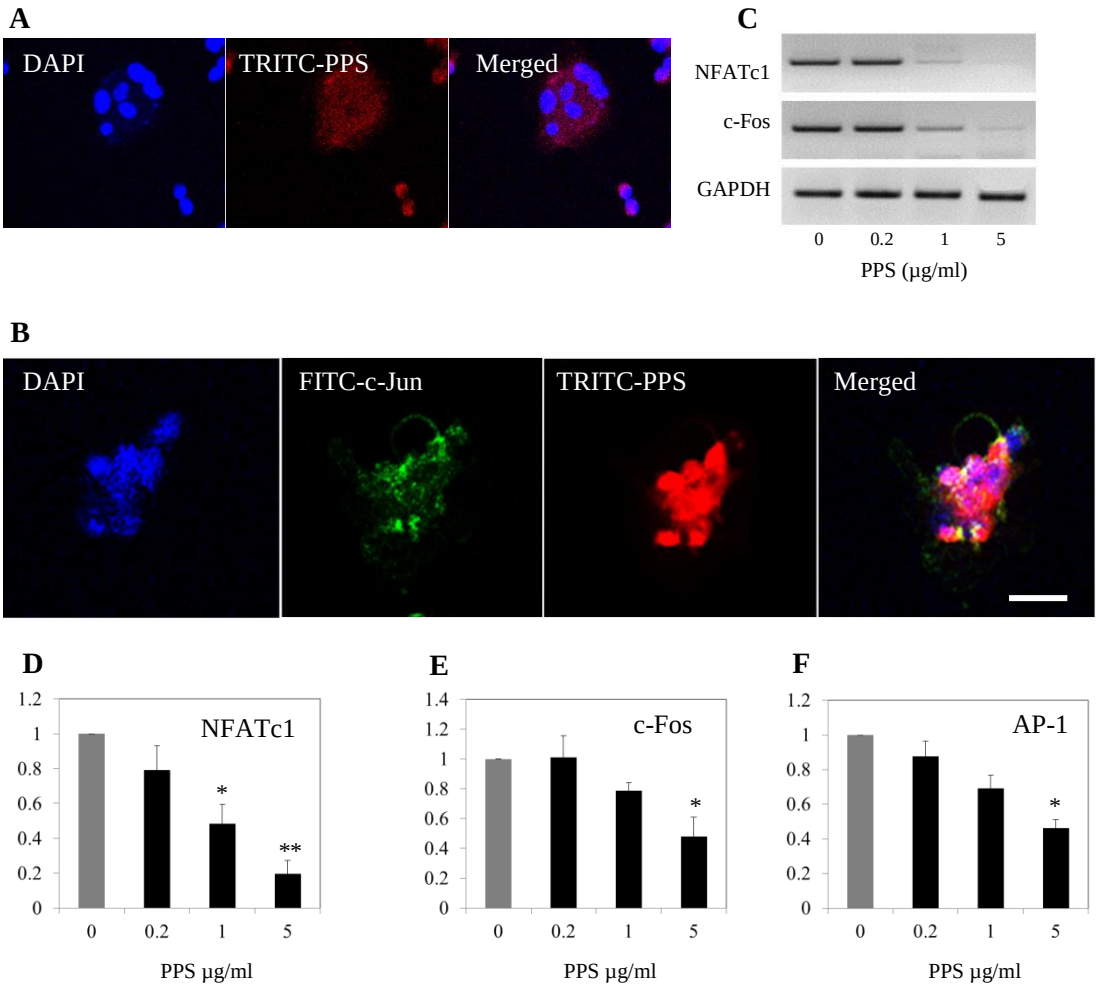

Fig. 15 Inhibitory and co-localization patterns of PPS with actively transcribed genes. Osteoclast differentiated from canine bone marrow with supplement of M-CSF (25 ng/ml) RANKL (50 ng/ml) together with absence and presence of PPS (0.2, 1, 5 μg/ml) for 7 days was done. **A**, Confocal microscopic images of invasion of TRITC-labeled PPS in to OC and **B** localization with c-Jun (subunit of AP-1 transcription complex) are shown. The orange in the overlay image indicates that PPS and gene activation proteins c-Jun (green) are in the same location. Nuclei were stained with 4,6-diamidino-2-phenylindole dye (DAPI). Scale bar- 100μm. **C**, Attenuation effect of PPS on master regulators of osteoclastogenesis (NFATc1, c-Fos) by dose dependent pattern are shown. **D**, **E** and **F**, Relative mRNA expression of NFATc1, c-Fos and AP-1 according to the PPS concentration gradient was significantly attenuated at 5 μg/ml. Data expressed as mean ± SE for each PPS concentration after normalizing for the expression of the GAPDH. Means with * are significantly different from 0 μg/mL of PPS (*: $p < 0.05$, **: $p < 0.01$).

Table 4 Primes used to polymerize the osteoclast-specific function genes

Target gene	Sense and anti-sense (5-3)	Annealing temperature(^{o}C)	Product (bp)
Carbonic anhydrase II	AAGGAGCCCATCAGCGTTAG	59.82	104
	GGGCGCCAGTTATCCATCAT	60.25	
NFATc1	CACAGGCAAGACTGTCTCCA	56.9	176
	TCCTCCCAATGTCTGTCTCC	67.9	
MMP9	GGCAAATTCCAGACCTTTGA	56.4	166
	TACACGCGAGTGAAGGTGAG	53.4	
c-Fos	GTCCGTACAGACCACAGACC	59.76	192
	CGCTCCACTTCATTGTGCTG	59.83	
RANK	CCCTGGACCAACTGTAGCAT	58.7	239
	ACCCAGTGCCACAAATTAGC	55.9	
Cathepsin K	ACCCATATGTGGGACAGGAT	57.79	169
	TGGAAAGAGGTCAGGCTTGC	60.25	
Activator protein-1	TCTACGACGATGCCCTCAAC	59.56	159
	TGAGCAGGTCCGAGTTCTTG	59.65	
GAPDH	CTGAACGGGAAGCTCACTGG	54.92	129
	CGATGCCTGCTTCACTACCT	54.03	

3.5 Discussion

In the present study, PPS exerted an inhibitory effect on canine osteoclastogenesis through the key transcription factors such as NFATc1, c-Fos and osteoclastogenesis-related other markers were also noted and colocalization with actively transcribed gene was visualized. To further study the effects of PPS on osteoclastogenesis, we examined whether PPS affected RANKL-induced OC function by bone resorption assays and actin formation. The results suggested that PPS suppressed RANKL-induced bone resorption activity and formation of actin-rings of matured OC. The stimulation of M-CSF and RANKL make mature OC result in resorption lacunae, pit formation and actin ring formation (Jun et al., 2012) which is a prerequisite for OC bone resorption and is the most obvious character of mature osteoclast during osteoclastogenesis (Hsu et al., 1999). Thus, OC play central role in pathologic bone destruction, manipulation of their differentiation and function by PPS might be a promising therapeutic strategy to treat bone disorders.

In this study, the noted inhibition of OC formation and TRAP activity indicated that PPS exerts an inhibitory effect on osteoclastogenesis and significantly reduction of density of pits by treatment, suggests that PPS exerted an inhibitory effect on mature OC function. The commonly used phenotype marker, TRAP is expressed particularly in OC and positive for TRAP stain after pre-OC cells differentiation with the supplement of RANKL (Jun et al., 2012). Detection of TRAP-positive cell formation is a renowned method of determining osteoclast formation and function (Tanabe et al., 2005; Tanaka et al., 2006).

In our study, PPS significantly suppressed the NFATc1 up-regulation in OC normally seen with RANKL treatment. In previous knock-out experiments has been

demonstrated that NFATc1 (Grigoriadis et al., 1994; Zhao et al., 2010) and c-Fos are an important transcription factors for RANKL-mediated OC differentiation, fusion, and activation (Matsuo et al., 2004). In addition, previous reports demonstrated that NFATc1 is not induced by RANKL stimulation in OC lacking c-Fos (Matsuo et al., 2004). Further, NFATc1 is the master regulator of osteoclastogenesis that is regulated by the AP-1 complex (Yagi et al., 2006). Dimeric transcription factor AP-1 is composed of members of the Jun and Fos protein family (Wagner and Eferl, 2005) and has a massive impact on OC differentiation and production of soluble mediators of bone erosion (Zenz et al., 2008).

Intracellular co-localization and interaction of PPS with c-Jun transcriptional factor was observed in this study by immunofluorescence assay emphasizing that the site of action of drug of interest. Thus, c-Fos up regulation is needed for NFATc1 induction (Ghayor et al., 2011) it is potential that the suppression of NFATc1 by PPS is the consequence of the down-regulation of c-Fos, with the subsequent down-regulation of AP-1 activity and attenuation of osteoclast–specific gene expression required for efficient OC differentiation and bone resorption. Previous reports also show that PPS possesses the ability to promote mesenchymal precursor cell proliferation and chondrogenic differentiation while suppressing osteogenic expression and bone formation (Ghosh et al., 2010).

Outcome of the present study confirmed that the inhibitory effect of PPS on canine OC differentiation and function, while additional investigations will be required to clarify the mechanism of action of PPS on OC in more detail. Based on the finding of current study, the effect of PPS on transcriptional factors, specific genes expression and cytoskeletal organization, further extension the study up to detailed work on gauging specific binding affinity of PPS with specific protein at nuclear, sub nuclear domain or

nuclear speckles would be much awarded the PPS as therapeutic perspective. Although the impact of PPS on cell signaling pathways of chondrocytes were well-recognized, invasion in to the osteoclast and its intracellular reactions, competence of osteoclastogenesis from stem cells and effect on functioning structural formation (actin ring) and transcriptional factors have not been considered until probing by this study. To our knowledge, this is the first study on dog's bone marrow derived osteoclast to demonstrate that the inhibitory effect of PPS through modulating the AP-1 and NFATc1 transcription factors and inhibits osteoclast function by reducing MMP-9 and CTK expression and disrupting bone resorption.

CHAPTER 4

Anti-arthritic effect of pentosan polysulfate in rats with collagen-induced arthritis

4.1 Summary

This study evaluated the anti-arthritic and anti-inflammatory activities of PPS, using a collagen-induced arthritis (CIA) model in rats. Model of arthritis was developed in Sprague Dawley rats by intradermal injection of bovine type II collagen emulsified with incomplete Freund's adjuvant. The rats were randomly divided into four groups: normal control, arthritic control, arthritic rats treated with PPS (at dose level 20 µg/g) and arthritic rats treated with meloxicam (2 µg/g). The treatment was continued daily until the day 30. Arthritic profiles based on clinical score, ankle size, radiography, and histological changes in joints were quantified. Concentration of cartilage oligomeric matrix protein (COMP) and tartrate-resistant acid phosphatase 5b (TRACP-5b) in synovial fluid and gene expression level of CTK, TRAP, IL-1β, and TNF-α in synovial membrane were measured. Daily administration of PPS to the arthritic rats significantly decreased the severity of arthritis by effectively suppressing the symptoms of arthritis and improving the functional recovery based on clinical score and histopathological evidence. Intriguingly, identical downregulation pattern of arthritis profiles, biological markers as well as relative mRNA levels of osteoclast markers and cytokines were monitored in CIA rats treated with PPS. In conclusion, PPS exerted anti-arthritic effects through regulating the clinical, histopathological and biological parameters. These results suggest that PPS is an effective candidate for therapeutic compounds of inflammatory arthritis by providing a cost-effective and safe alternative to existing disease-modifying osteoarthritis drugs.

4.2 Introduction

Rheumatoid arthritis (RA) is a chronic systemic autoimmune disease of unknown etiology. Inflammatory synovitis, neovascularization and pannus formation resulting joint destruction are major pathological outcomes of RA (Scott at al., 2010; Leonavičienė et al., 2008). Characterized by systemic involvement, RA affects the peripheral joints and causes chronic progressive inflammatory destruction starting at synovial membrane, cartilage and subchondral bone (Colmegna et al., 2012). Therapeutic studies on RA have shifted from symptomatic treatment to controlling the disease process together with obliteration of inflammation (Colmegna et al., 2012). The combination of therapies involving anti-inflammatory and structure-sparing effect for chronic forms of inflammatory arthropathy are interrelated since a potent anti-inflammatory approach also averts structural damage from the disease (Schett et al., 2008).

Although NSAID are used commonly to ease the symptoms of RA and OA, data on the potential of preserving cartilage and bone remains contentious. Therefore research has been focused on studying compounds which are capable of decreasing the inflammation while conserving structural silhouettes. This has yielded the creative approach to explore therapies which are termed as DMOAD or chondroprotective treatments due to their ability of preventing loss or encouraging the regrowth or healing of damaged articular cartilage (Blanco and Ruiz-Romero, 2013).

Previous studies on PPS have shown that this novel glycosaminoglycan is effective at promoting fibrinolysis, reducing joint inflammation, stimulating hyaluronan synthesis by synovial fibroblasts, stimulating proteoglycan synthesis by chondrocytes and downregulating matrix metallopeptidase-13 production at the gene promotor level

(Ghosh, 1999; Ghosh and Cheras, 2001; Andrews et al., 1983). Currently, PPS has been used for treating osteoarthritis in both veterinary and human practice with proven efficacy in experimental model (Ghosh, 1999; Burkhardt and Ghosh, 1987; Ghosh et al., 2005; Edelman et al., 1996; Ghosh et al., 1992; Smith et al., 1994). However, neither the antiarthritic activity of PPS nor its effect on inflammation-related biomarkers had been adequately investigated through the arthritis and histology profiles in RA animal models.

The aim of the present study was to evaluate the efficacy of PPS through clinical and histopathological outcomes compared with those in potential arthritic biological markers. To further this investigation, we developed the well-established rat CIA rat model which is able to closely reflect major features of human RA and used to extensively evaluate novel form of therapies (Joe and Wilder, 1999; Myers et al., 1997). Biochemical markers of cartilage and bone turnover, COMP and TRACP-5b are also receiving increasing attention (Karsdal et al., 2009) and have been applied to the current study to evaluate the degree of inflammation, damage and therapeutic effect. One NSAID, meloxicam, which is used widely to control symptoms of RA, was incorporated parallel to PPS in this study.

Using CIA rat model, efficacy of subcutaneously administered PPS was evaluated for disease progression, paw swelling and quantitative histopathological assessment, as well as inflammation-related markers in SF and its lining.

4.3 Materials and Methods

4.3.1 Animals

All experiments were carried out with female 8 weeks old Sprague Dawley (SD) rats (n=22) (body weight 191±3.8 g) purchased from Shimizu Laboratory Supply Co. (Kyoto, Japan). The rats were housed (2-3 per cage) in a temperature-controlled (20±2°C) and lit (lights on 08:00–20:00h) room. Food (Nosan Cooperation, Yokohama, Japan) and water were freely available. This experiment was carried out in accordance with the guidelines for animal experimentation of the Graduate School of Veterinary Medicine, Hokkaido University (approval No 14-0166/14050).

4.3.2 Induction of CIA

After acclimatization for approximately 1 week, 1.2 ml of emulation was administered, comprising 0.8 mg of bovine type II collagen (dissolved in 0.05 M acetic acid, Chondrex, Inc., Redmond, WA, USA) and incomplete Freund's adjuvant (Chondrex, Inc.) containing 0.4 mg of synthetic adjuvant N-acetylmuramyl-L-alanyl-D-isoglutamine (MDP, Chondrex, Inc.). The emulsion was injected as eight intradermal injections on the back and two injections to the base of the tail. The booster injection was given on 7 and 14 days after initial immunization.

4.3.3 Animal groups

Rats (n=22) were randomly allocated to four groups after immunization and received normal saline only for control CIA group (n=6) or PPS in saline administered daily as subcutaneous at a dose of 20 µg/g body weight (n=6) or meloxicam at a dose of 2 µg/g body weight (n=6) over the study period starting from day 0. Normal saline was

administered to normal healthy group (n=4) at the time of immunization of other three groups. This schedule is based on preliminary results showing that arthritis almost always developed by day 11 when the above protocol was used (Koga et al., 1980). Dose of PPS was determined by referring previous studies (Smith et al., 1999). Necropsy were performed on day 30 under general anesthesia by using isoflurane and euthanized by cervical dislocation following carbon dioxide (CO_2).

4.3.4 Severity of arthritis

Incident of CIA was considered when swelling was observed in at least one digit or paw. The severity of arthritis was graded in each paw according to the previous study (Jasemian et al., 2011). Briefly; grade 0= normal, 0.5= light redness of ankle or digits, 1= mild, but definite redness and swelling of the ankle or wrist, or apparent redness and swelling limited individual digits, regardless of the number of affected digits, 2= moderate redness and swelling of ankle, 3= severe redness and swelling of the entire paw including digits, more than two joints involved, 4= maximally inflamed limb with involvement of multiple joints. Each hind foot was scored (score left, score right), and a Score Index was calculated (SI = score left + score right). Further, skin temperature pattern (local inflammation response in hind feet) of the rats were visualized by infrared video camera (FLIR i3, FLIR systems Estonia, Estonia) while animals were under anesthesia with isoflurane. The body weights of the rats were measured from day-0 along with clinical scores. Animal were observed daily for the following: lameness, loss of body condition, pain, swelling, abscessation, fistula formation, infection and ulceration at or near the injection sites.

4.3.5 Evaluation of paw inflammation

Paw inflammation was quantified based on paw swelling and histological change. Edema of the hind foot measured by digital caliper (A & D Company Ltd., Tokyo, Japan), calculating the cross sectional area (in mm^2) of the paw and ankle of each hind foot (Paw: Ap, Ankle: Aa). Each of these areas was normalized to the same hind foot measured before the onset of treatment (Anormal p, Anormal a) and an Edema Index (EI) was calculated (Ap/ Anormal p, Aa/ Anormal a). The overall EI was determined by taking the average of the sum of EIleft and EIright (EI = (EIleft + EIright)/2). To calculate the area of the cross section (elliptical shape) of the paw and ankle two measurements were made for each section; paw: from side-to-side (a) and from top-to-bottom (b); ankle: from side-to-side (a) and from front to-back (b) at a 45° angle (Earp et al., 2008). The ellipse area was calculated by: Area= π. (a/2). (b/2). Paw volume was measured on days 0, 4, 8, 12, 18, 21, 26, 28 and 30.

On day 30, rats were euthanized by asphyxiation in CO_2 and the right hind limb of all the rats was fixed in 10% formaldehyde. Subsequently, the specimens were placed in formic acid containing decalcifying solution (Herbeta Arzneimittel, Berlin, Germany) for 1 week at 60°C. The decalcified hind legs were embedded in paraffin. Thereafter, 4-µm thick histological sections were cut and stained with H&E and safranin-O fast green. Comprehensive histologic scoring system with some modifications was used for grade the inflammatory severity of CIA rats (Brenner et al., 2005b). Briefly, tibiotalar, taluscalcaneal and midfoot joints were histologically scored for selected parameters as demonstrating in Table 4. Osteoclasts were quantified according to the following score: 0 = normal, 1 = few osteoclasts (5% of affected bone surface), 2 = some osteoclasts (5-

25% of affected bone surface), 3 = many osteoclasts (30-50% of affected bone surface), 4 = abundant osteoclast (>50% of affected bone surface) (Schett et al., 2009).

4.3.6 Synovial membrane analysis

Synovial membrane was collected at the end of the experiments. Total RNA from cells was extracted using RNeasy Mini Kit (QIAGEN, Germantown, Maryland, USA) according to the manufacture's protocol. Total RNA was quantified by spectrophotometry at 260 nm. RNA with a 260/280 nm ratio in the range 1.8–2.0 was considered high quality and then transcribed into cDNA with M-MLV RT kit (Takara Bio, Tokyo, Japan) according to manufacturer's recommended procedures. One microgram of total RNA derived was reverse-transcribed into cDNA with random hexamers. Cathespin K, TRAP, IL-1β and TNF-α primers (Table 5) were used and PCR conditions were as follows: denaturation at 95 ^{o}C for 30 seconds, annealing temperature for 1 min, extension at 72 ^{o}C for 1 min for 30 cycles, and final extension at 72 ^{o}C for 7 min. PCR products were separated on 1.5% agarose gel (BM Equipment, Tokyo, Japan) and stained with ethidium bromide (Nippon Gene, Tokyo, Japan).

4.3.7 Synovial fluid analysis for biologic markers by ELISA

Synovial fluid was collected at the end of the experiments. Biologic markers, COMP and TRACP-5b were assessed in synovial fluid by using MBS009757, MBS704438 rat ELISA kit (MyBiosource Inc., San Diego, CA, USA) according to the manufacturers' protocols. All assays were performed in triplicate. The overall procedures followed the manufacturer's instructions except for the following modifications: All samples were diluted with 1× phosphate buffered saline (PBS) before adding to the wells. No color-

giving reagents in the kit were used. The detection range of the COMP assay was 31.2 - 1000 ng/ml and TRACP-5b was 0.312 – 20 mlU/ml.

4.3.8 Statistical analysis

Data were analyzed using Statistical Package for the Social Sciences v.16 (SPSS inc., Chicago, IL, USA). Statistical significant of qRT-PCR results was determined by one-way analysis of variance (ANOVA) followed by Bonferroni post hoc test. ELISA data was analyzed using GraphPad Prism v.7.03 software (San Diego, CA, USA). Non-normally distributed data were analyzed using the Kruksal-Wallis test followed by the Mann-Whitney tests to compare two groups. Bonferroni corrections were applied for multiple comparisons. p-values were adjusted to a given control group for all comparisons and considered significant when alpha < 0.05 unless otherwise stated.

4.4 Results

4.4.1 The incidence and severity of arthritis between treatment groups

The macroscopic signs of severe arthritis from day 15 including swelling, redness, deformity and ankylosis in hind paws and ankle joints were observed. The hind paw of normal rats showed significant difference from the hind paw of rats from the vehicle group, whereas arthritic rats treated with PPS and meloxicam showed only redness and swelling (Fig. 16A). The sign of arthritis started from day 9 of post-collagen immunization with slight swelling and redness, reaching a significant level ($p<0.05$) at day 15 and maintaining its maximum clinical score until day 30 in rats of the vehicle group (Fig. 16B). On day 30, a significant reduction in the arthritis score was still observed in PPS and meloxicam treated rats with CIA (mean scores- 2.33 and 0.88, respectively), compared with that in arthritic rats (Table 6). Furthermore, a 100% incidence of CIA was observed by day 15 in the vehicle group, whereas 33.3% and 16.7% were seen among PPS and meloxicam by day 18 respectively (Table 6 and Fig. 16B). Thermographic color distribution pattern clearly indicated the variability of body surface temperature between rats from the four groups (Fig. 17A). Further, joint degradation of rats in vehicle groups was seen markedly in necropsy compared to that in rats from the control. There were mild pathological changes of joint components in rats from PPS and meloxicam groups (Fig. 17B). There was no macroscopic evidence of either hind paw erythema or edema in normal control rats. Calculated edema index was not progressively increased from day 21 in PPS and meloxicam groups ($p<0.05$) (Fig. 17C).

4.4.2 Effect of PPS on body weight

The rate and the absolute gain in body weight were comparable between SD rats from normal, vehicle, PPS and meloxicam groups at the first week. Beginning on day 14, the collagen-challenged rats gained less weight than the normal rats and this trend continue until day 30. Arthritic rats treated with PPS exhibited a shield on weight loss when compared with the respective control group (Fig. 17D).

4.4.3 Effect of PPS on CIA histopathology

On day 30, histological evaluation of the paws in the vehicle-treated arthritic animals revealed signs of severe arthritis with massive mixed (neutrophil, macrophage, and lymphocyte) inflammatory cell infiltration (Fig. 18A and Table 7 for damage score). In addition, various histological changes were seen including pronounced synovial hyperplasia, pannus formation, angiogenesis, synovial infiltration with mononuclear cells, extensive cartilage and bone destruction as well as cartilage loss of proteoglycan (proportional to safranin O staining) (Fig. 18B). However, PPS treated rats were able to preserve nearly normal histological architecture in ankle and knee joints, demonstrating mild of inflammatory changes as well as restoration of articular cartilage (Fig. 18B). Synovial mononuclear infiltration was comparatively and significantly attenuated (p<0.01) in both PPS and meloxicam when compared with CIA rats. No synovial hyperplasia or pannus extension was observed in the meloxicam group (p<0.01) and only mild focal synovial hyperplasia and pannus formation was observed in the PPS rat ankles (p<0.01) (Table 7). Focal and mild synovial fibrosis in PPS and meloxicam treated rats were also noticed. Marked loss of safranin O staining was observed in ankle joint of CIA rats was restored by PPS (p<0.05) (Fig. 18B and Table 7). Osteoclasts were quantified at the site of inflammation and the score of osteoclast in ankle joint of the PPS and

meloxicam-treated groups was significantly (p<0.05) lower than of the rat ankles from vehicle group (Fig. 19A, B).

4.4.4 Effect of PPS on mRNA expression and concentration of biomarkers

In order to demonstrate the effect of PPS at the level of mRNA, synovial membranes were collected to determine the relative expression levels of OC and cytokines gene markers. Non-immunized group of animals were used as control. Osteoclast marker genes, CTK and TRAP were markedly suppressed in synovial membrane derived from the PPS treated group compared with those in the vehicle group, whereas expression of the cytokines genes IL-1β and TNF-α were attenuated by both PPS and meloxicam treatment (Fig. 20A, B). The concentration of COMP and TRACP-5b in SF were considerably elevated with CIA (p<0.05) compared with those in normal rats, whereas dropped by PPS and meloxicam treatment (Fig. 20C, D).

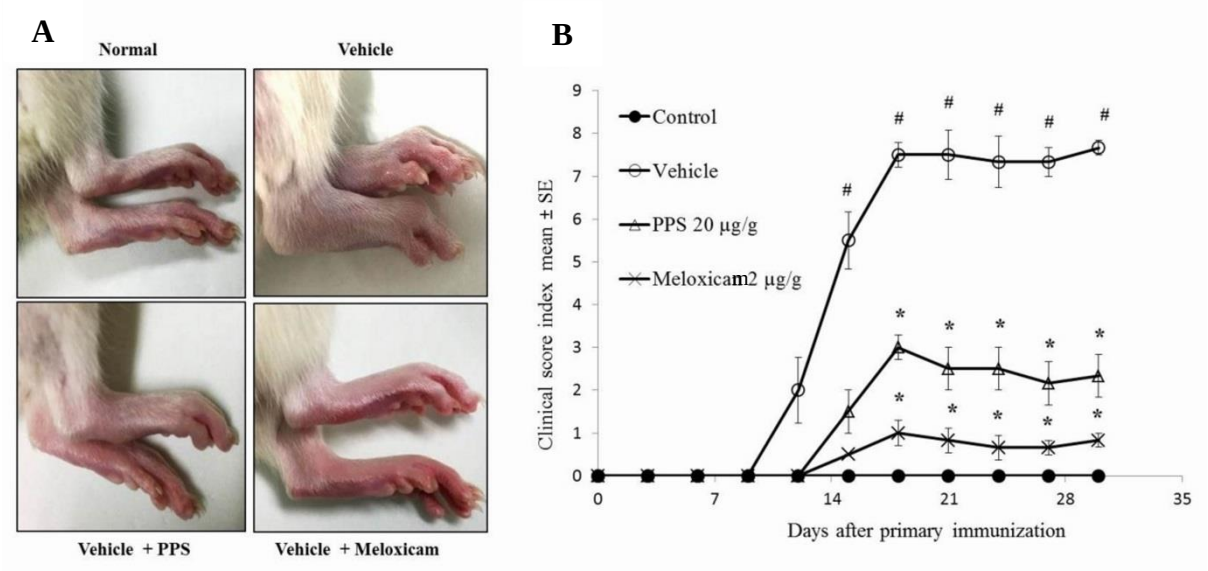

Fig. 16 Macroscopic observation of ankle joint of rats on day 30. Rats were immunized with collagen type II. **A**, Arthritic rats in vehicle group have shown redness, swelling, deformity and ankylosis with severe arthritis (symptoms maximum in the group), PPS (20 µg/g) treated rat with moderate arthritic symptoms; swelling only with moderate arthritis, meloxicam treated (2 µg/g) rat showing almost no sign of arthritis and appeared essentially normal. **B**, Mean clinical score index of CIA rats reached maximum score from day 18. Three days of delaying clinical signs were observed in rats treated with PPS and meloxicam. Data represent mean ± SEM and 6 rats per group. Significant difference normal vs vehicle is indicating as #: $p<0.05$. Significant difference of vehicle vs PPS/meloxicam is indicating as *: $p<0.05$.

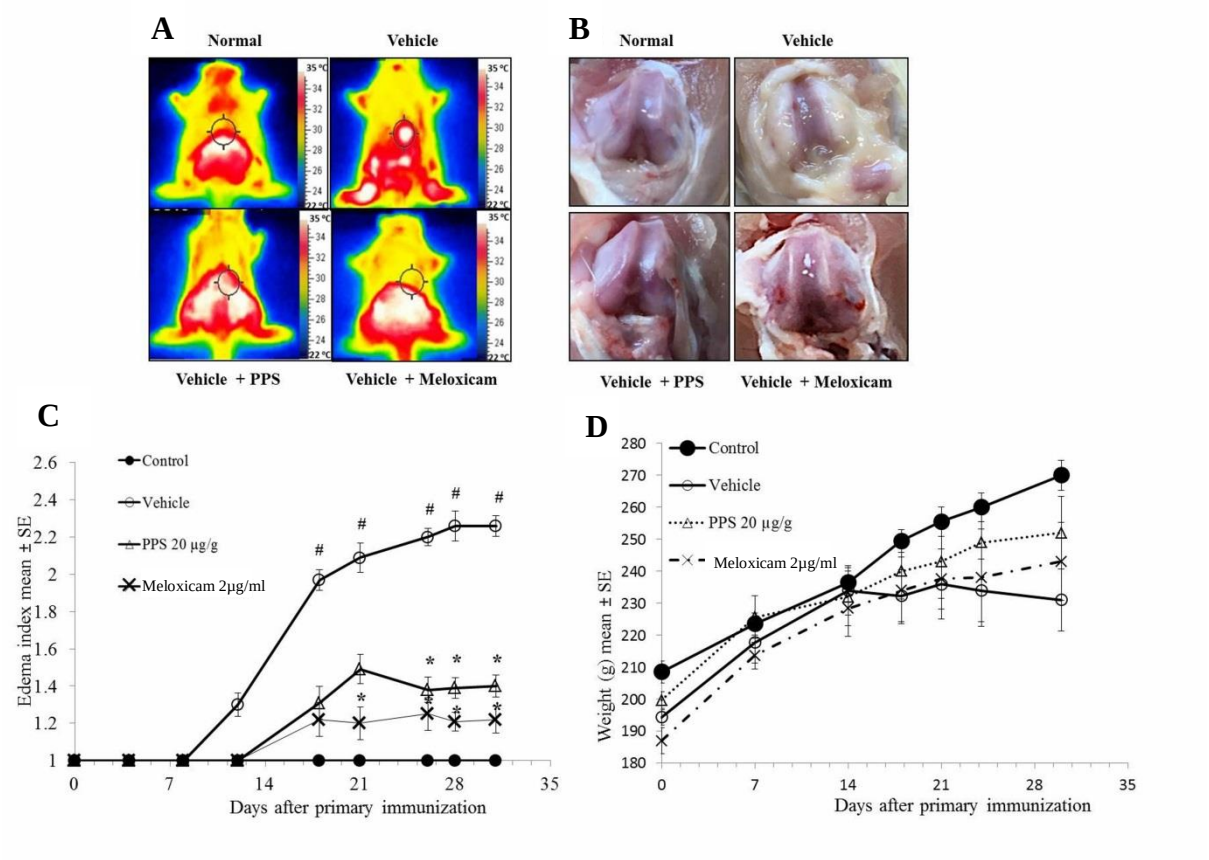

Fig. 17 Effect of PPS on arthritis-related clinic-pathological outcome was shown after 30 days from primary immunization. Rats were sensitized and challenged to type II bovine collagen in MDP and incomplete Freund's adjuvant. Pentosan polysulfate 20 µg/g and meloxicam 2 µg/g were given daily through subcutaneous. **A**, The infrared photos show an obvious temperature difference between groups. **B**, Joint degradation was shown in representative necropsy images. A smooth and glassy cartilage was observed in the normal group comparing that in vehicle group where surface abrasions and fibrotic tissue were observed. **C**, Mean edema index and **D** mean weight gain were shown accordingly. Data represent mean ± SEM and 6 rats per group. Significant difference normal vs vehicle is indicating as #: $p<0.05$. Significant difference of vehicle vs PPS/meloxicam is indicating as

* :$p<0.05$.

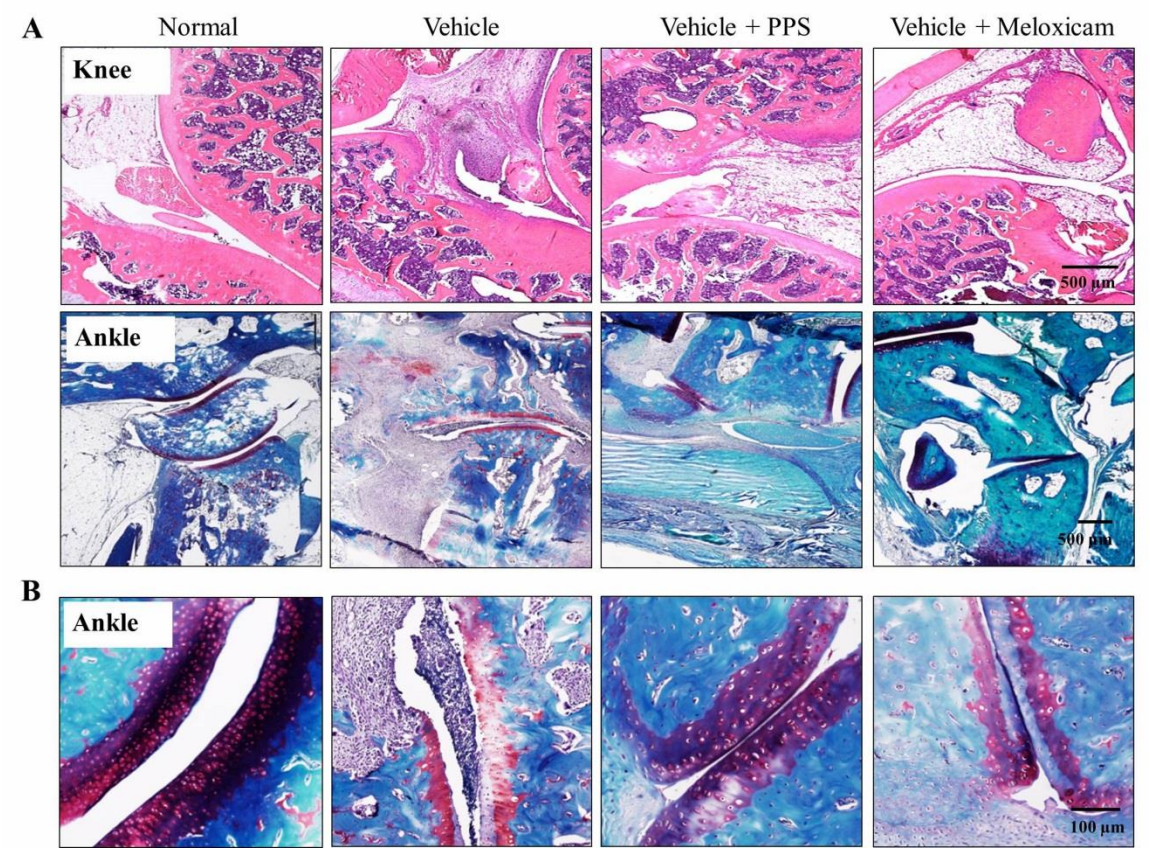

Fig. 18 Effect of PPS on arthritis-related microscopic changes. Sections were stained with H&E and safranin-O fast green. **A**, Histopathological changes of ankle and knee joints of each group were shown under low magnification. Significant differences in cellular infiltration, synovial hyperplasia, pannus formation, joint space narrowing, cartilage destruction and bone erosion in the synovial joints were found between the vehicle and normal rats. Ankle from an arthritis animal treated with 20 µg/g PPS has marked synovitis and mild cartilage damage with minimum pannus and bone resorption. Ankle from an animal treated with 2 µg/g meloxicam has mild inflammatory reactions. Images are representative of six distinct rats per group. **B,** Normal animal displays normal synovium and articular cartilage, whereas as knee from vehicle group displays severe synovitis and severe cartilage destruction which indicates with the color (red) intensity of safranin-O stain. Articular cartilage was restored with the treatment of PPS. Pictures are representative of 6 distinct rats per group.

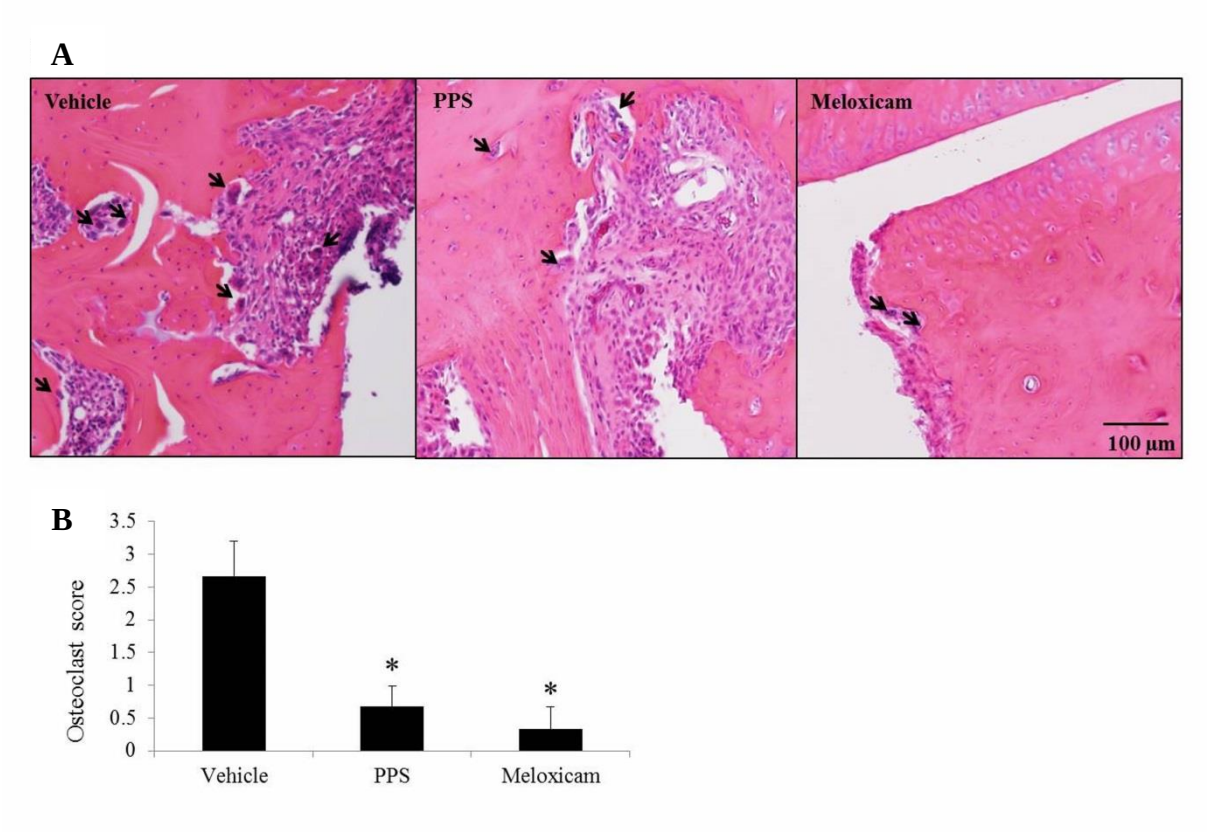

Fig. 19 Osteoclast observation in ankle joint from rats with collagen-induced arthritis treated with PPS. A, Tissue sections from vehicle group treated with normal saline; group treated with PPS concentration of 20 μg/g; group treated with meloxicam concentration of 2 μg/g were stained with H&E. **B**, Statistical data of osteoclast score in the knee joints of three different groups. *: $p < 0.05$ represents significant versus vehicle group. Data represent mean ± SEM and representative of 6 rats per group. Arrow denotes multinucleated osteoclast-like cells.

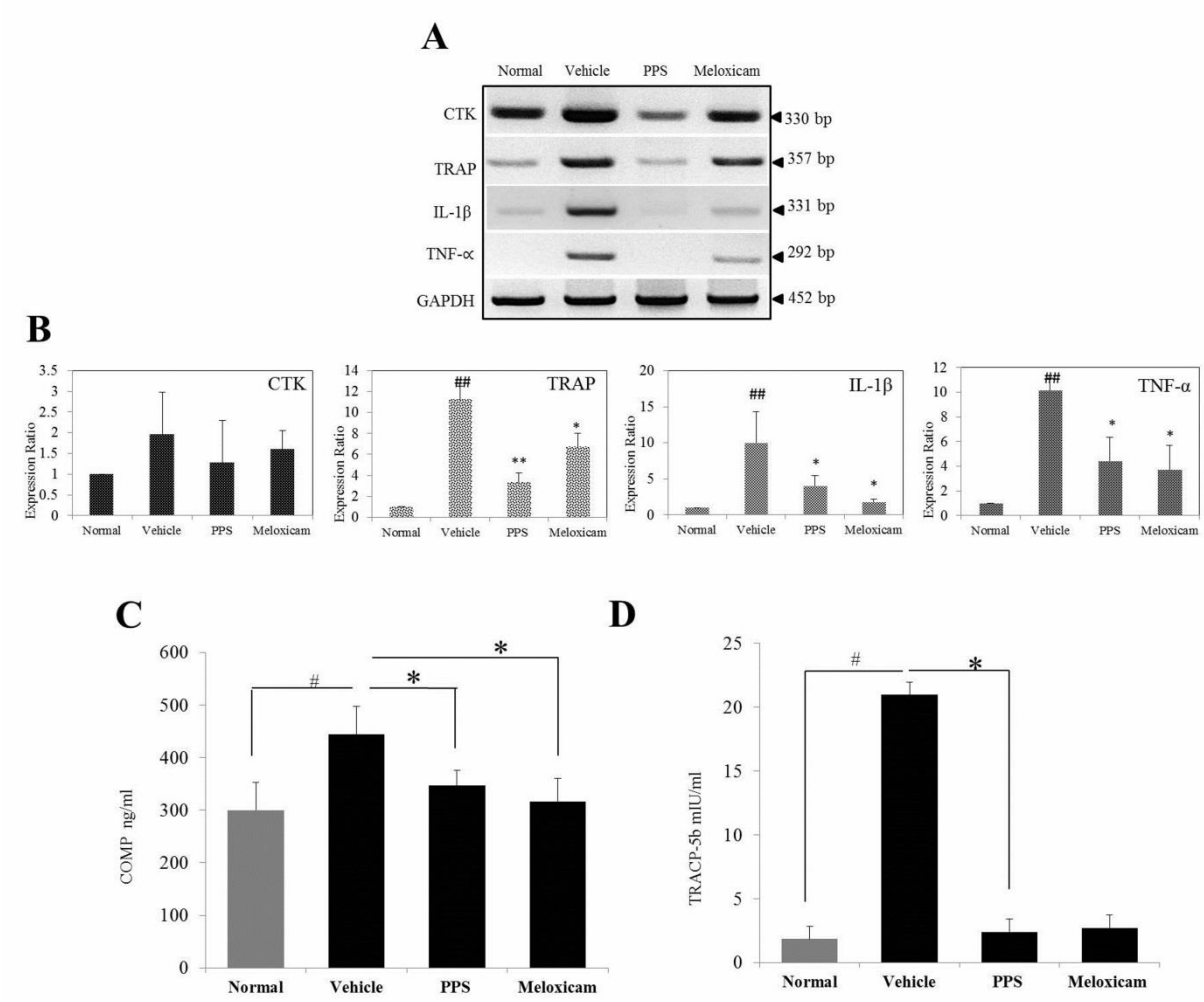

Fig. 20 Effect of PPS on inflammation-related markers of joints. (**A, B)** Relative mRNA expression was detected related to osteoclast specific genes; cathepsin k (CTK), tartrate-resistant acid phosphatase (TRAP) and cytokines, IL-1β, TNF-α in synovial membrane of rats. Remarkable reduction of osteoclast specific marker genes (PPS: $p<0.001$; meloxicam $p<0.05$) and inflammatory markers (PPS: $p<0.05$; meloxicam $p<0.05$) were detected in synovial membrane derived from rats treated with PPS and meloxicam. Bars represent mean relative values normalized to GAPDH expression ± SD**. (C, D)** Concentration of cartilage oligomeric matrix protein (COMP) and tartrate-resistant acid phosphatase 5b (TRACP-5b) in synovial fluid were measured and noted significant reduction ($p<0.05$) with both PPS and meloxicam treatment compared to those in vehicle group. Data represent mean ± SEM and 6 rats per group. Significant difference normal vs vehicle is indicating as # $p<0.05$. Significant difference of vehicle vs PPS/meloxicam is indicating as * $p<0.05$. (##, ** $p<0.001$).

Table 5 Histologic scoring parameters.

Parameters	Score 0	Score 1	Score 2	Score 3
1. Infiltrating mononuclear cells (five HMF)	Absent	Mild (1-10%)	Moderate (11-50%)	Severe (51-100%)
2. Synovial hyperplasia	Absent	Mild (5-10 layers)	Moderate (11-20 layers)	Severe (>20 layers)
3. Extension of pannus formation	Absent	Mild	Moderate	Severe
4. Synovial fibrosis	Absent	Mild (1-10%)	Moderate (11-50%)	Severe (51-100%)
5. Cartilage erosion	Absent	Mild (1-10%)	Moderate (11-50%)	Severe (51-100%)
6. Cartilage degradation (Based on safranin-O staining of proteoglycans)	Absent	Mild (1-10%)	Moderate (11-50%)	Severe (51-100%)
7. Bone erosion	None	Minor erosion (HMF)	Moderate erosion (LMF)	Transcortical erosion

HMF: high-power magnification fields, LMF: low-power magnification fields

Table 6 Primers used to polymerize the osteoclast and cytokine genes.

Molecule	Sense and anti-sense primer (5-3)	PCR fragment length (base pairs)	Sequence reference
Cathepsin K (Corisdeo et al., 2001)	CCCAGACTCCATCGACTATCG CTGTACCCTCTGCACTTAGCTGCC	330	AF010306
TRAP (Lang et al., 2001)	CGCCAGAACCGTGCAGA TCAGGCTGCTGGCTGAC	357	M76110
IL-1β (Kearsey et al., 1996)	CAACAAAAATGCCTCGTGC TGCTGATGTACCAGTTGGG	331	M98820
TNF-α (Kearsey et al., 1996)	TACTGAACTTCGGGGTGATCG CCTTGTCCCTTGAAGAGAACC	292	L00981
GAPDH (Heba et al., 2001)	ACCACAGTCCATGCCATCAC TCCACCACCCTGTTGCTGTA	452	NM017008

Table 7 Clinical outcome of rats with collagen–induced arthritis treated with PPS or meloxicam.

Treatment	CIA incidence	Day of onset	Score at onset	End score	Weight gain %
Vehicle	100%	12±0.57	2±0.76	7.66±0.16	18.86
PPS	33.33%	15±1	1.5±0.5	2.33±0.5*	26.61
Meloxicam	16.66%	15±0.154	0.5±0.5	0.83±0.16**	29.9

Collage-induced rats were dosed with 20µg/g PPS or meloxicam 2µg/g (once a day, from day 0 to day 30) and quantified incidence rate, clinical score and weight gain. Highest incidence rate was detected on 18^{th} day. Data are presented as mean ± SEM of six distinct rats. Findings of treatment groups were compared with vehicle group and represented significant difference as *: $p < 0.05$; **: $p < 0.01$.

Table 8 Histological score of rats with collagen-induced arthritis treated with PPS or meloxicam.

Histological parameter	Vehicle (n=6)	PPS (n=6)	Meloxicam (n=6)
Synovial mononuclear infiltrate (0–3)	2.8±0.20	0.5±0.22**	0.16±0.30**
Synovial hyperplasia (0–3)	2.8±0.20	0.83±0.30**	0**
Pannus extension (0–3)	2.8±0.20	0.16±0.16**	0**
Synovial fibrosis (0–3)	2.4±0.24	0.83±0.30**	0.16±0.16**
Cartilage erosions (0–3)	2.4±0.40	0.6±0.33**	0.1±0.16**
Safranin-O staining (0–3)	2±0.31	0.8±0.30*	1.16±0.30
Bone erosions (0–3)	2.8±0.20	0.16±0.16**	0.16±0.16**

Histopathological section stained with hematoxylin and eosin and safranin-O fast green were scaled according to the criteria mentioned in materials and methods. Data are presented as mean ± SEM in six distinct rats. Findings of treatment groups were compared with vehicle group and represented significant difference as *: $p < 0.05$; **: $p < 0.01$.

4.5 Discussion

Controlling inflammatory reactions is a feasible RA treatment method because the reaction creates the main problem in RA patients (McNamee et al., 2015; Xue et al., 2012). The results of the present study verified that the daily subcutaneous administration of the PPS effectively suppressed the arthritic symptoms of CIA in an animal model of RA. To discover the pharmacological mechanism of PPS, we investigated the effect of PPS on the expression of OC and cytokine marker genes as well as inflammatory response-related biologic markers. Quantitative clinical and histological arthritic scores consisted of mRNA expressions of osteoclast (CTK and TRAP) and cytokines-related (IL-1β and TNF-α) marker genes as well as the concentration of COMP and TRACP-5 released in SF. In various studies, COMP (Tseng et al., 2009) and TRACP-5b (Halleen et al., 2000) have shown promise as a diagnostic and prognostic indicator and as a marker of arthritis severity and the progress of treatment. Furthermore, both CTK and TRAP are highly expressed in lysosomal compartments of osteoclasts and are involved in the degradation of bone matrix throughout homeostatic and pathologic bone remodeling process and serve as characteristic markers of mature osteoclasts (Costa et al., 2011; Hayman, 2008). Crucially important two key pro-inflammatory cytokines, IL-1β and TNF-α in RA (Probert et al., 1995) were dropped with both PPS and meloxicam.

The most common clinical outcomes associated with RA are fatigue, malaise, arthralgia, fever and weight loss. Progressive reduction of body weight has been attained among arthritic animals during the development of arthritis (Jasemian et al., 2011; Busch and Engelhardt, 1990). But in the present study, a significant loss in body weight was not

detected during the period of study. Temperature of joint surface, which correlates with RA-related pain and stiffness (Jasemian et al., 2011) significantly declined with PPS and meloxicam treatment compared with that in CIA group. Meloxicam is an NSAID with analgesic effect and is especially suitable for the treatment of arthritis in animals (Fiorentino et al., 2008) apart from its gastrointestinal adverse effect (Bloom, 1989). During last decade, disease-modifying anti-rheumatic drugs and NSAID either concurrently or in combination has been the major therapy for RA (Gupta and Singh, 2013; Kremer, 2001; Moreland et al., 2001). Apart from their symptomatic relief, the value of these drugs along with prolong usage is restricted by their toxicity as well as no significant effect on the underlying disease process (Ahmed et al., 2005). However, during the period of this study, arthritic rats treated with meloxicam were able show the apparent clinical and biological improvement through its anti-inflammatory property as well as suspected chondroprotective effect which is not unanimously supported by literature reports (Blot et al., 2000; Engelhardt, 1996; Lemmel et al., 1997).

Currently, numerous investigations have demonstrated that naturally-derived compounds which carry least adverse effect might be useful as novel candidates for RA therapeutics formulas (Zheng et al., 2014; Choi et al., 2015). Beech wood-derived PPS is gaining more attention as a source of potential long-term safe pharmaceutical compound due to its pharmacologic properties (Ghosh and Cheras, 2001; Ghosh et al., 2005; Herrero et al., 2015; Bansal et al., 1993). From the results of previous in vitro and in vivo studies, the spectrum of pharmacological activities exhibited by PPS would qualify it as DMOAD because of its ability to preserve the integrity of the articular cartilage and bone while improving the quality of the joint SF (Ghosh, 1999; Burkhardt and Ghosh, 1987; Edelman et al., 1994; Ghosh et al., 1992). The findings of the current study from the RA

animal model treated with PPS, upgrades the significance of usage of this structure modifying glycosaminoglycan as an anti-arthritic compound.

On the other hand, OC score was impaired with the treatment of PPS implementing new target site of PPS and confirming our previous finding on *in vitro* assays in chapter 4. However, significant reduction of OC score in PPS and meloxicam groups was detected due to their anti-inflammatory property. Consisting with our previous data, PPS might carry synergistic effect over the bone erosion through its abilities of anti-inflammatory and anti-osteoclastogenesis.

Furthermore, a previous study reported that decreasing arthritic symptoms can occur via a reduction in the formation of new blood capillaries with some agents (angiogenesis) (Jasemian et al., 2011). The angiogenesis process worsens the inflammatory process as the fluid from the blood vessels is filtered out into the affected tissue area and causes edema. This process is very common in any inflammatory reactions, including the complex inflammatory reaction that occurs in the ankle joints of CIA rats. Another report revealed that PPS could reduce the expression of angiogenesis-related genes such as vascular endothelial growth factor (VEGF) and matrix metalloproteinase-9 (MMP9) plunging angiogenesis (Zaslau et al., 2006). Further, in the veterinary field from 1996 to date, there have been few reports about the use of pentosan for OA (Brunnberg et al., 2002; Henrotin et al., 2005). A recent report from our laboratory showed, PPS involves in the prevention of intracellular inflammatory responses induced by cytokine *in vitro* cultured canine articular chondrocytes (Bwalya et al., 2017). Therefore, current study might serve as another dimension for understanding the similarities and dissimilarities of PPS use in inflammation-related joint disease.

For the purpose of determining variation for each disease group, CIA model captured the data sufficiently well. Finally, several significant findings and trends were seen

demonstrating improvement with PPS at the day 30 time frame. A significant drawback for interpretation of these data is the small sample number in short study period with lack of well-defined endpoint. With that context, extended study period is needed providing more evidence, including immunohistochemical characterization of inflammatory infiltrates and fibroblastic transformation to highlight the specific action of both PPS and meloxicam. These data suggest that there might be a potential to show treatment effect of PPS for model of RA with greater sample number and selected drug dosing within their safe margins or even with perhaps sequential evaluation in further clinical trials.

5. General Conclusions

One of the primary aims of this thesis was studying the differentiation ability of synoviocytes-derived from inflamed synovial joint of the dogs. Second chapter of this thesis confirms that the severity of inflammation of joint diseases might affect multipotency of SM-derived stem cells while maintaining the stem cell population. In addition, pre-activated MSCs by inflammatory factors might offer a method of improving the potency of these cells without the need for additional cell number. Further we can speculate that these SM-derived stem cells are liable to re-establish the imbalance between OA catabolism and joint anabolism. This study might serve as a platform for understanding the similarities and dissimilarities of the cellularity in synovitis associated with common knee injuries. This basic understanding might need to approach therapeutic targets in inflammation-related arthritis.

One important caveat to these experiments is the method used for canine osteoclastogenesis from bone marrow-derived hematopoietic stem cells. Variations of OC differentiation ability of pro-inflammatory cytokines was studied and validated that cytokines have specific characteristics throughout the osteoclastogenesis process. Regardless temporal differentiation, TNF-α and IL-17 enhanced OC formation and their function at particular concentrations. But IL-1β suppressed the osteoclastogenesis at early phase of the process while stimulating at the late stage. Therefore, additional studies are needed to test differential effect of other cytokines involved in canine osteoclastogenesis to identify their roles and implement the therapeutics strategies targeting bone resorption. Moreover, this study might be a manifesto for future investigation of finding other factors involved in the IL-1β–induced inhibition of canine osteoclastogenesis and to unveil the rationale of MMP9 downregulation by IL-17 in

addition to determine the mechanisms of action of IL-17 in bone erosion. Collectively, understanding the precise mechanisms of immune-mediated bone destruction would increase opportunities for target-specific inhibition of bone erosion or osteoporosis. The identification of the OC and its role in joint destruction has enabled the development of therapies aimed at reducing its resorptive capacity. Thereby, therapeutic interventions specifically targeting osteoclastogenesis might enable veterinarians to spare bone mass in canine patients with arthritis.

The second goal of this study was to identify the effect of pentosan over the osteoclastogenesis and its function. Thus OC play major role in bone homeostasis, this study would be a platform and promising launch for further investigation to identify the intracellular acting sites of PPS and more detailed protein interactions for detailed therapeutic mechanism of action. In conclusion, PPS exerts its great therapeutic value in treating osteoporosis and other bone-erosive diseases such as rheumatoid arthritis and bone diseases associated with excessive bone resorption.

To the best of our knowledge, the present investigation is the first report to evaluate the therapeutic effects of PPS on RA in the CIA animal model. The present investigation demonstrates that PPS possesses promising anti-arthritic effects on CIA in rats. The potential pharmacological mechanism for these effects might be related to the inhibition of inflammatory reactions during the RA process, whereby PPS suppresses the expression of pro-inflammatory cytokines, OC markers and concentration of arthritis biomarkers. Therefore, our results suggest that PPS might be a novel candidate for RA therapeutic protocol as a safe alternative to existing DMOAD and NSAID.

6. References

Ahmed, S., Anuntiyo, J., Charles, J., Haqqi, T. M., 2005. Biological basis for the use of botanicals in osteoarthritis and rheumatoid arthritis: A review. *Evid. Based Complement Alternat. Med.* **2**, 301–308.

Altman, R., 2004. Measurement of structural modification in osteoarthritis. *Osteoarthr Cartil.* **12**, 69-76.

Andrews, J. L., Ghosh, P., Lentini, A., Ternai, B. 1983. The interaction of pentosan polysulphate (SP54) with human neutrophil elastase and connective tissue matrix components. *Chem. Biol. Interact.* **47**, 157-173.

Anger, J. T., Zabihi, N., Clemens, J. Q., Payne, C. K., Saigal, C. S., Rodriguez, L. V., 2011. Treatment choice, duration, and cost in patients with interstitial cystitis and painful bladder syndrome. *Int. Urogynecol.* J. **22**, 395–400.

Bajayo, A., Goshen, I., Feldman, S., Csernus, V., Iverfeldt, K., Shohami, E., Yirmiya, R., Bab, I. 2005. Central IL-1 receptor signaling regulates bone growth and mass. *Proc. Natl. Aca. Sci. USA.* **102**: 12956-12961.

Bansal, M. K., Smith, M. M., Numata, Y., Ghosh, P., 1993. The effects of calcium pentosan polysulfate on inflammatory mediators in the rat air-pouch model of inflammation. *Curr. Ther. Res.* **54**, 714-730.

Barbero, A., Ploegert, S., Heberer, M., Martin, I., 2003. Plasticity of clonal populations of dedifferentiated adult human articular chondrocytes. *Arthritis and Rheum.* **48**, 1315–1325.

Bertram, K. L., Krawetz, R. J., 2012. Osmolarity regulates chondrogenic differentiation potential of synovial fluid derived mesenchymal progenitor cells. *Biochem. Biophys. Res. Commun.* **422**, 455-461.

Blanco, F. J., Ruiz-Romero, C., 2013. New targets for disease modifying osteoarthritis drugs: chondrogenesis and Runx1. *Ann. Rheum. Dis.* **72**(5), 61-634.

Bloom, B. S., 1989. Risk and cost of gastrointestinal side effect associated with non-steroid anti-inflammatory drugs. *Arch. Intern. Med*. **149**, 1019-1022.

Blot, L., Marcelis, A., Devogelaer, J. P., Manicourt, D. H. 2000. Effects of diclofenac, aceclofenac and meloxicam on the metabolism of proteoglycans and hyaluronan in osteoarthritic human cartilage. *Br. J. Pharmacol.* **131**, 1413–1421.

Boyce, B. F., Yao, Z., Xing, L., 2009. Osteoclasts have Multiple Roles in Bone in Addition to Bone Resorption. *Crit. Rev. Eukaryot. Gene. Expr*. **19**, 171–180.

Boyle, W. J., Simonet, W. S., Lacey, D. L., 2003. Osteoclast differentiation and activation. *Nature* **423**, 337–342.

Branco De Sousa, E., Casado, P. L., Neto, V. M., Leite Duarte, M. E., Aguiar, D. P., 2014. Synovial fluid and synovial membrane mesenchymal stem cells: latest discoveries and therapeutic perspectives. *Stem cell Res.* Ther. **5**,112.

Brandt, K. D., Myers, S. L., Burr, D., Albrecht, M., 1991. Osteoarthritic changes in canine articular cartilage, subchondral bone and synovium fifty four months after transection of the anterior cruciate ligament. *Arthritis Rheum*. **34**, 1560-1570.

Breedveld, F. C., 2002. Current and future management approaches for rheumatoid arthritis. *Arthritis Res.* **4** (suppl 2):S16-S21.

Brennan, F. M. and McInnes, I. B., 2008. Evidence that cytokines play a role in rheumatoid arthritis. *J. Clin. Invest.* **118**: 3537-3545.

Brenner, M., Meng, H. C., Yarlett, N. C., Joe, B., Griffiths, M. M., Remmers, E. F., Ronald, L.W., Gulko, P. S., 2005a. The non-MHC quantitative trait locus Cia5 contains three major arthritis genes that differentially regulate disease severity, pannus formation, and joint damage in collagen- and pristane-induced arthritis. *J. Immunol*. **174**, 7894–7903.

Brenner, M., Meng, H., Yarlett, N. C., Griffiths, M. M., Remmers, E. F., Wilder, R. L., Gulko, P. S., 2005b. The non-MHC quantitative trait locus Cia10 contains a major arthritis gene and regulates disease severity, pannus formation and joint damage. *Arthritis Rheum*. **52**, 322-332.

Brunnberg, L., Gebski, V., Cullis-Hill, D., 2002. A multi-center clinical study of the efficacy of sodium pentosan polysulfate and carprofen in canine osteoarthritis (osteoarthrosis). *Veterinärmötet*. 123-130.

Burkhardt, D., Ghosh, P., 1987. Laboratory evaluation of antiarthritic drugs as potential chrondroprotective agents. *Semin. Arthritis Rheum*. **17**(2 Suppl 1), 3–34.

Burmester, G. R., Jahn, B., Rohwer, P., Zacher, J., Winchester, R. J., Kalden, J. R., 1987. Differential expression of la antigens by rheumatoid synovial lining cells. *J. Clin. Invest.* **80**, 595–604.

Busch, U., Engelhardt, G., 1990. Distribution of [14C] meloxicam in joints of rats with adjuvant arthritis. *Drugs Exp. Clin. Res*. **16**, 49–52.

Bwalya, E. C., Kim, S., Fang, J., Wijekoon, H. M. S., Hosoya, K., Okumura, M., 2017. Pentosan polysulfate inhibits IL-1β-induced iNOS, c-Jun and HIF-1α upregulation in canine articular chondrocytes. *PLoS ONE* **12**(5), e0177144.

Candela, M. E., Yasuhara, R., Iwamoto, M., Enomoto-Iwamoto, M. 2014. Resident mesenchymal progenitors of articular cartilage. *Matrix Biol.* **39**, 44–49.

Chatzidionysiou, K., Lie, E., Nasonov, E., Lukina, G., Hetland, M. L., Tarp, U., van Riel, P. L., Nordström, D. C., Gomez-Reino, J., Pavelka, K., Tomsic, M., Kvien, T. K., van Vollenhoven, R. F., Gabay, C. 2012. Effectiveness of disease-modifying antirheumatic drug co-therapy with methotrexate and leflunomide in rituximab-treated rheumatoid arthritis patients: results of a 1-year follow-up study from the CERERRA collaboration. *Ann. Rheum. Dis.* **71**(3), 374-377.

Choi, J. K., Oh, H. M., Park, J. H., Choi, J. H., Sa, K. H., Kang, Y. M., Park, P. H., Shin, T. Y., Rho, M. C., Kim, S. H., 2015. Salvia plebeia extract inhibits the inflammatory response in human rheumatoid synovial fibroblasts and a murine model of arthritis. *Phytomedicine* **22**, 415–422.

Colmegna, I., Ohata, B. R., Menard, H. A., 2012. Current understanding of rheumatoid arthritis therapy. *Clin. Pharmacol. Ther*. **91**, 607–620.

Corisdeo, S., Gyda, M., Zaidi, M., Moonga, B. S., Troen, B. R., 2001. New insights into the regulation of cathepsin K gene expression by osteoprotegerin ligand. *Biochem. Biophys. Res. Commun.* **285**, 335–9.

Corral, D. A., Amling, M., Priemel, M., Loyer, F., Fuchs, S., Ducy, P., Baron, R., Karsenty, G., 1998. Dissociation between bone resorption and bone formation in osteopenic transgenic mice. *Proc. Natl. Acad.Sci. USA.* **95**, 13835–13840.

Costa, A. G., Cusano, N. E., Silva, B. C., Cremers, S., Bilezikian, J. P., 2011. Cathepsin K: its skeletal actions and role as a therapeutic target in osteoporosis. *Nat. Rev. Rheumatol*. **7**, 447-56.

Danks, L., Sabokbar, A., Gundle, R., Athanasou, N.A., 2002. Synovial macrophage-osteoclast differentiation in inflammatory arthritis. *Ann. Rheum. Dis.* **61**, 916–921.

De Bari, C., Dell 'accio, F., Tylzanowski, P., Luyten, F. P.,2001. Multipotent mesenchymal stem cells from adult human synovial membrane. *Arthritis Rheum.* **44**, 1928–1942.

Dominici, M., Le Blanc, K., Mueller, I., Slaper-Cortenbach, I., Marini, F., Krause, D., Deans, R.J., Keating, A., Prockop, D.J., Horwitz, E., 2006. Minimal criteria for defining multipotent mesenchymal stromal cells. *Cytotherapy* **8**, 315–317.

Doom, M., de Bruin, T., de Rooster, H., van Bree, H., Cox, E., 2008. Immunopathological mechanisms in dogs with rupture of the cranial cruciate ligament. *Vet. Immunol. Immunopathol.* **125**, 143–161.

Earp, J. C., DuBois, D. C., Molano, D. S., 2008. Modeling corticosteroid effects in a rat model of rheumatoid arthritis I: Mechanistic disease progression model for the time course of collagen-induced arthritis in Lewis rats. *J. Pharmacol. Exp. Therap.* **326**, 532–45.

Edelman, J., March, L., Ghosh, P., 1994. A double-blind placebo-controlled clinical study of a pleotropic osteoarthritis drug (pentosan polysulphate Cartrophen v) in 105 patients with osteoarthritis of the knee and hip joints. *Osteoarthr. Cartil*. **2**, 35.

Edelman, J., March, L., Ghosh, P., 1996. Disease modification in osteoarthritis: Relationship of macrophage procoagulant activity and haematological parameters to symptoms in patients receiving pentosan polysulfate. *Osteoarthr. Cartil*. **4** Suppl :4-5.

Endres, M., Andreas, K., Kalwitz, G., Freymann, U., Neumann, K., Ringe, J., Sittinger, M., Häupl, T., Kaps, C., 2010. Chemokine profile of synovial fluid from normal, osteoarthritis and rheumatoid arthritis patients: CCL25, CXCL10 and XCL1 recruit human subchondral mesenchymal progenitor cells. *Osteoarthr. Cartil.* **18**, 1458–1466.

Engelhardt, G. 1996. Pharmacology of meloxicam, a new non-steroidal anti-inflammatory drug with an improved safety profile through preferential inhibition of COX-2. *British J. Rheumatol.* **35**, 4–12.

Fiorentino, P. M., Tallents, R. H., Miller, J. N., Brouxhon, S. M., O'Banion, M. K., Puzas, J. E., Kyrkanides, S., 2008. Spinal interleukin-1b in a mouse model of arthritis and joint pain. *Arthritis Rheum*. **58**, 3100–3109.

Firestein, G. S., 2003. Evolving concepts of rheumatoid arthritis. *Nature* **423**:35661.

Firestein, G. S., Harris, R. C. B., Edward, D., Genovese, Mark C., Gary S., Clement, B., 2005. Etiology and Pathogenesis of Rheumatoid Arthritis. Kelley's Textbook of Rheumatology. Vol.7. Philadelphia, PA, USA: Elsevier Saunders; 996-1042.

Fujikawa, Y., Sabokbar, A., Neale, S., Athanasou, N. A., 1996. Human osteoclast formation and bone resorption by monocytes and synovial macrophages in rheumatoid arthritis. *Ann. Rheum. Dis.* **55**, 816–822.

Gao, Y., Ryan, M. R., Terauchi, M., Page, K., Yang, X., Weitzmann, M. N. and Pacifici, R. 2007. IFN-γ stimulates osteoclast formation and bone loss in vivo via antigen-driven T cell activation. *J. Clin. Invest.* **117**: 122-132.

Ghayor, C., Correro, R. M., Lange, K., Karfeld-Sulzer, L. S., Gra¨tz, K. W., Weber, F. E., 2011. Inhibition of osteoclast differentiation and bone resorption by N-Methylpyrrolidone. *J. Biol. Chem.* **286**(27), 24458-24466.

Ghosh, P., 1999. The pathobiology of osteoarthritis and the rationale for the use of pentosan polysulfate for its treatment. *Semin. Arthritis Rheum*. **28**, 211-267.

Ghosh, P., Cheras, P., 2001. Vascular mechanism in osteoarthritis. *Best Pract. Res. Clin. Rheumatol.* **15**, 693-709.

Ghosh, P., Edelman, J., March, L., Smith, M., 2005. Effects of Pentosan Polysulfate in Osteoarthritis of the Knee: A Randomized, Double-Blind, Placebo-Controlled Pilot Study. *Curr. Ther. Res.* **66**, 552- 571.

Ghosh, P., Smith, M., Wells, C., 1992. Second line agents in osteoarthritis. In Dixon JS, Furst DE Eds. Second Line Agents in the Treatment of Rheumatic Diseases. New York: *Marcel Dekker Inc.*363-427.

Ghosh, P., Wu, J., Shimmon, S., Zannettino, A. C. W., Gronthos, S., Itescu, S., 2010. Pentosan polysulfate promotes proliferation and chondrogenic differentiation of adult human bone marrow-derived mesenchymal precursor cells. *Arthritis Res. Ther.* **12**, 28.

Grigoriadis, A. E., Wang, Z. Q., Cecchini, M. G., Hofstetter, W., Felix, R., Fleisch, H. A., Wagner, E. F., 1994. c-Fos: a key regulator of osteoclast-macrophage lineage determination and bone remodeling. *Science* **226**, 443-448.

Gupta, A. and Singh, A. (2013). Evaluation of anti-inflammatory effect of Withania somnifera root on collagen-induced arthritis in rats. *Pharm. Biol.* **52**, 308-320.

Halleen, J. M., Alatalo, S. L., Suominen, H., Cheng, S., Janckila, A. J., Vaatanen, H. K. 2000. Tartrate resistant acid phosphatase 5B: a novel serum marker of bone resorption. *J. Bone Miner. Res.* **15**, 1337–1345.

Hanno, P. M., Burks, D. A., Clemens, J. Q., Dmochowski, R. R., Erickson, D., FitzGerald, M. P., Forrest, J.B., Gordon, B., Gray, M., Mayer, R. D., Moldwin, R., Newman, D. K., Nyberg, L., Payne, C. K., Wesselmann, U., Faraday, M. M., 2011. AUA guideline for the diagnosis and treatment of interstitial cystitis/bladder pain syndrome. *J. Urol.* **185**, 2162–2170.

Harrison, E. T., Luyten, F. P., Reddi, A. H., 1991. Osteogenin promotes reexpression of cartilage phenotype by dedifferentiated articular chondrocytes in serum-free medium. Experimental Cell Research. *Exp. Cell Res.* **192**, 340-334.

Hayman, A. R., 2008. Tartrate-resistant acid phosphatase (TRAP) and the osteoclast/immune cell dichotomy. *Autoimmunity* **41**, 218-223.

Heba, G., Krzeminski, T., Porc, M., Grzyb, J., Dembinska-Kiec, A., 2001. Relation between expression of TNF , iNOS, VEGF mRNA and development of heart failure after experimental myocardial infarction in rats. *J. Physiol. Pharmacol*. **52**, 39–52.

Henrotin, Y., Christelle, S., Balligand, M., 2005. Pharmaceutical and nutraceutical management of canine osteoarthritis: Present and future perspectives. *Vet. J.* **170**, 113-123.

Herrero, L. J., Foo, S., Sheng, K., Chen, W., Forwood, M. R., Bucala, R., Mahalingam, S., 2015. Pentosan Polysulfate: a novel glycosaminoglycan-like molecule for effective treatment of alphavirus-induced cartilage destruction and inflammatory disease. *J. Virol.* **89**, 8063-8076.

Hsu, H., Lacey, D. L., Dunstan, C. R., Solovyev, I., Colombero, A., Timms, E., Tan, H. L., Elliott, G., Kelley, M. J., Sarosi, I., Wang, L., Xia, X. Z., Elliott, R., Chiu, L., Black, T., Scully, S., Capparelli, C., Morony, S., Shimamoto, G., Bass, M. B., Boyle, W. J., 1999. Tumor necrosis factor receptor family member RANK mediates osteoclast differentiation and activation induced by osteoprotegerin ligand. *Proc. Natl. Acad. Sci. USA.* **96**, 3540-3545.

Hurst, R., Zuo, J., Holliday, L. S., 2004. Actin-related protein 2/3 complex is required for actin ring formation. *J. Bone Miner. Res.* **19**, 499-506.

Itonaga, I., Fujikawa, Y., Sabokbar, A., Murray, D. W., Athanasou, N. A., 2000. Rheumatoid arthritis synovial macrophage-osteoclast differentiation is osteoprotegerin ligand-dependent. *J. Pathol.* **192**, 97–104.

Itonaga, I., Sabokbar, A., Sun, S. G., Kudo, O., Danks, L., Ferguson, D., Fujikawa, Y., Athanasou, N. A., 2004. Transforming growth factor-β induces osteoclast formation in the absence of RANKL. *Bone.* **34**, 57-64.

Jackson, D. W., Lalor, P. A., Aberman, H. M., Simon, T. M., 2001. Spontaneous repair of full- thickness defects of articular cartilage in a goat model a preliminary study. *J. Bone Joint Surg*. **83**, 53-64.

Jasemian Y, Svendsen P, Deleuran B, Dagnaes-Hansen F, 2011. Refinement of the Collagen Induced Arthritis Model in Rats by Infrared Thermography. *Br. J. Med. Res.* **1**(4):469-477.

Jimi, E., Nakamura, I., Duong, L. T., Ikebe, T., Takahashi, N., Rodan, G. A. and Suda, T. 1999. Interleukin 1 induces multinucleation and bone-resorbing activity of osteoclasts in the absence of osteoblasts/stromal cells. *Exp. Cell. Res.* **247**, 84-93.

Jimi, E., Shuto, T. and Koga, T. 1995. Macrophage colony-stimulating factor and interleukin-1 alpha maintain the survival of osteoclast-like cells. *J. Endocrinol.* **136**, 808-811.

Joe, B., Wilder, R., 1999. Animal model of RA. *Mol. Med. Today* **5**, 367-369.

Joffe, S., 1976. Drug prevention of postoperative deep vein thrombosis. A compararative study of calcium heparinate and sodium pentosan polysulfate. *Arch. Surg*. **111**, 37-40.

Jun, A. Y., Kim, H. J., Park, K. K., Son, K. H., Lee, D. H., Woo, M. H., Kim, Y. S., Lee, S. K., Chung, W. Y., 2012. Extract of Magnoliae Flos inhibits ovariectomy-induced osteoporosis by blocking osteoclastogenesis and reducing osteoclast-mediated bone resorption. *Fitoterapia* **83**, 1523-1531.

Karsdal, M. A., Henriksen, K., Leeming, D. J., Mitchell, P., Dun, K., Barascuk, N., Klickstein, L., Aggarwal, P., Nemirovskiy, O., Byrjalsen, I., Qvist, P., Bay-Jensen, A. C., Dam, E. B., Madsen, S. H., Christiansen, C., 2009. Biochemical markers and the FDA Critical Path: how biomarkers may contribute to the understanding of pathophysiology and provide unique and necessary tools for drug development. *Biomarkers* **14**, 181-202.

Karsenty, G., Wagner, E. F., 2002. Reaching a genetic and molecular understanding of skeletal development. *Dev. Cell.* **2**, 389–406.

Kearsey, J. A., Standnyk, A. W., 1996. Isolation and characterization of highly purified rat intestinal intraepithelial lymphocytes. *J. Immunol. Methods*. **194**, 35–48.

Kim, J., Kim, E., Lee, B., Min, J., Song, D., Lim, J., Eom, J. W., Yeom, M., Jung, H., Sohn, Y., 2016. The effects of Lycii Radicis Cortex on RANKL-induced osteoclast differentiation and activation in RAW 264.7 cells. *Int. J. Mol. Med*. **37**, 649-658.

Kisiel, H., McDuffee, L., Masaoud, E., Bailey, T. R., Esparza Gonzalez, B. P., Nino-Fong, R., 2012. Isolation, characterization and in vitro proliferation of canine mesenchymal stem cells derived from bone marrow, adipose tissue, muscle, and periosteum. *Am. J. Vet. Res.* **73**, 1305–1317.

Kitami, S., Tanaka, H., Kawato, T., Tanabe, N., Katono-Tani, T., Zhang, F., Suzuki, N., Yonehara, Y. and Maeno, M. 2010. IL-17A suppresses the expression of bone resorption-related proteinases and osteoclast differentiation via IL-17RA or IL-17RC receptors in RAW264.7 cells. *Biochimie*. **92**, 398-404.

Kitazawa, R., Kimble, R. B., Vannice, J. L., Kung, V. T. and Pacifici, R. 1994. Interleukin-1 receptor antagonist and tumor necrosis factor binding protein decrease osteoclast formation and bone resorption in ovariectomized mice. *J. Clin. Invest.* **94**, 2397-2406.

Kobayashi, K., Takahashi, N., Jimi, E., Udagawa, N., Takami, M., Kotake, S., Nakagawa, N., Kinosaki, M., Yamaguchi, K., Shima, N., Yasuda, H., Morinaga, T., Higashio, K., Martin, T. J. and Suda, T. 2000. Tumor necrosis factor alpha stimulates osteoclast differentiation by a mechanism independent of the ODF/RANKL-RANK interaction. *J. Exp. Med.* **191**, 275-286.

Koga, T., Sakamoto, S., Onoue, K., Kotani, S., Sumiyoshi, A., 1980. Efficient induction of collagen arthritis by the use of a synthetic muramyl dipeptide. *Arthritis Rheum.* **23**, 993-997.

Kong, Y. Y., Yoshida, H., Sarosi, I., Tan, H. L., Timms, E., Capparelli, C., Morony, S., Oliveira-dos-Santos, A. J., Van, G., Itie, A., Khoo, W., Wakeham, A., Dunstan, C. R., Lacey, D. L., Mak, T. W., Boyle, W. J., Penninger, J. M., 1999. OPGL is a key

regulator of osteoclastogenesis, lymphocyte development and lymph-node organogenesis. *Nature* **397**, 315-323.

Kotake, S., Nanke, Y., Yago, T., Kawamoto, M. and Yamanaka, H. 2009. Human osteoclastogenic T cells and human osteoclastology. *Arthritis Rheum*. **60**, 3158-3163.

Kremer, J. M., 2001. Rational use of new and existing disease modifying agents in rheumatoid arthritis. *Ann. Intern. Med*. **134**, 695–706.

Krenn, V., Morawietz, L., Burmester, G. R., Kinne, R. W., Mueller-Ladner, U., Muller, B., Haupl, T., 2006. Synovitis score: Discrimination between chronic low-grade and high-grade synovitis. *Histopathology* **49**, 358–364.

Kumagai, K., Shirabe, S., Miyata, N., Murata, M., Yamauchi, A., Kataoka, Y., Niwa, M., 2010. Sodium pentosan polysulfate resulted in cartilage improvement in knee osteoarthritis - An open clinical trial. *Clin. Pharmacol*. **10**, 7.

Kwan, C., Bell, R., Koenig, T., Bischofberger, A., Horadagoda, N., Perkins, N. R., Jeffcott, L. B., Dart, A. J., 2012. Effects of intra-articular sodium pentosan polysulfate and glucosamine on the cytology, total protein concentration and viscosity of synovial fluid in horses. *Aust. Vet. J.* **90**, 315–320.

Lang, P., Schultzberg, M., Andersson, G., 2001. Expression and distribution of tartrate-resistant purple acid phosphatase in the rat nervous system. *J. Histochem. Cytochem.* **49**, 379–396.

Lee, B., Kim, T. H., Jun, J. B., Yoo, D. H., Woo, J. H., Choi, S. J., Lee, Y. H., Song, G. G., Sohn, J., Park-Min, K. H., Ivashkiv, L. B. and Ji, J. D. 2010. Direct inhibition of human RANK+ osteoclast precursors identifies a homeostatic function of IL-1β. *J. Immunol.* **185**, 5926-5934.

Lee, S. E., Chung, W. J., Kwak, H. B., Chung, C. H., Kwack, K. B., Lee, Z. H. and Kim, H. H. 2001. Tumor necrosis factor-alpha supports the survival of osteoclasts through the activation of Akt and ERK. *J. Biol. Chem*. **276**, 49343-49349.

Lemburg, A. K., Meyer-Lindenberg, A., Hewicker-Trautwein, M., 2004. Immunohistochemical characterization of inflammatory cell populations and

adhesion molecule expression in synovial membranes from dogs with spontaneous cranial cruciate ligament rupture. *Vet. Immunol. Immunopathol.* **97**, 231–240.

Lemmel, E. M., Bolten, W., Burgos-Vargas, R., Platt, P., Nissilä, M., Sahlberg, D., Björneboe, O., Baumgartner, H., Valat, J. P., Franchimont, P., Bluhmki, E., Hanft, G., Distel, M., 1997. Efficacy and safety of meloxicam in patients with rheumatoid arthritis. *J. Rheumatol.* **24**, 282-290.

Leonavičienė, L., Bradūnaitė, R., Vaitkienė, D., Vasiliauskas, A., Keturkienė, A., 2008. Collagen-induced arthritis and pro-/antioxidant status in Wistar and Lewis rats. *Biologija* **54**, 290–300.

Lerner, U. H. and Ohlin, A. 1993. Tumor necrosis factors alpha and beta can stimulate bone resorption in cultured mouse calvariae by a prostaglandin-independent mechanism. J. *Bone. Miner. Res.* **8**, 147-155.

Li, F., Chung, H., Reddy, S. V., Lu, G., Kurihara, N., Zhao, A. Z., Roodman, G. D., 2005. Annexin II Stimulates RANKL Expression Through MAPK. *J. Bone Miner. Res.* **20**, 1161-1167.

Little, J. P., Bleedorn, J. A., Sutherland, B. J., Sullivan, R., Kalscheur, V. L., Ramaker, M. A., Schaefer, S.L., Hao, Z., Muir, P., 2014. Arthroscopic assessment of stifle synovitis in dogs with cranial cruciate ligament rupture. PLoS One 9(6), e97329.

MacDonald, B. R., Takahashi, N., McManus, L. M., Holahan, J., Mundy, G. R., Roodman, G. D., 1987. Formation of multinucleated cells that respond to osteotropic hormones in long term human bone marrow cultures. *Endocrinology* **120**, 2326–2333.

Matei, I. and Matei, L. 2002. Cytokine patterns and pathogenicity in autoimmune diseases. *Rom. J. Intern. Med.* **40**, 27-41.

Matsuo, K., Galson, D. L., Zhao, C., Peng, L., Laplace, C., Wang, K. Z., Bachler, M. A., Amano, H., Aburatani, H., Ishikawa, H., Wagner, E. F., 2004. Nuclear factor of activatedvT-cells (NFAT) rescues osteoclastogenesis in precursors lacking c-Fos. *J. Biol. Chem.* **279**, 26475–26480.

McIlwraith, C. W., Frisbie, D. D., Kawcak, C. E., 2012. Evaluation of intramuscularly administered sodium pentosan polysulfate for treatment of experimentally induced osteoarthritis in horses. *Am. J. Vet. Res.* **73**, 628-633.

McInnes, I. B., Schett, G., 2007. Cytokines in the pathogenesis of rheumatoid arthritis. *Nat. Rev. Immunol.* **7**, 42942.

McNamee, K., Williams, R., Seed, M., 2015. Animal models of rheumatoid arthritis: How informative are they? *Eur. J. Pharmacol*. **759**, 278–286.

Mobasheri, A., 2013. The Future of Osteoarthritis Therapeutics: Emerging Biological Therapy, *Curr. Rheumatol. Rep.* **15**(12), 385.

Mochizuki, T., Muneta, T., Sakaguchi, Y., Nimura, A., Yokoyama, A., Koga, H., Sekiya, I., 2006. Higher chondrogenic potential of fibrous synovium- and adipose synovium-derived cells compared with subcutaneous fat-derived cells: Distinguishing properties of mesenchymal stem cells in humans. *Arthritis and Rheum.* **54**, 843–853.

Moon, S. J., Ahn, I. E., Jung, H., Yi, H., Kim, J., Kim, Y., Kwok, S. K., Park, K. S., Min, J. K., Park, S. H., Kim, H. Y. and Ju, J. H. 2013. Temporal differential effects of pro-inflammatory cytokines on osteoclastogenesis. *Int. J. Mol. Med.* **31**, 769-777.

Moreland, L. W., Russel, A. S., Paulus, H. E., 2001. Management of rheumatoid arthritis: the historical context. *J. Rheumatol.* **28**, 1431-1452

Muir, P., Schamberger, G. M., Manley, P. A., Hao, Z., 2005. Localization of cathepsin k and tartrate-resistant acid phosphatase in synovium and cranial cruciate ligament in dogs with cruciate disease. *Vet. Surg.* **34**, 239–246.

Mulherin, D., Fitzgerald, O., Bresnihan, B., 1996. Synovial tissue macrophage populations and articular damage in rheumatoid arthritis. *Arthritis Rheum.* **39**,115–124.

Myers, L. K., Rosloneic, E. F., Cremer, M. A., Kang, A. H., 1997. Collagen induced arthritis and animal model of autoimmune. *Life Sci.* **61**, 1861-1878.

Nagase, T., Muneta, T., Ju, Y. J., Hara, K., Morito, T., Koga, H., Nimura, A., Mochizu, T., Sekiya, I., 2008. Analysis of the chondrogenic potential of human synovial stem

cells according to harvest site and culture parameters in knees with medial compartment osteoarthritis. *Arthritis Rheum.* **58**, 1389–1398.

Nakagawa, N., Kinosaki, M., Yamaguchi, K., Shima, N., Yasuda, H., Yano, K., Morinaga, T., Higashio, K., 1998. RANK is the essential signaling receptor for osteoclast differentiation factor in osteoclastogenesis. *Biochem. Biophys. Res. Commun.* **253**, 395-400.

Nakamura, I., Takahashi, N., Jimi, E., Udagawa, N., Suda, T., 2012. Regulation of osteoclast function. *Mod. Rheumatol.* **22**, 167-177.

Nishimura, K., Solchaga, L. A., Caplan, A. I., Yoo, J. U., Goldberg, V. M., Johnstone, B., 1999. Chondroprogenitor cells of synovial tissue. *Arthritis Rheum*. **42**, 2631–2637.

Paleolog, E. M., 2002. Angiogenesis in rheumatoid arthritis. *Arthritis Res*. **4**, S8190.

Pei, M., He, F., Vunjak-Novakovic, G., 2008. Synovium-derived stem cell-based chondrogenesis. *Differentiation* **76**, 1044–1056.

Pfeilschifter, J., Chenu, C., Bird, A., Mundy, G.R. and Roodman, G.D. 1989. Interleukin-1 and tumor necrosis factor stimulate the formation of human osteoclast-like cells in vitro. *J. Bone. Miner. Res.* **4**, 113-118.

Probert, L., Plows, D., Kontogeorgos, G., Kollias, G., 1995. The type I interleukin-1 receptor acts in series with tumor necrosis factor (TNF) to induce arthritis in TNF-transgenic mice. *Eur. J. Immunol*. **25**, 1794-1797.

Quan, L., Thiele, G. M., Tian, J., Wang, D., 2008. The Development of Novel Therapies for Rheumatoid Arthritis. *Expert Opin. Ther.* **18**, 723–738.

Qvist, P., Bay-Jensena, A., Christiansena, C., Dama, E. B., Pastoureaub, P., Karsdal, M. A., 2008. The disease modifying osteoarthritis drug (DMOAD): Is it in the horizon? *Pharmacol. Res.* **58**, 1–7.

Redlich, K., Hayer, S., Ricci, R., David, J. P., Tohidast-Akrad, M., Kollias, G., 2002. Osteoclasts are essential for TNF-alpha-mediated joint destruction. *Eur. J. Clin. Invest.* **110**, 1419–27.

Reponen P., Sahlberg C., Munaut C., Thesleff I., Tryggvason K. 1994. High expression of 92-kDa type IV collagenase (gelatinase) in the osteoclast lineage during mouse development. *Ann. N.Y. Acad. Sci.* **732**, 472–475.

Ritchlin, C. 2000. Fibroblast biology: Effector signals released by the synovial fibroblast in arthritis. *Arthritis. Res. Ther.* **2**, 356-360.

Ritchlin, C. T., Haas-Smith, S. A., Li, P., Hicks, D. G., Schwarz, E. M., 2003. Mechanisms of TNF-alpha- and RANKL-mediated osteoclastogenesis and bone resorption in psoriatic arthritis. *J. Clin. Invest.* **111**, 821–31.

Sakaguchi, Y., Sekiya, I., Yagishita, K., Muneta, T., 2005. Comparison of human stem cells derived from various mesenchymal tissues: Superiority of synovium as a cell source. *Arthritis Rheum.* **52**, 2521–2529.

Sakkas, L. I., Platsoucas, C. D., 2007. The role of T cells in the pathogenesis of osteoarthritis. *Arthritis Rheum.* **56**, 409-424.

Schett, G., 2007. Cells of the synovium in rheumatoid arthritis. *Arthritis Res. Ther.* **9**, 203.

Schett, G., Gravallese, E. 2012. Bone erosion in rheumatoid arthritis: mechanisms, diagnosis and treatment. Nat. Rev. Rheumatol. 8, 656-664.

Schett, G., Stach, C., Zwerina, J., Voll, R., Manger, B., 2008. How anti-rheumatic drugs protect joints rom damage in rheumatoid arthritis. *Arthritis Rheum.* **58**, 2936–2948.

Schett, G., Stolina, M., Dwyer, D., Zack, D., Uderhardt, S., Krönke, G., Kostenuik, P., Feige, U., 2009. Tumor necrosis factor α and RANKL blockade cannot halt bony spur formation in experimental inflammatory arthritis. *Arthritis Rheum*. **60**, 2644–2654.

Schonthaler, H. B., Guinea-Viniegra, J., Wagner, E. F., 2011. Targeting inflammation by modulating the Jun/AP‐1 pathway. *Ann. Rheum. Dis*. **70**, 109–112.

Schumacher, H. R., Newton, C., Halliwell, R. E., 1980. Synovial pathologic changes in spontaneous canine rheumatoid-like arthritis. *Arthritis Rheum*. **23**, 412-423.

Schwarz, E. M., Looney, R. J., Drissi, M. H., O'Keefe, R. J., Boyce, B. F., Xing, L., Ritchlin, C. T., 2006. Autoimmunity and bone. *Ann N Y Acad Sci.* **1068**, 275–83.

Scott, D. L., Wolfe, F., Huizinga, T. W., 2010. Rheumatoid arthritis. *Lancet* **376**, 1094-1108.

Shirasawa, S., Sekiya, I., Sakaguchi, Y., Yagishita, K., Ichinose, S., Muneta, T., 2006. In vitro chondrogenesis of human synovium-derived mesenchymal stem cells: Optimal condition and comparison with bone marrow-derived cells. *J. Cell. Biochem.* **97**, 84–97.

Smith, M. D., 2011. The Normal Synovium. *Open Rheumatol. J.* **5**, 100-106.

Smith, M. D., Walker, J. G., 2011. The synovium. Rheumatology Editors Hochberg, Silman, Smolen, Weinblatt, Weisman, Eds. 5th ed. vol **1**, 51-56.

Smith, M. M., Ghosh, P., Numata, Y. and Bansal, M. K., 1994. The effects of orally administered calcium pentosan polysulphate on inflammation and cartilage degradation produced in rabbit joints by intra-articular injection of a hyaluronate-polylysine complex. *Arthritis Rheum.* **37**, 125-136.

Smith, M. M., Numata, Y. and Ghosh, P. 1999. Effects of Calcium Pentosan Polysulfate on Joint Inflammation and Pouch Fluid Levels of Leukocytes, Nitric Oxide, and Interleukin-6 in a Rat Model of Arthritis. *Curr. Ther. Res*. **60**, 561-576.

Smolen, J. S. and Steiner, G. 2013. Therapeutic strategies for rheumatoid arthritis. *Nat. Rev. Drug Discov.* **2**, 473-488.

Smolen, J. S., Aletaha, D., Koeller, M., Weisman, M.H. and Emery, P. 2007. New therapies for treatment of rheumatoid arthritis. *The Lancet* **370**, 1861-1874.

Smolen, J. S., Steiner, G., 2003. Therapeutic strategies for rheumatoid arthritis. *Nat. Rev. Drug Discov.* **2**, 47388.

Suda, T., Takahashi, N., Martin, T. J., 1992. Modulation of osteoclast differentiation. *Endocr. Rev.* **13**, 66-80.

Takayanagi, H., 2007. Osteoimmunology: shared mechanisms and crosstalk between the immune and bone systems. *Nat. Rev. Immunol.* **7**, 292–304.

Takayanagi, H., Kim, S. and Taniguchi, T. 2002. Signaling crosstalk between RANKL and interferons in osteoclast differentiation. *Arthritis. Res. Ther.* **3**, 227.

Takeshita, S., kaji, K., Kudo, A. 2000. Identification and characterization of the new osteoclast progenitor with macrophage phenotypes being able to differentiate into mature osteoclasts. *J. Bone Miner. Res.* **15**, 1477-1488.

Takizawa, M., Yatabe, T., Okada, A., Chijiiwa, M., Mochizuki, S., Ghosh, P., Okada, Y., 2008. Calcium pentosan polysulfate directly inhibits enzymatic activity of ADAMTS4 (aggrecanase-1) in osteoarthritic chondrocytes. *FEBS Lett.* **582,** 2945–2949.

Tanabe, N., Maeno, M., Suzuki, N., Fujisaki, K., Tanaka, H., Ogiso, B., Ito, K., 2005. IL-1 alpha stimulates the formation of osteoclast-like cells by increasing M-CSF and PGE2 production and decreasing OPG production by osteoblasts. *Life Sci*. **77**, 615-626.

Tanaka, H., Tanabe, N., Shoji, M., Suzuki, N., Katono, T., Sato, S., Motohashi, M., Maeno, M., 2006. Nicotine and lipopolysaccharide stimulate the formation of osteoclast-like cells by increasing macrophage colony-stimulating factor and prostaglandin E2 production by osteoblasts. *Life Sci.* **78**, 1733-1740.

Taylor, P. C., Moore, A., Vasilescu, R., Alvir, J., Tarallo, M., 2016. A structured literature review of the burden of illness and unmet needs in patients with rheumatoid arthritis: a current perspective. *Rheumatol Int*. **36**, 685–95.

Teitelbaum, S. L., 2000. Bone resorption by osteoclasts. *Science* **289**,15048.

Tharasanit, T., Phutikanit, N., Wangdee, C., Soontornvipart, K., Tantrajak, S., Kaewamatawong, T., Suwimonteerabutr, J., Supaphol, P., Techakumphu, M., 2011. Differentiation potentials of canine bone marrow mesenchymal stem cells. *Thai J. Vet. Sci.* **41**, 79-86.

Thomson, B.M., Mundy, G.R. and Chambers, T.J. 1987. Tumor necrosis factors alpha and beta induce osteoblastic cells to stimulate osteoclastic bone resorption. *J. Immunol.* **138**, 775-779.

Tseng, S., Reddi, H. A., Cesare, P. E. D., 2009. Oligomeric Matrix Protein (COMP): A Biomarker of Arthritis. *Biomark. Insights* **4**, 33-44.

van der Pluijm G., Most W., van der Wee-Pals L., de Groot H., Papapoulos S. and Löwik C. 1991. Two distinct effects of recombinant human tumor necrosis factor-alpha on osteoclast development and subsequent resorption of mineralized matrix. *Endocrinology* **129**, 1596-604.

Vargas, S. J., Naprta, A., Glaccum, M., Lee, S. K., Kalinowski, J. and Lorenzo, J. A. 1996. Interleukin-6 expression and histomorphometry of bones from mice deficient in receptors for interleukin-1 or tumor necrosis factor. *J. Bone. Miner. Res.* **11**, 1736-1744.

Vinazzer, H., 1989. Antithrombotic therapy in patients with known risk factors for thromboembolism. Folia Haematol Int Mag Klin Morphol Blutforsch. **116,** 927-934.

Wagner, E. F. 2010. Bone development and inflammatory disease is regulated by AP‐1 (Fos/Jun). *Ann. Rheum. Dis.* **1**, 86–88.

Wagner, E. F., Eferl, R. 2005. Fos/AP-1 proteins in bone and the immune system. *Immunol. Rev.* **208**, 126-132.

Wagner, E. F., Matsuo, K., 2003. Signalling in osteoclasts and the role of Fos/AP1 proteins. *Ann. Rheum. Dis.* **62**, 83-85.

Wallace, J. L. 1997. Nonsteroidal anti-inflammatory drugs and gastroenteropathy: the second hundred years. *J. Gastroenterol.* **112,** 1000-1016.

Walsh, D. A., McWilliams, D. F., 2014. Mechanisms, impact and management of pain in rheumatoid arthritis. *Nat. Rev. Rheumatol*. **10**, 581–92.

Witsberger, T. H., Armando, V.J., Schultz, L. G., Hahn, A. W., 2008. Prevalence of and risk factors for hip dysplasia and cranial cruciate ligament deficiency in dogs. *J. Am. Vet. Med. Assoc.* **232,** 1818-1824.

Xue, M., Jiang, Z. Z., Wu, T., Li, J., Zhang, L., Zhao, Y., Li, X. J., Zhang, L. Y., Yang, S. Y., 2012. Anti-inflammatory effects and hepatotoxicity of Tripterygium-loaded solid lipid nanoparticles on adjuvant-induced arthritis in rats. *Phytomedicine* **19**, 998–1006.

Yagi, M., Miyamoto, T., Sawatani, Y., Iwamoto, K., Hosogane, N., Fujita, N., Morita, K., Ninomiya, K., Suzuki, T., Miyamoto, K., Oike, Y., Takeya, M., Toyama, T., Suda, T., 2005. DC-STAMP is essential for cell-cell fusion in osteoclasts and foreign body giant cells. *J. Exp. Med.* **2020**, 345-351.

Yagi, M., Miyamoto, T., Toyama, Y., Suda, T., 2006. Role of DC-STAMP in cellular fusion of osteoclasts and macrophage giant cells. *J. Bone. Miner. Metab*. **24**, 355-358.

Zaslau, S., Sparks, S., Riggs, D., Jackson, B., Kandzari, S. J., 2006. Pentosan polysulfate (Elmiron): in vitro effects on prostate cancer cells regarding cell growth and vascular endothelial growth factor production. *Ame. J. Surg.* **192**, 640–643.

Zenz, R., Eferl, R., Scheinecker, C., Redlich, K., Smolen, J., Schonthaler, H. B., Kenner, L., Tschachler, E., Wagner, E. F., 2008. Activator protein 1 (Fos/Jun) functions in inflammatory bone and skin disease. *Arthritis Res. Ther.* **10**, 201.

Zhao, Q., Wang, X., Liu, Y., He, A., Jia, R., 2010. NFATc1: functions in osteoclasts. Int. J. Biochem. *Cell Biol.* **45**, 576-579.

Zheng, C. J., Zhao, X. X., Ai, H. W., Lin, B., Han, T., Jiang, Y. P., Xing, X., Qin, L. P., 2014. Therapeutic effects of standardized Vitex negundo seeds extract on complete Freund's adjuvant induced arthritis in rats. *Phytomedicine* **21**, 838–846.

Zupan, J., Jeras, M. and Marc, J. 2013. Osteoimmunology and the influence of pro-inflammatory cytokines on osteoclasts. *Biochem Med.* **23**, 43-63.

7. Abstract of the Dissertation

Pentosan polysulfate: an effective treatment for model of rheumatoid arthritis and a novel candidate for inhibition of cytokines-induced osteoclastogenesis

Inflammatory joint diseases characterized by abnormal synovial proliferation and destruction of articular cartilage and bone. The degree of joint damage in inflammatory joint diseases such as, rheumatoid arthritis (RA) correlates with the number of synovial macrophages and inflammatory mediators appeared in the thickened synovial lining and synovial fluid. Comprehensive investigation of biological reaction of inflamed synovial joints is essential for implementing the treatment strategies by considering pathological changes. This study was constructed based on two major purposes. Primary objective was to identify the differentiation potential of synoviocytes and osteoclast; key effector cells in RA and second is to study the effectiveness of pentosan polysulfate (PPS) over the osteoclastogenesis and inflammation-related arthritis.

The synovial membrane (SM) is the central area of pathology of osteoarthritis (OA), RA and other inflammatory joint diseases including canine common knee injuries such as cranial cruciate ligament rupture (CCLr) and medial patella luxation (MPL). Findings of current study showed, differentiation capability of SM-derived multipotent stem cells varies with inflammatory severity occurring in CCLr and MPL. Further, current study was able to emphasize that pre-activated MSCs by inflammatory factors might offer a method of improving the potency of these cells without the need for additional cell number.

Several studies have shown that RA synovial cells release proinflammatory prostaglandins and cytokines, such as interleukin (IL)-1, tumour necrosis factor alpha (TNFα), and IL-17, all of which are known to promote osteoclastic bone resorption. Osteoclastogenic properties of inflammatory cytokines at different time-points of

osteoclastogenesis were identified. This study might be a manifesto for future investigation of finding other factors involved in the IL-1β–induced inhibition of canine osteoclastogenesis and to unveil the rationale of MMP9 downregulation by IL-17 in addition to determine the mechanisms of action of IL-17 in bone erosion.

Pentosan polysulfate sodium is a semi-synthetic sulfated polysaccharide drug manufactured from European beech-wood hemicellulose by sulfate esterification. From the results of previous *in vitro* and *in vivo* studies, the spectrum of pharmacological activities exhibited by PPS would qualify it as disease-modifying osteoarthritis drug (DMOAD) because of its ability to preserve the integrity of the articular cartilage and bone while improving the quality of the joint synovial fluid. Findings of current study provide useful preliminary information of inhibitory effect of PPS on OC differentiation and bone resorption by proving treatment option for osteoporosis or other bone diseases associated with excessive bone resorption and provides useful information for future pharmacokinetic studies and clinical trials *in vivo*. Pentosan has been used as a treatment for variety of inflammatory conditions with an excellent long-term safety profile. One of the aims of this study was to investigate potential anti-arthritic activity of PPS in collagen induced arthritis rat. The results of the current *in vivo* study confirmed that PPS upgrades the clinical outcome of RA animal model while conserving structural silhouettes of the joints by possessing its anti-arthritis effect.

Collectively this whole study was able to emphasis that the anti-arthritis and anti-inflammatory effect of PPS in RA animal model while unveiling it’s another dimension of mechanism of action on osteoclastogenesis. To achieve this phenomenon, clustered studies including, understanding differentiation potential of synoviocytes and OC at inflammatory background added the contextual value and fundamental theories to the whole study.

8. Japanese Summary

多硫酸ペントサン：関節リウマチの効果的な治療法およびサイトカイン誘発破骨細胞分化制御の新規薬剤としての検討

炎症性関節症では、滑膜の異常増殖と関節を構成する骨軟骨の著しい破壊がみられる。関節リウマチなど、関節炎における関節破壊は、肥厚した滑膜内や滑液中に増加するマクロファージの数に比例して悪化する。炎症を発現した関節構造の生物学的な反応に対する多角的な研究は、関節の病理学的変化を理解することとそれによる治療法の開発には不可欠である。本研究は、次の二つ事象について検討した。まず、犬の関節リウマチにおいて重要な役割を持つ滑膜細胞と破骨細胞の分化能を解明すること、次に、破骨細胞分化および炎症性関節症における多硫酸ペントサン（PPS）の病態修飾効果を評価することを目的にした。

滑膜には、変形性関節症、関節リウマチ、前十字靭帯断裂や膝蓋骨内方脱臼などに関連した関節疾患における主要な病態生理が存在する。検討の結果、前十字靭帯断裂や膝蓋骨内方脱臼に関連した関節炎では、それらによって誘導される関節内の炎症の度合いによって滑膜に存在する多分化細胞の分化能が変化することがわかった。さらに、炎症性因子によって刺激を受けた間葉系幹細胞はその分化能が高まることが示された。関節リウマチ罹患関節内の滑膜細胞からは炎症性プロスタグランディンや、インターロイキン（IL）-1、腫瘍壊死因子（TNF）-α、IL-17などの炎症性サイトカインが産生されることがわかっており、それらはすべて破骨細胞による骨破壊を誘導する因子であるが、ここではIL-1βによる犬破骨細胞分化抑制、骨破壊におけるIL-17のメカニズムの解明に

加え、IL-17によるマトリックスメタロプロテイナーゼ（MMP）9発現抑制の根拠を明らかにした。

PPSは半合成硫酸化多糖であり、西洋ブナから硫酸エステル化によって薬剤として製造されている。過去の *in vitro* や *in vivo* の研究成果から、PPSには関節軟骨・骨の保護効果や滑膜炎の制御など変形性関節症に対する病態修飾薬（DMOAD）としての能力があることが示されている。本研究では、PPSは破骨細胞分化を抑制し、骨粗鬆症や他の過剰な骨吸収を伴う骨疾患の治療薬になる可能性および臨床試験における薬理作用の検討に有益な情報が示された。PPSはその長期間投与における高い安全性から、炎症性病態への治療に活用しうることが示されてきた。そこで、コラーゲン誘発性関節炎（ラット）に対する抗関節炎効果について検討した。その結果、関節炎による関節破壊を抑制し、関節炎の進行を遅らせることができることが示唆された。

以上の結果から、関節リウマチモデル動物におけるPPSの特筆すべき抗関節炎効果が示され、このことはPPSの破骨細胞分化抑制効果と関連していると考えられた。このことを結論付けるため、滑膜細胞や破骨細胞の分化様式を再現し、それにおけるPPSの関与を明らかにした。

9. Acknowledgments

The completion of this thesis would not have been possible without the scientific and personal support of many. Firstly, I would like to express my sincere gratitude to my advisor Prof. Masahiro Okumura for the continuous support of my Ph.D study and related research, for his patience, motivation, and immense knowledge has made it a pleasure to work with him for the past several years. His guidance helped me in all the time of research and writing of this thesis. I could not have imagined having a better advisor and mentor for my Ph.D study. Besides my advisor, I would like to thank the rest of my co-supervisors and thesis committee: Associate Prof. Kenji Hosoya, Assistant Prof. Sangho Kim and Prof. Yasuhiro Kon for their insightful comments and encouragement, but also for the hard question which incented me to widen my research from various perspectives. My sincere thanks go to Associate Prof. Kentaro Sakamoto and Assistant Prof. Keisuke Aoshima for their immense support for the success of animal experiments and hisopathology. My sincere thanks also go to Prof. Steven Teitelbaum (Washington University in St. Louis), Prof. Ians McInnes and Dr. Carl Goodyear (Glasgow University) who provided me an opportunity to join their team as intern, gave access to the laboratory and research facilities. I would like to offer my thanks to Dr. David Cullis-Hill, Arthropharm Pty. Ltd., Australia for proving fluorescence labeled PPS.

Working in the surgery lab has also provided me with the opportunity to have as my colleagues a wonderful group of inquisitive and supportive people. Specially, I would like to thank Jing Fang for her patience in teaching me many basic things about cell culture at 1 st year of PhD, Eugene Bwalya for tolerating my physical extremity as a

bench-mate and hood-mate as well as his constant encouragements, Tatsuya Deguchi , Yusuke Murase, Mijiddorj Tsogbadrakh and Akaraphutiporn Ekkapol for their enormous help for sampling, and Mika Sumita for your kind support during the study period. Working in the surgery lab has also given me the chance to receive the input from many of the world's leading experts in bone biology through participating conferences and internship trainings. Finally, studying at the graduate school of veterinary medicine has given me the chance to interact with a number of scientists.

Last but not the least, I would like to thank my family for all their love and encouragement: my parents who raised me with a love of science and supported me in all my pursuits and to my father and mother-in-law, sister and brother-in-low and little Aanya for supporting me spiritually throughout writing this thesis and my life in general.

And most of all for my loving, supportive, encouraging and patient husband, Nuwan Wijekoon and daughter Abhimani Wijekoon for providing me with unfailing support and continuous encouragement throughout my years of study and through the process of researching and writing this thesis. This accomplishment would not have been possible without you.

Thank you.

H. M. Suranji Wijekoon

Hokkaido University

2018